PilT and PilU are homohexameric ATPases that coordinate to retract type IVa pili

Jennifer L. Chlebek[1], Hannah Q. Hughes[1], Aleksandra S. Ratkiewicz[2], Rasman Rayyan[2], Joseph Che-Yen Wang[3], Brittany E. Herrin[1], Triana N. Dalia[1], Nicolas Biais[2], and Ankur B. Dalia[1,*]

[1]Department of Biology, Indiana University, 1001 E. 3rd Street, Bloomington, IN 47405.

[2]Biology Department, CUNY Brooklyn College, 2900 Bedford Avenue, Brooklyn, NY 11210 and Graduate Center of CUNY, 365 5th Avenue, NY 10016.

[3]Electron Microscopy Center, Indiana University, Bloomington, IN 47405.

*Correspondence to: ankdalia@indiana.edu.

Short Title: PilU is a PilT-dependent type IVa pilus retraction ATPase

Abstract

Bacterial type IV pili are critical for diverse biological processes including horizontal gene transfer, surface sensing, biofilm formation, adherence, motility, and virulence. These dynamic appendages extend and retract from the cell surface. In many type IVa pilus systems, extension occurs through the action of an extension ATPase, often called PilB, while optimal retraction requires the action of a retraction ATPase, PilT. Many type IVa systems also encode a homolog of PilT called PilU. However, the function of this protein has remained unclear because *pilU* mutants exhibit inconsistent phenotypes among type IV pilus systems and because it is relatively understudied compared to PilT. Here, we study the type IVa competence pilus of *Vibrio cholerae* as a model system to define the role of PilU. We show that the ATPase activity of PilU is critical for pilus retraction in PilT Walker A and/or Walker B mutants. PilU does not, however, contribute to pilus retraction in Δ*pilT* strains. Thus, these data suggest that PilU is a *bona fide* retraction ATPase that supports pilus retraction in a PilT-dependent manner. We also found that a Δ*pilU* mutant exhibited a reduction in the force of retraction suggesting that PilU is important for generating maximal retraction forces. Additional *in vitro* and *in vivo* data show that PilT and PilU act as independent homo-hexamers that may form a complex to facilitate pilus retraction. Finally, we demonstrate that the role of PilU as a PilT-dependent retraction ATPase is conserved in *Acinetobacter baylyi*, suggesting that the role of PilU described here may be broadly applicable to other type IVa pilus systems.

Author Summary

Almost all bacterial species use thin surface appendages called pili to interact with their environments. These structures are critical for the virulence of many pathogens and represent one major way that bacteria share DNA with one another, which contributes to the spread of antibiotic resistance. To carry out their function, pili dynamically extend and retract from the bacterial surface. Here, we show that retraction of pili in some systems is determined by the combined activity of two motor ATPase proteins.

Introduction

Type IV pili are ubiquitous surface appendages in Gram-negative bacteria that promote diverse activities including attachment, virulence, biofilm formation, horizontal gene transfer, and twitching motility [1-5]. These structures can dynamically extend and retract from the cell surface, which is often critical for their function. A detailed mechanistic understanding of pilus dynamic activity, however, remains lacking.

Type IV pili are composed almost exclusively of a single protein called the major pilin, which forms a helical fiber that extends from the cell surface [6]. Extension and retraction of the pilus is hypothesized to occur through the interaction of cytoplasmic hexameric ATPases with the inner membrane platform of the pilus machine, whereby ATP hydrolysis likely facilitates turning of the platform in order to incorporate or remove major pilin subunits from the pilus fiber [7-9]. All type IV pilus systems encode a predicted ATPase, often called PilB, that facilitates pilus extension [7, 10-12]. Many type IVa pilus systems also contain a retraction ATPase, called PilT, which depolymerizes the pilus fiber and recycles pilin subunits into the inner membrane. Many type IVa pilus systems also encode another putative ATPase called PilU. PilU is a homolog of the retraction ATPase PilT, however, the function of this protein has remained unclear because PilU is relatively understudied compared to PilT and because of phenotypic inconsistency for *pilU* mutants in different organisms. For example, a *pilU* mutant of *Pseudomonas aeruginosa*, exhibits reduced twitching motility [13], but in other type IV pilus systems, including the *V. cholerae* competence pilus, loss of *pilU* does not reveal any overt phenotypes.

The facultative bacterial pathogen *Vibrio cholerae* uses a type IV competence pilus for DNA uptake during natural transformation. We have recently demonstrated that the type IV competence pili of *V. cholerae* can be fluorescently labeled by using a technique [14-16] in which an amino acid of the major pilin subunit PilA is replaced with a cysteine ($PilA^{S56C}$ based on the mature pilin sequence, which was previously misannotated $PilA^{S67C}$ [17] and $PilA^{S81C}$ [18]), which allows for subsequent labeling with a fluorescently-labeled thiol-reactive maleimide dye (AF488-mal). This labeling approach does not impede dynamic pilus activity and allows for the direct observation and measurement of pilus extension and retraction by time-lapse epifluorescence microscopy. Using this labeling technique, we have recently demonstrated that the retraction of DNA-bound type IV competence pili is required to initiate the process of DNA uptake during natural transformation [18].

Here, we employ our pilus labeling approach and complementary molecular methods to address the role that PilU plays in type IV competence pilus retraction, and we extend our findings to the type IVa competence pilus of *Acinetobacter baylyi*. Our results indicate that PilT and PilU form

independent homo-hexamers and that the ATPase activity of PilU promotes type IV pilus retraction in a PilT-dependent manner.

Results

PilU promotes type IV competence pilus retraction in a PilT-dependent manner

In order to study the function and role of ATPases in the retraction of type IV competence pili in *V. cholerae*, we utilize two main methods: (1) our labeling approach to directly measure pilus retraction via epifluorescence time-lapse microscopy and (2) assessing natural transformation, which is dependent on competence pilus retraction [18, 19]. Also, as for other pili [20-22], competence pili can mediate cell to cell interactions [17], which causes hyperpiliated strains to aggregate and pellet to the bottom of culture tubes. Consistent with prior work [19, 23-28], mutant strains that lack the retraction ATPase PilT are poorly transformable, exhibit markedly reduced rates of pilus retraction, aggregate, and are hyperpiliated (≥3 pili per cell) compared to the parent strain (**Fig 1A, 1B, 1D** and **1E**). Also, the number of cells that exhibit dynamic pilus activity is reduced in the Δ*pilT* strain as observed by time-lapse epifluorescence microscopy, which is consistent with the hyperpiliated phenotype of this mutant (**Fig 1C**). Because the frequency of retraction was reduced by ~2 logs in the Δ*pilT* strain (**Fig 1C**), we could not obtain enough events to make rigorous statistical comparisons. In the rare events observed, however, the retraction rate is reduced, albeit not significantly, ~50-fold in the Δ*pilT* background.

The residual retraction in a Δ*pilT* strain is not due to PilU because a Δ*pilT* Δ*pilU* double mutant strain displays the same phenotype as a Δ*pilT* strain (**Fig 1A-E**). By contrast, Δ*pilU* mutants are highly transformable, do not aggregate, exhibit normal numbers of pili and are largely indistinguishable from the parent strain (**Fig 1A** and **1C-E**) aside from a significant 1.3-fold reduction in retraction rates compared to the parent strain (**Fig 1B**). This effect of PilU on retraction rate is much smaller compared to the ~50-fold reduction in retraction rate observed in the Δ*pilT* and Δ*pilT* Δ*pilU* mutants (**Fig 1B**). This suggests that PilT can still mediate retraction in a Δ*pilU* strain (because retraction frequency and rates for Δ*pilU* are closer to the parent than the Δ*pilT* Δ*pilU* strain), while PilU cannot mediate retraction in a Δ*pilT* strain (since the Δ*pilT* strain resembles the Δ*pilT* Δ*pilU* strain). Thus, these data support a model where PilT plays the dominant role in pilus retraction, which is consistent with prior reports [18, 19, 26].

112 PilT is a predicted ATPase and its ATPase activity has been shown to be important in the
113 function of other type IV pilus systems [12, 29]. Therefore, we hypothesized that the ATPase
114 activity of PilT would be required for retraction of the competence pilus. In order to answer this
115 question, we putatively ablated the ATPase activity of PilT by introducing a mutation in either an
116 invariantly conserved lysine in the Walker A motif required for ATP binding (*pilT*^{K136A}), a mutation
117 in a conserved glutamic acid in the Walker B motif required for ATP hydrolysis (*pilT*^{E204A}), or by
118 making a double mutant containing both mutations (*pilT*$^{E204A/K136A}$). Though these Walker A and
119 Walker B mutations have not been well studied in *V. cholerae* PilT-like ATPases, the effect of
120 these mutations has been well characterized in other systems and we assume that they ablate
121 the ATPase activity of this protein in a similar manner [30]. Interestingly, we found that strains
122 harboring mutations in PilT that putatively ablate the ATPase activity of this protein (*pilT*^{K136A},
123 *pilT*^{E204A}, *pilT*$^{E204A/K136A}$) all transform similarly to the parent strain and retract competence pili at
124 rates that are at most ~4-fold lower than the parent (**Fig 1A-B**). This is in stark contrast to a
125 Δ*pilT* strain where the transformation frequency is reduced ~4-logs and retraction is >50-fold
126 slower compared to the parent strain (**Fig 1A-B**). These results were quite surprising and
127 suggested that either (1) the ATPase activity of the retraction machinery is not critical for
128 promoting pilus retraction, (2) that the mutations to the Walker motifs do not ablate PilT ATPase
129 activity, or (3) that another retraction ATPase may promote retraction in the absence of PilT
130 ATPase activity.

131 We tested the third model and specifically assessed whether PilU could promote retraction in
132 predicted PilT ATPase-deficient mutants. Indeed, we found that *pilT*^{K136A}Δ*pilU*, *pilT*^{E204A}Δ*pilU*
133 and *pilT*$^{E204A/K136A}$Δ*pilU* strains all display reduced transformation, are hyperpiliated, aggregate,
134 exhibit markedly reduced retraction frequency, and reduced retraction rates similar to a Δ*pilT*
135 Δ*pilU* strain (**Fig 1A-E**). This is consistent with PilU promoting retraction in the *pilT*^{K136A}, *pilT*^{E204A}
136 and *pilT*$^{E204A/K136A}$ backgrounds. Importantly, the *pilT*^{K136A}Δ*pilU*, *pilT*^{E204A}Δ*pilU* and
137 *pilT*$^{E204A/K136A}$Δ*pilU* strains could be complemented via ectopic expression of *pilT* or *pilU* (**S1**
138 **Fig**). Since loss of *pilT* alone (i.e. Δ*pilT*) results in a phenotype comparable to a Δ*pilT* Δ*pilU*
139 mutant, this result indicates that PilU is not sufficient to drive pilus retraction in the absence of
140 PilT (**Fig 1A-E**). Consistent with this, ectopic expression of *pilU* does not rescue the
141 transformation deficit of a Δ*pilT* Δ*pilU* mutant (**S1 Fig**). Together, these data suggest that PilU
142 supports pilus retraction in a PilT-dependent manner.

143 Interestingly, whereas a *pilT*^{K136A} Walker A mutant displays normal piliation, the *pilT*^{E204A}Walker
144 B mutant is hyperpiliated (**Fig 1D-E**). The frequency of cells that exhibit pilus retraction in the

145 *pilT*^{E204A} mutant is much lower than the parent and comparable to the Δ*pilT* Δ*pilU* strain (**Fig**
146 **1C**), which may explain this hyperpiliated phenotype; however, when pilus retraction is
147 observed, the rate of retraction is closer to that of the parent than the Δ*pilT* Δ*pilU* mutant (**Fig**
148 **1B**). Considering the canonical functions of the Walker A and B motifs in ATP-binding and
149 hydrolysis, respectively, the *pilT*^{E204A} Walker B mutant should be able to bind to ATP but not
150 hydrolyze it. Because the putative ATP-binding deficient *pilT*^{K136A} Walker A mutant exhibited
151 parental levels of piliation (**Fig 1D-E**), we hypothesized that the hyperpiliation observed in
152 *pilT*^{E204A} may be due to the fact that this protein may be locked in an ATP-bound state. A recent
153 preprint shows that different ATP-bound states of PilT exhibit different conformations [31]. This
154 may suggest that the conformation adopted by PilT^{E204A} reduces the ability of PilU to facilitate
155 retraction. Because ATP-binding must precede hydrolysis, we hypothesized that a Walker A and
156 B double mutant (*pilT*$^{E204A/K136A}$) should restore the ability of PilU to mediate normal piliation
157 because this would prevent the formation of the ATP-bound conformation of PilT. Consistent
158 with this, we observed that the phenotype of the putative ATP-binding deficient Walker A
159 mutation (*pilT*^{K136A}) is dominant over the putative ATP-hydrolysis deficient *pilT*^{E204A} Walker B
160 mutation (**Fig 1D-E**). Both the Walker A and Walker B mutations should result in loss of ATPase
161 activity. Therefore, to avoid phenotypic consequences associated with the ATP-bound state of
162 the *pilT*^{E204A} mutant, we utilized the *pilT*^{K136A} mutant as a putative ATPase-defective allele of PilT
163 moving forward.

164

165 **PilU is required for forceful retraction**

166 The data thus far suggest that PilU is capable of supporting pilus retraction in putative PilT
167 ATPase-deficient mutants, but that PilU is not necessary to mediate pilus retraction (since Δ*pilU*
168 mutants transform at frequencies that are similar to the parent). PilU, however, is present in
169 many type IVa pilus systems, so the question remains: Why is PilU so widely conserved if it is
170 not necessary for pilus retraction? Recent work in *Pseudomonas aeruginosa* indicates that PilU
171 may be required for forceful retraction [32]. Our data thus far indicate that the Δ*pilU* mutant only
172 causes a modest reduction in the retraction rate (**Fig 1A**), which does not have a phenotypic
173 consequence on pilus-dependent DNA uptake (**Fig 1C**); however, these measurements are
174 based on free pili that are not retracting under load. We hypothesized that PilU might be
175 required for forceful retraction, such as when pili are attached to a surface. To test this, we
176 assessed pilus retraction using a micropillar assay in which binding of pili to micropillars and
177 subsequent retraction results in measurable bending and displacement of the micropillars.

178 These data can then be used to calculate the rates and force of pilus retraction [33]. In
179 agreement with our cell biological approach (i.e. pilus labeling), the micropillar assay showed
180 that retraction rates were reduced in both Δ*pilU* and Δ*pilT* strains; with PilT having a larger effect
181 on this rate (2-fold reduction for Δ*pilU* vs 14-fold reduction for Δ*pilT*) (**Fig 1B** and **1F**).
182 Importantly, the micropillar assay is more sensitive at detecting rare pilus retraction, which
183 allowed us to collect enough events to show that Δ*pilT* mutants are statistically significantly
184 reduced for retraction rates compared to the parent strain, which is consistent with previous
185 work [18]. In contrast, the Δ*pilU* and Δ*pilT* strains exhibited a similar reduction in the retraction
186 force (~2-fold for both) compared to the parent strain (**Fig 1G**). As other groups have also
187 reported, data collected on pilus retraction forces tend to be highly variable [18, 32, 34], which
188 we also observed here (**Fig 1G-H**). Despite this variability, a histogram reveals that PilT and
189 PilU promote retraction forces >12 pN because retraction events exceeding this force are
190 relatively rare in the Δ*pilT* and Δ*pilU* strains (**Fig 1H**). Thus far, we have shown that Δ*pilU* and
191 Δ*pilT* mutants display distinct phenotypes for transformation frequency (**Fig 1A**), retraction rates
192 (**Fig 1B** and **1F**) and piliation state (**Fig 1D-E**). Interestingly, the micropillar data reveal that
193 Δ*pilU* and Δ*pilT* mutants have a similar effect on retraction force (**Fig 1G-H**). This suggests that
194 PilU and PilT are both necessary for generating maximal retraction forces in the *V. cholerae*
195 competence pilus.

196

197 The ATPase activities of PilT and PilU define the rate of type IV competence pilus 198 retraction

199 Just like PilT, PilU is a PilT-like ATPase with a conserved lysine in its Walker A motif. Because
200 we observed that PilU supports pilus retraction in the $pilT^{K136A}$ mutant (**Fig 1B**), we hypothesized
201 that the ATPase activity of PilU may be important for supporting pilus retraction. To test the
202 relative roles of each of these ATPases in pilus retraction, we mutated the conserved lysine in
203 the Walker A motifs of PilT and/or PilU. The $pilU^{K134A}$ strain retracts ~1.5-fold slower than the
204 parent strain, similar to the Δ*pilU* mutant (**Fig 2A**). There may be a limited effect of the $pilU^{K134A}$
205 mutation on pilus retraction because this strain still has a functional PilT ATPase. However, we
206 hypothesized that PilU ATPase activity may be critical for retraction in a background where PilT
207 ATPase activity is also inactivated. Consistent with this, we found that a $pilT^{K136A}$ $pilU^{K134A}$ strain
208 is indistinguishable from a $pilT^{K136A}$ Δ*pilU* strain for pilus retraction, piliation, aggregation, and
209 transformation (**Fig 2A-C**). Together, these data suggest that PilU ATPase activity promotes
210 type IV competence pilus retraction.

211 The data above suggest that the ATPase activities of PilT and PilU are critical for pilus
212 retraction. These ATPases are predicted to be motor proteins that facilitate the depolymerization
213 of pilus fibers. Thus, if we alter the ATPase rates of these motors, we hypothesized that this
214 should alter the rates of pilus retraction. To test this hypothesis, we mutated a leucine in the
215 Walker B domain of PilT and PilU to a cysteine, which was previously shown to reduce the rate
216 of ATP hydrolysis of *Neisseria gonorrhoeae* PilT ~2-fold [26]. When these Walker B mutations
217 were tested in isolation, they did not alter the rate of pilus retraction (comparing the parent strain
218 to *pilT*^{L201C} and *pilU*^{L199C}) (**Fig 2A**). This may be due to the fact that these cells still have one fully
219 functional retraction ATPase (i.e. *pilT*^{L201C} still has a fully functional PilU and *pilU*^{L199C} still has a
220 fully functional PilT). We hypothesized that these putatively Walker B "slow" ATPase mutations,
221 however, may have an impact on pilus retraction if they represented the sole functional
222 retraction ATPase in the cell. To that end, we generated both a *pilT*^{L201C} Δ*pilU* strain and a
223 *pilT*^{K136A} *pilU*^{L199C} strain. The *pilT*^{L201C} Δ*pilU* mutant showed a slight (1.3 fold), but significant,
224 reduction in retraction rate compared to the Δ*pilU* strain (**Fig 2A**), which provides genetic
225 evidence to suggest that the ATPase rate of PilT may be linked to the retraction rate of the type
226 IV competence pilus and further supports the idea that PilT promotes pilus retraction through its
227 ATPase activity. The *pilT*^{K136A} *pilU*^{L199C} mutant also showed a slight (1.5-fold) reduction in
228 retraction rate compared to *pilT*^{K136A}, although this difference was not statistically significant (**Fig
229 2A**). Because this difference was not statistically significant, it may suggest that the ATPase
230 rate of PilU does not dictate the retraction rate of competence pili even when it is the sole
231 retraction ATPase; however, because this mutant trended towards a decreased retraction rate,
232 this result may still suggest that the ATPase rate of PilU is linked to retraction rates.

233

234 PilT and PilU directly interact with one another

235 All of these data presented above indicate that PilT and PilU can both support pilus retraction.
236 Therefore, we hypothesized that PilT and PilU may interact to form a complex that supports
237 pilus retraction. To address this, we utilized a Bacterial Adenylate Cyclase Two-Hybrid (BACTH)
238 assay [35, 36]. As expected for predicted hexameric proteins like PilT and PilU, the BACTH
239 analysis showed PilT-PilT and PilU-PilU self-interactions (**Fig 3** and **S2 Fig**). Additionally, the
240 BACTH assay showed that PilT and PilU interact with one another, which is consistent with prior
241 work in other systems [35, 37], and further demonstrated that Walker A mutations in either
242 protein (PilT^{K136A} and PilU^{K134A}) did not disrupt this interaction (**Fig 3** and **S2 Fig**). Thus, our
243 BACTH results suggest that PilT and PilU may form a complex. These results do not, however,

244 indicate whether PilU and PilT form heteromeric complexes or homomeric complexes to
245 facilitate pilus retraction. We test this further below.

246

247 PilT and PilU form independent homohexameric rings *in vitro* and *in vivo*

248 PilT in other systems has been shown to form a hexameric complex [38], and by homology we
249 hypothesized that PilU also forms a hexamer. Based on transformation frequency assays, N-
250 terminally tagged ^{6X}His-PilT and ^{6X}His-PilU were fully functional (**S3A Fig**). Therefore, we used
251 our purified ^{6X}His-PilT and ^{6X}His-PilU to characterize these proteins *in vitro*. Negative stain
252 transmission electron microscopy revealed that both ^{6X}His-PilT and ^{6X}His-PilU formed hexameric
253 ring complexes (**Fig 4A**). These results indicate that these proteins are capable of forming
254 independent homohexameric complexes *in vitro*. PilT and PilU have both sequence (~65%
255 similarity) and structural similarity to one another (**Fig 4A**), thus it is also possible that these
256 proteins can be incorporated into one ring and form heterohexameric complexes that facilitate
257 pilus retraction *in vivo*.

258 In order to test if PilT and PilU form heterohexamers or independent homohexamers to facilitate
259 pilus retraction *in vivo*, we hypothesized that overexpression of putative ATPase-inactive
260 mutants (i.e. PilT^{K136A} and PilU^{K134A}) in backgrounds that have native PilT and PilU would allow
261 us to distinguish between these two models. For example, if these proteins form heteromeric
262 complexes, then we would predict that overexpression of either putative ATPase-inactive
263 protein (PilT^{K136A} or PilU^{K134A}) should result in complexes that are mostly composed of ATPase-
264 inactive proteins and result in inhibition of pilus retraction (yielding a hyperpiliated phenotype)
265 and reduce rates of natural transformation (**Fig 4B**). If these proteins solely form homomeric
266 complexes, however, then we would predict that overexpression of only one ATPase-inactive
267 protein (PilT^{K136A} or PilU^{K134A}) should only inhibit the activity of one motor complex (PilT or PilU,
268 respectively) and should not have a dramatic effect on pilus retraction or natural transformation
269 because the other retraction motor would still be intact (**Fig 4B**).

270 In order for us to successfully test this question, we needed to: (1) be able to ectopically
271 overexpress ATPase deficient alleles of PilT or PilU, (2) demonstrate that ATPase deficient
272 alleles can interact with their ATPase sufficient counterparts and form proper hexamers, and (3)
273 show that ectopic expression of ATPase deficient alleles of PilT or PilU can inhibit the activity of
274 their respective natively expressed ATPase. We test each of these in turn below. First, we
275 confirmed that we could ectopically overexpress PilT and PilU. Using functional 3xFLAG-tagged

276 versions of PilT and PilU (**S3A-B Fig**), we show that our chromosomal P_{tac} regulated constructs
277 resulted in dramatic overexpression of these proteins (**S3C Fig**). Importantly, overexpression of
278 WT PilT and PilU did not affect pilus activity or natural transformation (**S1, S3B and S3D Figs**).
279 Next, we purified 6xHis-PilT^{K136A} and 6xHis-PilU^{K134A} and demonstrated that they formed ring
280 structures *in vitro* (**S3E Fig**), indicating that these proteins should form complexes with ATPase
281 sufficient alleles. This is also supported by our BACTH data (**Fig 3**). Finally, we wanted to
282 confirm that overexpressing the ATPase-inactive PilT^{K136A} or PilU^{K134A} could effectively impede
283 the function of the natively expressed ATPase-active PilT or PilU. To test this, we genetically
284 isolated either PilT or PilU as the sole functional retraction ATPase (i.e. PilT activity is isolated in
285 a Δ*pilU* background, while PilU activity is isolated in a *pilT*^{K136A} background) and then
286 overexpressed the cognate ATPase-inactive allele (P_{tac}-*pilT*^{K136A} or P_{tac}-*pilU*^{K134A}, respectively).
287 We assessed piliation, aggregation, and natural transformation as indicators of pilus retraction.
288 We found that, as expected, overexpression of ATPase-inactive alleles was sufficient to disrupt
289 the activity of the natively expressed ATPase (**Fig 4C-D** - compare Δ*pilU* to Δ*pilU* P_{tac}-*pilT*^{K136A}
290 and *pilT*^{K136A} to *pilT*^{K136A} P_{tac}-*pilU*^{K134A}). Also, as expected, overexpression of both ATPase-
291 deficient alleles together (P_{tac}-*pilT*^{K136A} and P_{tac}-*pilU*^{K134A}) in a background that has natively
292 expressed PilT and PilU, results in hyperpiliation, aggregation and reduced natural
293 transformation (**Fig 4C-D**), which further demonstrates that overexpression of these ATPase-
294 deficient proteins inhibits the activity of their natively expressed ATPase–sufficient versions.

295 The experiments above indicated that it would be feasible to test whether PilT and PilU formed
296 homomeric or heteromeric complexes *in vivo* as described in our model (**Fig 4B**). When we
297 overexpressed only one ATPase-deficient protein (P_{tac}-*pilT*^{K136A} or P_{tac}-*pilU*^{K134A}) in a background
298 that has natively expressed PilT and PilU, we found that piliation and transformation were
299 indistinguishable from the parent (**Fig 4C-D**). Thus, these data are consistent with PilT and PilU
300 forming independent homohexamers to facilitate pilus retraction.

301 Using our purified PilT and PilU, we also attempted to directly measure the ATPase activity of
302 these proteins. Unfortunately, the ATPase activity of these purified proteins was
303 indistinguishable from contaminating ATPases and/or below our detection limit (~1 nmol
304 pi/min/mg protein). Poor ATPase activity in purified retraction ATPases is not unique to our
305 system [12, 29, 39]. Alternatively, these results may suggest that the ATPase activities of these
306 proteins are stimulated *in vivo* via interaction with the proteins that compose the pilus machine,
307 as previously suggested [12]. Regardless, our previous *in vivo* data (**Fig 1A-D**) are consistent
308 with the *pilT*^{K136A} mutant being ATPase deficient.

309

310 The presence of PilT is not required for PilU to interact with the pilus platform 311 PilC.

312 Our data thus far indicate that PilU requires the presence of PilT (whether it is a functional
313 ATPase or not) to support optimal pilus retraction. The extension and retraction ATPases are
314 hypothesized to interact with the platform protein PilC to mechanically facilitate polymerization
315 and depolymerization of the pilus fiber [7, 37, 40]. Because PilU is dependent on the presence
316 of PilT to mediate retraction, we hypothesized that PilT can interact with PilC, but that PilU
317 cannot. To test this, we utilized the BACTH assay to test the interactions of PilT and PilU with
318 PilC. This assay showed that PilT and PilU could both interact with PilC, and that the Walker A
319 mutations of these ATPases ($PilT^{K136A}$ and $PilU^{K134A}$) did not affect these interactions (**Fig 3**). It
320 is necessary to point out, however, that the BACTH assay cannot address relative affinities of
321 protein interactions due to non-native expression levels, but instead indicates the potential
322 presence or absence of an interaction. The biological relevance of these interactions will
323 depend on the relative affinities and concentrations of these proteins in their natural context.
324 The interaction between PilC and PilT supports the canonical model that retraction ATPases
325 interact with PilC to facilitate depolymerization of the pilus fiber. Interestingly, our data suggest
326 that PilC and PilU interact independently of PilT. This result is also supported by prior BACTH
327 analysis of *P. aeruginosa* pilus components [37]. Thus, the simple model of PilU requiring PilT
328 for interaction with the platform PilC appears to be incorrect.

329

330 The function of PilU as a PilT-dependent retraction ATPase is conserved in the 331 *Acinetobacter baylyi* competence pilus

332 As mentioned earlier, many type IVa pilus systems encode PilU in addition to the canonical
333 retraction ATPase PilT. Therefore, we sought to assess whether PilU could facilitate PilT-
334 dependent retraction in other type IV pilus systems. To test this, we studied the type IVa
335 competence pili of a distinct gammaproteobacterium *Acinetobacter baylyi*. *A. baylyi* competence
336 pili also mediate DNA-uptake and the genetic organization of *pilT* and *pilU* is similar to that
337 observed in *V. cholerae*.

338 The competence pili of *A. baylyi* likely facilitate DNA uptake in a retraction-dependent manner,
339 similar to the competence pili of *V. cholerae*. Thus, we employed natural transformation assays

340 to dissect the role that PilT and PilU play in *A. baylyi* competence pilus retraction. These assays
341 showed that the PilT and PilU of *A. baylyi* behave largely like the PilT and PilU of *V. cholerae*.
342 The *pilU* mutant of *A. baylyi* displays a significant (~13-fold) reduction in natural transformation
343 (**Fig 5**), unlike what is observed in *V. cholerae* (**Fig 1A**). This may be because DNA uptake in *A.*
344 *baylyi* requires more forceful retraction or because PilU plays a more important role in pilus
345 retraction in this species. Most importantly, however, we found that PilU facilitates natural
346 transformation (and therefore pilus retraction) in backgrounds where the ATPase activity of PilT
347 is putatively inactivated (by mutation of the invariantly conserved lysine in the Walker A
348 domain), but not in backgrounds where *pilT* is absent (**Fig 5** – compare $pilT^{K136A}$ to $pilT^{K136A}$
349 Δ*pilU* and Δ*pilT*). Also, a strain where the ATPase activity of both PilT and PilU were putatively
350 inactivated ($pilT^{K136A}$ $pilU^{K137A}$) resulted in the loss of transformation equivalent to a retraction
351 deficient background (e.g. Δ*pilTU*) or a strain lacking competence pili (Δ*comP*). Importantly,
352 strains lacking *pilT* (i.e. Δ*pilT* and Δ*pilTU*) could only be complemented via ectopic expression of
353 *pilT* but not *pilU*, while strains that contained an ATPase defective allele of *pilT* (i.e. $pilT^{K136A}$
354 Δ*pilU* or $pilT^{K136A}$ $pilU^{K137A}$) could be complemented by ectopic expression of either *pilT* or *pilU*
355 (**S4 Fig**). These data are consistent with what was observed for *V. cholerae* competence pili
356 (**Fig 1A** and **S1 Fig**). Additionally, it was very recently shown that PilU from *Pseudomonas*
357 *aeruginosa* can also promote retraction in a PilT-dependent manner [41]. Together, these
358 results demonstrate that PilU ATPase activity facilitates pilus retraction in a PilT-dependent
359 manner in at least three gammaproteobacteria (*V. cholerae*, *A. baylyi* and *P. aeruginosa*) and
360 suggests that this phenomenon may also extend to other type IVa pilus systems.

361

362 Discussion

363 This study sheds light on the function of PilU as a retraction ATPase of type IVa competence pili
364 in *V. cholerae*. Specifically, our data indicate that PilU can mediate pilus retraction in a PilT-
365 dependent manner likely through its ATPase activity. Our results also show that PilT and PilU
366 form independent homohexamers and that these proteins likely interact with each other and the
367 platform protein PilC. Furthermore, we demonstrate that the role of PilU in supporting pilus
368 retraction is conserved in at least one other type IVa pilus system.

369 Interestingly, previous work in other species has shown that ATPase mutations in PilT have a
370 greater effect on pilus function compared to the results we present here for both *A. baylyi* and *V.*
371 *cholerae* competence pili [12, 42]. It is possible that PilT ATPase mutations have a greater

372 effect on retraction depending on the pilus activity in question (for example twitching motility vs
373 DNA uptake). It is also possible that previous reports may have overlooked subtle effects of
374 mutations within the *pilT* gene on the expression of *pilU*, which is generally found downstream in
375 the same operon. Finally, it is also possible that PilU may not be able to compensate for the loss
376 of PilT ATPase activity in some pilus systems.

377 Our results indicate that PilU can only facilitate pilus retraction in the presence of PilT,
378 regardless of whether that PilT is a functional ATPase. These results are also supported by a
379 recent report from the Blokesch lab, which was published while our manuscript was in revision
380 [41]. We initially tested the hypothesis that this was due to a requirement for PilT to bridge PilU
381 with the platform protein PilC. Our BACTH results, however, indicated that PilU may directly
382 interact with PilC in the absence of PilT (**Fig 3** and **S2 Fig**). While they may interact, it is
383 possible that PilU does not bind and engage the PilC platform in a conformation that would
384 facilitate retraction. Alternatively, it is possible that PilU does bind PilC in a conformation that
385 can facilitate retraction but additional interactions with PilT are required to stimulate PilU
386 ATPase activity. Another possibility is that PilT interacts with other components of the pilus
387 machine that are required for stimulating retraction, and that PilU lacks these interactions. Yet
388 another possibility is that PilU enhances the processivity of the PilT ATPase. Future efforts
389 focused on the interaction network of the retraction ATPases with the pilus machine should
390 shed light on these various hypotheses.

391 Previous reports have shown that PilU is necessary for twitching motility in *P. aeruginosa* [13],
392 an activity that likely requires forceful retraction [32]. Consistent with this, our results indicate
393 that PilU is necessary for maximal retraction force for the competence pilus in *V. cholerae* (**Fig**
394 **1G-H**). Interestingly, because the Δ*pilU* mutant transforms similarly to the parent strain (**Figs 1A**
395 and **2B**), the forceful retraction mediated by PilU does not seem to be necessary for the function
396 of the *V. cholerae* competence pilus in DNA uptake under the conditions tested. However,
397 forceful PilU-dependent retraction may be necessary for DNA uptake when tDNA is absorbed
398 onto surfaces and/or in complex environments like biofilms.

399 Beyond altering the force of retraction, many mutants in PilT and PilU also reduced the speed of
400 pilus retraction relative to the parent strain (i.e. Δ*pilU* = ~1.3-fold, $pilT^{K136A}$ = ~4.3-fold, $pilT^{K136A}$
401 $pilU^{L199C}$ = ~6.5-fold, $pilU^{K134A}$ = ~1.5-fold, $pilT^{L201C}$ Δ*pilU* = ~1.7-fold) (**Figs 1B** and **2A**). This
402 revealed that altering the rates of these motor ATPases results in a corresponding reduction in
403 the rate of pilus retraction [43]. Additionally, despite this reduction in the speed of pilus
404 retraction, these mutants still transformed at levels that were comparable to the parent strain

405 (**Figs 1A** and **2B**). Thus, these results suggest that the absolute speed of competence pilus
406 retraction is not critical for DNA uptake during natural transformation. On the other hand, all
407 mutants that lack a functional retraction ATPase (Δ*pilT*, Δ*pilT*Δ*pilU*, *pilT*^{K136A} Δ*pilU*, *pilT*^{E204A}
408 Δ*pilU*, *pilT*$^{K136A/E204A}$ Δ*pilU*) showed a ~2-log reduction in the frequency of pilus retraction (**Fig**
409 **1C**). This revealed that functional retraction ATPases are crucial for generating high numbers of
410 retraction events, which may increase the likelihood of retracting a DNA-bound pilus. Further
411 experiments will focus on defining the parameters that are essential for DNA uptake.

412 Mutants that completely inactivated the retraction machinery (e.g. Δ*pilT*, Δ*pilT* Δ*pilU*, *pilT*^{K136A}
413 Δ*pilU*, *pilT*^{K136A} *pilU*^{K134A}) resulted in a hyperpiliated phenotype, lower transformation frequency
414 and a marked reduction in the frequency of pilus retraction (**Figs 1A, 1C-E**, **2A** and **2C**). These
415 strains, however, did display rare pilus retraction, which occurred at rates that were markedly
416 slower than the parent (>40-fold), and which was independent of PilT and PilU (**Figs 1B** and
417 **2A**). Recent work in *Neisseria* indicates that PilTU-independent retraction is not unique to the *V.*
418 *cholerae* type IVa competence pilus [34]. The mechanism underlying PilTU-independent
419 retraction remains unclear. One possibility is that an extension ATPase for another type IV pilus
420 system promotes this retraction. We have tested this in *V. cholerae* by mutating the extension
421 ATPases of the two other type IV pilus systems (MSHA and TCP) and found that PilTU-
422 independent retraction of the competence pilus still occurs in this background (**S5 Fig**). Thus,
423 suggesting that these other ATPases likely do not contribute to PilTU-independent retraction. It
424 remains possible that the competence pilus extension ATPase PilB supports PilTU-independent
425 retraction as suggested for the type IVc tad pili of *Caulobacter crescentus* where the same
426 ATPase bifunctionally promotes both pilus extension and retraction [43]. It is also possible that
427 PilTU-independent pilus retraction is due to an inherent instability of the pilus fiber. Uncovering
428 the mechanism underlying PilTU-independent retraction of the type IVa competence pilus [5] will
429 be the focus of future work.

430

431 # Materials and Methods

432

433 ## Bacterial strains and culture conditions

434 *Vibrio cholerae* and *A. baylyi* strains were routinely grown in LB Miller broth and on LB Miller
435 agar supplemented with erythromycin (10 µg/mL), kanamycin (50 µg/mL), and/or carbenicillin
436 (50 µg/mL) when appropriate.

437

438 ## Construction of mutant strains

439 All *V. cholerae* strains used throughout this study are derivatives of the El Tor isolate E7946. All
440 *A. baylyi* strains used were derivatives of strain ADP1 [44]. All mutant strains were constructed
441 via MuGENT and natural transformation using transforming DNA products made by splicing-by-
442 overlap extension (SOE) PCR exactly as previously described [45-48]. For a detailed list of all
443 mutant strains used throughout this study see **Table S1**. For a detailed list of all primers used to
444 construct mutant strains see **Table S2**.

445

446 ## Natural transformation assays

447 In order to induce competence in *V. cholerae* strains, the master competence regulator TfoX
448 was overexpressed using an IPTG-inducible or constitutive P_{tac} promoter and the cells were
449 genetically locked in a state of high cell density via deletion of *luxO* [46, 49-53]. Chitin-
450 independent transformation assays were performed exactly as previously described [47]. Briefly,
451 strains were grown overnight rolling at 30 ^{o}C with 100 μM IPTG then ~10^8 colony forming units
452 (CFU) were subcultured into 3mL of LB + 100 μM IPTG + 20 mM $MgCl_2$ + 10 mM $CaCl_2$ and
453 grown to late log. Next, ~10^8 CFU of this culture was diluted into instant ocean medium (7 g/L;
454 Aquarium Systems) supplemented with 100 μM IPTG and 500ng of transforming DNA was
455 added to each reaction and incubated statically at 30 ^{o}C overnight. The tDNA targeted VC1807,
456 a frame-shifted transposase, for deletion as previously described [45]. Negative control
457 reactions where no tDNA was added were also performed for each strain. After incubation with
458 tDNA, reactions were outgrown by adding 1mL of LB to each reaction and shaking (250 rpm) at
459 37 ^{o}C for ~2 hours. Reactions were then plated for quantitative culture onto medium selecting for
460 transformants (LB + 10 μg/mL Erythromycin) or onto plain LB for total viable counts. The
461 transformation frequency is defined as the number of transformants divided by the total viable
462 counts. For reactions where no transformants were obtained, a limit of detection was calculated
463 and plotted.

464 In order to sensitize natural transformation assays to differences in the efficiency of DNA
465 uptake, reactions were incubated with transforming DNA for shorter periods of time. These
466 assays were prepared exactly as described above, except that 10 units of DNase I (NEB) was

467 added to reactions 7 minutes after incubation with 500ng of transforming DNA. Reactions were
468 then incubated statically at 30°C overnight, outgrown, and plated exactly as described above.

469 For *A. baylyi*, transformations were performed exactly as previously described [54]. Briefly,
470 strains were grown overnight in LB medium. Then, ~10^8 cells were diluted into fresh LB
471 medium, and tDNA was added (~100 ng). Reactions were incubated at 30°C with agitation for 5
472 h and then plated for quantitative culture as described above to determine the transformation
473 frequency.

474

475 **Pilin labelling, imaging and quantification**

476 In order to label pili for observation with epifluorescence microscopy, strains were grown to the
477 late-log phase exactly as described above for natural transformation assays. Then, ~10^8 CFU
478 were spun down at 18,000 x g for 1 min and resuspended in instant ocean medium. Cells were
479 then incubated with 25 µg/mL AF488-mal for 15 minutes statically at room temperature in the
480 dark. Cells were washed twice using 100µL of instant ocean medium and resuspended to a final
481 concentration of ~10^7 CFU. Next, 2µL of these labeled cells were placed under an 0.2% gelzan
482 pad (made in instant ocean medium) on a coverslip and imaged on an inverted Nikon Ti-2
483 microscope with a Plan Apo ×60 objective, a green fluorescent protein filter cube, a Hamamatsu
484 ORCAFlash 4.0 camera and Nikon NIS Elements imaging software. In order to measure
485 retraction events, labelled cells were imaged by time-lapse microscopy in which a phase-
486 contrast (to image cell bodies) and fluorescent (to image labeled pili) image were taken every
487 second for 1-2 minutes or every 10 seconds for 10-15 minutes. Rates were calculated manually
488 using measurement tools in the NIS Elements analysis software. Only pili that were longer than
489 0.3 µm and completed retracting within the time-lapse window were analyzed.

490 In order to calculate the number of pili per cell, static images of cell bodies and labeled pili were
491 captured using phase-contrast and epifluorescence microscopy, respectively. Images from 3
492 independent biological replicates were sectioned into areas containing ~100-200 cells and the
493 total number of cells and the number of pili displayed on each cell was manually determined.
494 Representative images of the piliation state of strains were gathered and the lookup tables for
495 each phase or fluorescent image were adjusted to the same range.

496 In order to calculate the retraction frequency, time-lapse videos of cell bodies and labeled pili
497 were captured using phase-contrast and epifluorescence microscopy, respectively. Time-lapses

498 from 3 independent biological replicates were sectioned into areas containing ~300-1000 cells.
499 The number of cells that exhibited a pilus retraction event and the total number of cells in the
500 field was manually counted. This analysis was constrained to measuring pili that are greater
501 than 0.1 μM because shorter pili cannot be resolved by our pilus labeling approach.

502 To assess aggregation and pelleting of cultures, strains were grown to late log under the
503 conditions described above. Cultures were then allowed to sit statically at room temperature for
504 30-60 mins. Images of cultures were then taken against a white background.

505

506 **Protein expression and purification**

507 His tagged (6xHis) versions of PilT, PilT^{K136A}, PilU and PilU^{K134A} were cloned into a pHis
508 expression vector and verified by DNA sequencing (Eurofins). Vectors were transformed into *E.*
509 *coli* BL21 DE3 for expression and purification.

510 For purification of His-PilU and His-PilU^{K134A}, cells were grown in a 1L flask at 37°C with aeration
511 to an OD_{600} = 0.6. The culture was then induced by adding IPTG (1 mM) and grown to a final
512 OD_{600} = 4.0 at 30°C with aeration. Cells were harvested by centrifugation at 8,000 x g for 15 min
513 at room temperature and then resuspended in Buffer A [100 mM Tris pH 8.5, 300 mM KCl, 10%
514 glycerol, 20 mM Imidazole] and stored at -80°C. Pellets were thawed on ice and then lysozyme
515 (1 mg/mL) and DNase I (2 mg/L) were added before lysing via sonication with a probe tip
516 sonicator. The soluble fraction was clarified by centrifugation at 12,000 x g for 1 hour at 4°C.
517 The supernatant was loaded onto a nickel-charged HisTrap HP column (1mL; GE) using an
518 ÄKTA FPLC at room temperature. The column was then washed with Buffer A and the protein
519 was eluted with a gradient of Buffer B [100 mM Tris pH 8.5, 300 mM KCl, 10% glycerol, 500 mM
520 imidazole] and fractions were collected on ice. Elution fractions were separated on 15% SDS-
521 PAGE gels and stained with Coomassie Brilliant Blue R-250 (BioRad). Peak fractions were
522 pooled and dialyzed (Fisher, MWCO 12 kDa) into 500 mL Buffer C [100 mM Tris pH 8.5, 300
523 mM KCl, 10% glycerol] overnight, on a stir plate at 4°C. Then a second round of dialysis was
524 performed using 500 mL Buffer C for 4-6 hours, on a stir plate at 4°C. Following dialysis, the
525 protein concentration was determined using a Bradford Assay and aliquots were stored at -80C.

526 For purification of His-PilT and His-PilT^{K136A}, cells were grown in a 1L flask at 37°C with aeration
527 to an OD_{600} = 0.6. The culture was then induced by adding IPTG (1 mM) and grown overnight at
528 22°C with aeration. Cells were harvested by centrifugation at 8,000 x g for 15min at room

529 temperature and then resuspended in Buffer A [25 mM Tris pH 8.5, 300 mM KCl, 10% glycerol,
530 1 mM EDTA, 1 mM $MgCl_2$, 5 mM β-mercaptoethanol, 20 mM Imidazole] and stored at -80°C.
531 Pellets were thawed on ice and lysozyme (1 mg/mL), DNase I (2 mg/L) and PMSF (1 mM) were
532 added before lysing via sonication with a probe tip sonicator. The soluble fraction was clarified
533 by centrifugation at 12,000 x g for 1 hour at 4°C. The supernatant was loaded onto a nickel-
534 charged HisTrap HP column (1 mL; GE) using an ÄKTA FPLC at room temperature. The
535 column was then washed with Buffer A and the protein was eluted with a gradient of Buffer B
536 [25 mM Tris pH 8.5, 300 mM KCl, 10% glycerol, 1 mM EDTA, 1 mM $MgCl_2$, 5 mM β-
537 mercaptoethanol, 500 mM Imidazole] and fractions were collected on ice. Elution fractions were
538 separated on 15% SDS-PAGE gels and stained with Coomassie Brilliant Blue R-250 (BioRad).
539 Peak fractions were pooled and dialyzed (Fisher, MWCO 12 kDa) into 500 mL Buffer C [25 mM
540 Tris pH 8.5, 50 mM KCl, 10% glycerol, 1 mM EDTA, 1 mM $MgCl_2$, 0.5mM TCEP] overnight, on a
541 stir plate at 4°C. The next day, the eluate was concentrated with an Amicon conical filter
542 (MWCO 30 kDa) at 4,000 x g for 15 min at 4°C and resuspended to the original volume in Buffer
543 C twice. The protein concentration was determined using a Bradford Assay and then aliquots of
544 protein were snap-frozen with liquid nitrogen and stored at -80C.

545

546 **Bacterial Adenylate Cyclase Two-hybrid (BACTH) Assays**

547 The Bacterial Adenylate Cyclase Two-Hybrid (BACTH) system was employed to study protein
548 interactions. Gene inserts were amplified by PCR and cloned into pUT18C ($Carb^{R}$) and pKT25
549 (Kan^{R}) vectors to generate N-terminal fusions to the T18 and T25 fragments of adenylate
550 cyclase, respectively. Miniprepped vectors (Qiagen plasmid miniprep kit) were then
551 cotransformed into *E. coli* BTH101 and outgrown with 500 µL LB for 1 hour at 37°C with
552 shaking. Transformations were isolation streak plated on LB plates containing kanamycin 50
553 µg/mL and carbenicillin 100 µg/mL to select for transformants that had received both plasmids.
554 Strains were then grown statically at 30°C from frozen stocks overnight in LB supplemented with
555 kanamycin 50 µg/mL and carbenicillin 100 µg/mL and 3.5µL of each strain was then spotted
556 onto LB plates containing kanamycin 50 µg/mL, carbenicillin 100µg/mL, 0.5 mM IPTG and 40
557 µg/mL X-gal and incubated at 30°C for 48 hours.

558

559 **BACTH Miller Assays**

560 For BACTH Miller assays strains were prepared by growing the BTH101 strains with the
561 indicated pUT18C and pKT25 vectors statically overnight at 30°C in LB supplemented with
562 kanamycin 50 µg/mL and carbenicillin 100 µg/mL. Then 5 µL of this overnight culture was
563 subcultured into 3mL of LB supplemented with kanamycin 50 µg/mL, carbenicillin 100µg/mL and
564 0.5 mM IPTG and grown rolling at 30°C overnight. Cultures were then pelleted and resuspended
565 in 1 mL of Z buffer [60 mM Na_2HPO_4-$7H_2O$, 40 mM NaH_2PO_4-H_2O, 10 mM KCl, 2 mM $MgSO_4$-
566 $7H_2O$] to an OD_{600} = 0.5. 50µL of 1% SDS was added to each reaction and vortexed. 100µL of
567 chloroform was added to each reaction, vortexed again and then centrifuged for 1 min at 18,000
568 x g. The aqueous fraction was then mixed with ONPG (2.5 mg/mL) in a 96-well plate and the
569 OD_{420} and OD_{550} were measured every 5 minutes for 10 hours. Miller units were then calculated
570 at the time (in mins) when the A_{420} reached 0.3 or at 10 hours using the formula: [1000*(A_{420}-
571 (1.75*A_{550}))/ (mins*0.2 mL*A_{600})].

572

573 **Western Blotting**

574 Strains were grown to mid-log phase in LB with 100 µM IPTG if applicable and then
575 resuspended to an OD_{600} = 100 in TBS containing 1 mM PMSF. Cells were then lysed using a
576 FastPrep-24 (MP Bio). Lysates were centrifuged at 16,000 x g for 10 min at 4°C, and the
577 supernatant was then mixed 1:1 with 2X SDS sample buffer [220 mM Tris pH 6.8, 25% glycerol,
578 1.8% SDS, 0.02% Bromophenol Blue, 5% β-mercaptoethanol] and then 2uL of each sample
579 was separated on a 15% SDS PAGE gel. Proteins were transferred to a PVDF membrane and
580 incubated with one of the following primary antibodies: α-FLAG polyclonal rabbit (Sigma) or α-
581 RpoA monoclonal mouse (Biolegend). Then, blots were washed and incubated with a α-rabbit
582 or α-mouse secondary antibodies conjugated to IRdye 800CW. Blots were then imaged using
583 an Odyssey classic LI-COR system.

584

585 **Negative-stain electron microscopy**

586 Negative stain specimens were prepared by applying 4 µL of protein solution (0.1 mg/mL + 1
587 mM AMP-PnP) onto a glow-discharged 300-mesh copper grid coated with continuous carbon
588 film (EMS). After 30 s the protein solution was blotted with a piece of filter paper. The grid was
589 washed with 4 µL of milli-Q water and stained with 4 µL of stain solution (1% (w/v) uranyl
590 acetate, 0.5% (w/v) trehalose). The excess stain solution was removed by filter paper and the
591 grid was left to air dry. Due to the availability of the instrument, we used two different

592 transmission electron microscopes for data collection. For PilU, the data were collected on a
593 300-kV JEM-3200FS TEM equipped with FEG source and 8k x 8k Direct Electron DE-64
594 camera. A total of 32 micrograph images were taken at a nominal magnification of 60,000x,
595 which is equivalent to 1.56 Å per pixel. For PilT, the data were collected on a 120-kV JEM-
596 1400plus TEM equipped with LaB_6 source and a Gatan Oneview camera. A total of 59 images
597 were taken at a nominal magnification of 60,000x and the pixel size is 1.94 Å. To avoid potential
598 beam induced damage, minimum dose system was employed during data collection. Note that
599 PilU data were collected on a direct electron detector; therefore, each image contains 50 frames
600 and the frame alignment was performed using unblur program with exposure filter applied.
601 Particle picking, defocus estimation and phase flipped particles were all done using EMAN2
602 software package [55]. These particles were then imported into RELION (v3.0.7) for 2D
603 classification, Initial model building, 3D refinement, and 3D classification [56]. From 2D
604 classification results, we observed clear hexameric density organization [7, 57]. No symmetry
605 was applied for subsequent 3D refinement and 3D classification. The final 3D reconstructions
606 were computed from 45204 particles to 16.6 Å for PilU and 17472 particles to 20.8 Å for PilT.
607 The resolution estimation was calculated using gold-standard method at Fourier shell correlation
608 of 0.143 as implemented in RELION. The 3D reconstructions were rendered using UCSF
609 Chimera where the handedness of PilU was chosen to be consistent with PilT [58]. The
610 negative stain 3D reconstruction of PilU and PilT have been deposited into EMDB (ID: EMD-
611 20757, EMD-20758 respectively).
612

613 **Micropillar retraction assay**

614 To ensure that all measurements recorded were due to type IV competence pili, all the
615 experiments were performed with *V. cholerae* strains lacking all external appendages other than
616 type IV competence pili as well as exopolysaccharide production (i.e. mutants lacking flagella,
617 MSHA pili, TCP pili and *Vibrio* polysaccharide (VPS) production). Strains were grown overnight
618 in LB either directly from frozen stocks or from a single colony from an LB agar plate. Of the
619 overnight liquid culture, 50 µl was subcultured into 3 ml LB + 100 µM IPTG + 20 mM $MgCl_2$ + 10
620 mM $CaCl_2$ and allowed to grow at 30°C for 4h. Then, 100 µl of this culture was centrifuged for 5
621 min at 20,000 x *g* and the bacteria were resuspended in instant ocean medium. At different
622 times, 23 µl of the resuspension were added to micropillars in an observation chamber as
623 previously reported [15]. Briefly, silica molds were inverted on activated coverslips with
624 polyacrylamide gels in between. The result is an array of flexible micropillars in a hexagonal

array of 3 μm × 3 μm.Once the bacteria were in contact with the micropillars, 10-Hz movies of the top of the pillars were recorded. The motion of the tips of the pillars was tracked using a cross-correlation algorithm in ImageJ. The amplitude and speeds of the pillars' motions were then analyzed using MATLAB. Finally, we calibrated the pillars' stiffness constant using optical tweezers as previously described [33]. The pillars used in this study have a stiffness constant of 17±4pNμm−1.

Statistics

Statistical differences were assessed by one-way ANOVA tests followed by a multiple comparisons post test (either Tukey's or Dunnett's) using GraphPad Prism software. For all transformation frequency experiments and frequency of pilus retraction experiments, statistical analyses were performed on log transformed data. All means and statistical comparisons can be found in **S3** and **S4 Tables**.

Acknowledgements

We would like to thank CK Ellison for helpful discussions. We would like to acknowledge JD Newman and CE Dann III for their advice during protein purification. We thank JC van Kessel for providing strains associated with BACTH assays. We would like to thank L Khosla and V Deopersaud for technical assistance with micropillar experiments. We also thank JA Lorah for assistance with statistical analyses.

References

1. Burrows LL. Pseudomonas aeruginosa twitching motility: type IV pili in action. Annu Rev Microbiol. 2012;66:493-520. Epub 2012/07/04. doi: 10.1146/annurev-micro-092611-150055. PubMed PMID: 22746331.

2. Maier B, Wong GCL. How Bacteria Use Type IV Pili Machinery on Surfaces. Trends Microbiol. 2015;23(12):775-88. doi: 10.1016/j.tim.2015.09.002. PubMed PMID: 26497940.

652 3. Hospenthal MK, Costa TRD, Waksman G. A comprehensive guide to pilus biogenesis in Gram-
653 negative bacteria. Nat Rev Microbiol. 2017;15(6):365-79. Epub 2017/05/13. doi:
654 10.1038/nrmicro.2017.40. PubMed PMID: 28496159.
655 4. Proft T, Baker EN. Pili in Gram-negative and Gram-positive bacteria - structure, assembly and
656 their role in disease. Cell Mol Life Sci. 2009;66(4):613-35. Epub 2008/10/28. doi: 10.1007/s00018-008-
657 8477-4. PubMed PMID: 18953686.
658 5. Craig L, Forest KT, Maier B. Type IV pili: dynamics, biophysics and functional consequences. Nat
659 Rev Microbiol. 2019. Epub 2019/04/17. doi: 10.1038/s41579-019-0195-4. PubMed PMID: 30988511.
660 6. Craig L, Pique ME, Tainer JA. Type IV pilus structure and bacterial pathogenicity. Nat Rev
661 Microbiol. 2004;2(5):363-78. doi: 10.1038/nrmicro885. PubMed PMID: 15100690.
662 7. McCallum M, Tammam S, Khan A, Burrows LL, Howell PL. The molecular mechanism of the type
663 IVa pilus motors. Nat Commun. 2017;8:15091. doi: 10.1038/ncomms15091. PubMed PMID: 28474682;
664 PubMed Central PMCID: PMCPMC5424180.
665 8. Bischof LF, Friedrich C, Harms A, Sogaard-Andersen L, van der Does C. The Type IV Pilus
666 Assembly ATPase PilB of Myxococcus xanthus Interacts with the Inner Membrane Platform Protein PilC
667 and the Nucleotide-binding Protein PilM. J Biol Chem. 2016;291(13):6946-57. doi:
668 10.1074/jbc.M115.701284. PubMed PMID: 26851283; PubMed Central PMCID: PMCPMC4807279.
669 9. Chang YW, Rettberg LA, Treuner-Lange A, Iwasa J, Sogaard-Andersen L, Jensen GJ. Architecture
670 of the type IVa pilus machine. Science. 2016;351(6278):aad2001. doi: 10.1126/science.aad2001.
671 PubMed PMID: 26965631; PubMed Central PMCID: PMCPMC5929464.
672 10. Chiang P, Habash M, Burrows LL. Disparate subcellular localization patterns of Pseudomonas
673 aeruginosa Type IV pilus ATPases involved in twitching motility. J Bacteriol. 2005;187(3):829-39. doi:
674 10.1128/JB.187.3.829-839.2005. PubMed PMID: 15659660; PubMed Central PMCID: PMCPMC545728.
675 11. Craig L, Volkmann N, Arvai AS, Pique ME, Yeager M, Egelman EH, et al. Type IV pilus structure by
676 cryo-electron microscopy and crystallography: implications for pilus assembly and functions. Mol Cell.
677 2006;23(5):651-62. doi: 10.1016/j.molcel.2006.07.004. PubMed PMID: 16949362.
678 12. Jakovljevic V, Leonardy S, Hoppert M, Sogaard-Andersen L. PilB and PilT are ATPases acting
679 antagonistically in type IV pilus function in Myxococcus xanthus. J Bacteriol. 2008;190(7):2411-21. doi:
680 10.1128/JB.01793-07. PubMed PMID: 18223089; PubMed Central PMCID: PMCPMC2293208.
681 13. Whitchurch CB, Mattick JS. Characterization of a gene, pilU, required for twitching motility but
682 not phage sensitivity in Pseudomonas aeruginosa. Mol Microbiol. 1994;13(6):1079-91. Epub
683 1994/09/01. PubMed PMID: 7854122.

684 14. Blair KM, Turner L, Winkelman JT, Berg HC, Kearns DB. A molecular clutch disables flagella in the
685 Bacillus subtilis biofilm. Science. 2008;320(5883):1636-8. Epub 2008/06/21. doi:
686 10.1126/science.1157877. PubMed PMID: 18566286.
687 15. Ellison CK, Kan J, Dillard RS, Kysela DT, Ducret A, Berne C, et al. Obstruction of pilus retraction
688 stimulates bacterial surface sensing. Science. 2017;358(6362):535-8. Epub 2017/10/28. doi:
689 10.1126/science.aan5706. PubMed PMID: 29074778; PubMed Central PMCID: PMCPMC5805138.
690 16. Ellison CK, Dalia TN, Dalia AB, Brun YV. Real-time microscopy and physical perturbation of
691 bacterial pili using maleimide-conjugated molecules. Nat Protoc. 2019. doi: 10.1038/s41596-019-0162-6.
692 PubMed PMID: 31028374.
693 17. Adams DW, Stutzmann S, Stoudmann C, Blokesch M. DNA-uptake pili of Vibrio cholerae are
694 required for chitin colonization and capable of kin recognition via sequence-specific self-interaction. Nat
695 Microbiol. 2019. doi: 10.1038/s41564-019-0479-5. PubMed PMID: 31182799.
696 18. Ellison CK, Dalia TN, Vidal Ceballos A, Wang JC, Biais N, Brun YV, et al. Retraction of DNA-bound
697 type IV competence pili initiates DNA uptake during natural transformation in Vibrio cholerae. Nat
698 Microbiol. 2018;3(7):773-80. Epub 2018/06/13. doi: 10.1038/s41564-018-0174-y. PubMed PMID:
699 29891864.
700 19. Seitz P, Blokesch M. DNA-uptake machinery of naturally competent Vibrio cholerae. Proc Natl
701 Acad Sci U S A. 2013;110(44):17987-92. Epub 2013/10/16. doi: 10.1073/pnas.1315647110. PubMed
702 PMID: 24127573; PubMed Central PMCID: PMCPMC3816411.
703 20. Bieber D, Ramer SW, Wu CY, Murray WJ, Tobe T, Fernandez R, et al. Type IV pili, transient
704 bacterial aggregates, and virulence of enteropathogenic Escherichia coli. Science. 1998;280(5372):2114-
705 8. PubMed PMID: 9641917.
706 21. Chamot-Rooke J, Mikaty G, Malosse C, Soyer M, Dumont A, Gault J, et al. Posttranslational
707 modification of pili upon cell contact triggers N. meningitidis dissemination. Science.
708 2011;331(6018):778-82. doi: 10.1126/science.1200729. PubMed PMID: 21311024.
709 22. Helaine S, Carbonnelle E, Prouvensier L, Beretti JL, Nassif X, Pelicic V. PilX, a pilus-associated
710 protein essential for bacterial aggregation, is a key to pilus-facilitated attachment of Neisseria
711 meningitidis to human cells. Mol Microbiol. 2005;55(1):65-77. doi: 10.1111/j.1365-2958.2004.04372.x.
712 PubMed PMID: 15612917.
713 23. Dietrich M, Mollenkopf H, So M, Friedrich A. Pilin regulation in the pilT mutant of Neisseria
714 gonorrhoeae strain MS11. FEMS Microbiol Lett. 2009;296(2):248-56. doi: 10.1111/j.1574-
715 6968.2009.01647.x. PubMed PMID: 19486161; PubMed Central PMCID: PMCPMC4428587.

716 24. Merz AJ, So M, Sheetz MP. Pilus retraction powers bacterial twitching motility. Nature.
717 2000;407(6800):98-102. doi: 10.1038/35024105. PubMed PMID: 10993081.
718 25. Pujol C, Eugene E, Marceau M, Nassif X. The meningococcal PilT protein is required for induction
719 of intimate attachment to epithelial cells following pilus-mediated adhesion. Proc Natl Acad Sci U S A.
720 1999;96(7):4017-22. PubMed PMID: 10097155; PubMed Central PMCID: PMCPMC22412.
721 26. Hockenberry AM, Hutchens DM, Agellon A, So M. Attenuation of the Type IV Pilus Retraction
722 Motor Influences Neisseria gonorrhoeae Social and Infection Behavior. MBio. 2016;7(6). doi:
723 10.1128/mBio.01994-16. PubMed PMID: 27923924; PubMed Central PMCID: PMCPMC5142622.
724 27. Wolfgang M, Lauer P, Park HS, Brossay L, Hebert J, Koomey M. PilT mutations lead to
725 simultaneous defects in competence for natural transformation and twitching motility in piliated
726 Neisseria gonorrhoeae. Mol Microbiol. 1998;29(1):321-30. PubMed PMID: 9701824.
727 28. Leighton TL, Dayalani N, Sampaleanu LM, Howell PL, Burrows LL. Novel Role for PilNO in Type IV
728 Pilus Retraction Revealed by Alignment Subcomplex Mutations. J Bacteriol. 2015;197(13):2229-38. doi:
729 10.1128/JB.00220-15. PubMed PMID: 25917913; PubMed Central PMCID: PMCPMC4455263.
730 29. Aukema KG, Kron EM, Herdendorf TJ, Forest KT. Functional dissection of a conserved motif
731 within the pilus retraction protein PilT. J Bacteriol. 2005;187(2):611-8. doi: 10.1128/JB.187.2.611-
732 618.2005. PubMed PMID: 15629932; PubMed Central PMCID: PMCPMC543540.
733 30. Hanson PI, Whiteheart SW. AAA+ proteins: have engine, will work. Nat Rev Mol Cell Biol.
734 2005;6(7):519-29. doi: 10.1038/nrm1684. PubMed PMID: 16072036.
735 31. McCallum M, Benlekbir S, Nguyen S, Tammam S, Rubinstein JL, Burrows LL, et al. Multiple
736 conformations facilitate PilT function in the type IV pilus. bioRxiv. 2019. doi:
737 https://doi.org/10.1101/672212.
738 32. Tala L, Fineberg A, Kukura P, Persat A. Pseudomonas aeruginosa orchestrates twitching motility
739 by sequential control of type IV pili movements. Nat Microbiol. 2019. Epub 2019/02/26. doi:
740 10.1038/s41564-019-0378-9. PubMed PMID: 30804544.
741 33. Biais N, Higashi D, So M, Ladoux B. Techniques to measure pilus retraction forces. Methods Mol
742 Biol. 2012;799:197-216. doi: 10.1007/978-1-61779-346-2_13. PubMed PMID: 21993648; PubMed
743 Central PMCID: PMCPMC5160128.
744 34. Zollner R, Cronenberg T, Maier B. Motor properties of PilT-independent type 4 pilus retraction in
745 gonococci. J Bacteriol. 2019. doi: 10.1128/JB.00778-18. PubMed PMID: 30692169.
746 35. Georgiadou M, Castagnini M, Karimova G, Ladant D, Pelicic V. Large-scale study of the
747 interactions between proteins involved in type IV pilus biology in Neisseria meningitidis: characterization

748 of a subcomplex involved in pilus assembly. Mol Microbiol. 2012;84(5):857-73. doi: 10.1111/j.1365-
749 2958.2012.08062.x. PubMed PMID: 22486968.
750 36. Karimova G, Pidoux J, Ullmann A, Ladant D. A bacterial two-hybrid system based on a
751 reconstituted signal transduction pathway. Proc Natl Acad Sci U S A. 1998;95(10):5752-6. Epub
752 1998/05/20. PubMed PMID: 9576956; PubMed Central PMCID: PMCPMC20451.
753 37. McCallum M, Tammam S, Little DJ, Robinson H, Koo J, Shah M, et al. PilN Binding Modulates the
754 Structure and Binding Partners of the Pseudomonas aeruginosa Type IVa Pilus Protein PilM. J Biol Chem.
755 2016;291(21):11003-15. doi: 10.1074/jbc.M116.718353. PubMed PMID: 27022027; PubMed Central
756 PMCID: PMCPMC4900251.
757 38. Forest KT, Satyshur KA, Worzalla GA, Hansen JK, Herdendorf TJ. The pilus-retraction protein PilT:
758 ultrastructure of the biological assembly. Acta Crystallogr D Biol Crystallogr. 2004;60(Pt 5):978-82. Epub
759 2004/04/23. doi: 10.1107/S0907444904006055. PubMed PMID: 15103158.
760 39. Jones CJ, Utada A, Davis KR, Thongsomboon W, Zamorano Sanchez D, Banakar V, et al. C-di-GMP
761 Regulates Motile to Sessile Transition by Modulating MshA Pili Biogenesis and Near-Surface Motility
762 Behavior in Vibrio cholerae. PLoS Pathog. 2015;11(10):e1005068. doi: 10.1371/journal.ppat.1005068.
763 PubMed PMID: 26505896; PubMed Central PMCID: PMCPMC4624765.
764 40. Takhar HK, Kemp K, Kim M, Howell PL, Burrows LL. The platform protein is essential for type IV
765 pilus biogenesis. J Biol Chem. 2013;288(14):9721-8. doi: 10.1074/jbc.M113.453506. PubMed PMID:
766 23413032; PubMed Central PMCID: PMCPMC3617274.
767 41. Adams DW, Pereira JM, Stoudmann C, Stutzmann S, Blokesch M. The type IV pilus protein PilU
768 functions as a PilT-dependent retraction ATPase. PLoS Genet. 2019;15(9):e1008393. doi:
769 10.1371/journal.pgen.1008393. PubMed PMID: 31525185.
770 42. Chiang P, Sampaleanu LM, Ayers M, Pahuta M, Howell PL, Burrows LL. Functional role of
771 conserved residues in the characteristic secretion NTPase motifs of the Pseudomonas aeruginosa type IV
772 pilus motor proteins PilB, PilT and PilU. Microbiology. 2008;154(Pt 1):114-26. doi:
773 10.1099/mic.0.2007/011320-0. PubMed PMID: 18174131.
774 43. Ellison CK, Kan J, Chlebek JL, Hummels KR, Panis G, Viollier PH, et al. A bifunctional ATPase drives
775 tad pilus extension and retraction. bioRxiv. 2019:616128. doi: 10.1101/616128.
776 44. Juni E, Janik A. Transformation of Acinetobacter calco-aceticus (Bacterium anitratum). J
777 Bacteriol. 1969;98(1):281-8. PubMed PMID: 5781579; PubMed Central PMCID: PMCPMC249934.

778 45. Dalia AB. Natural Cotransformation and Multiplex Genome Editing by Natural Transformation
779 (MuGENT) of Vibrio cholerae. Methods Mol Biol. 2018;1839:53-64. Epub 2018/07/27. doi: 10.1007/978-
780 1-4939-8685-9_6. PubMed PMID: 30047054.
781 46. Dalia AB, McDonough E, Camilli A. Multiplex genome editing by natural transformation. Proc
782 Natl Acad Sci U S A. 2014;111(24):8937-42. Epub 2014/06/04. doi: 10.1073/pnas.1406478111. PubMed
783 PMID: 24889608; PubMed Central PMCID: PMCPMC4066482.
784 47. Dalia TN, Yoon SH, Galli E, Barre FX, Waters CM, Dalia AB. Enhancing multiplex genome editing
785 by natural transformation (MuGENT) via inactivation of ssDNA exonucleases. Nucleic Acids Res.
786 2017;45(12):7527-37. Epub 2017/06/03. doi: 10.1093/nar/gkx496. PubMed PMID: 28575400; PubMed
787 Central PMCID: PMCPMC5499599.
788 48. Dalia AB, Lazinski DW, Camilli A. Characterization of undermethylated sites in Vibrio cholerae. J
789 Bacteriol. 2013;195(10):2389-99. Epub 2013/03/19. doi: 10.1128/JB.02112-12. PubMed PMID:
790 23504020; PubMed Central PMCID: PMCPMC3650525.
791 49. Zhu J, Miller MB, Vance RE, Dziejman M, Bassler BL, Mekalanos JJ. Quorum-sensing regulators
792 control virulence gene expression in Vibrio cholerae. Proc Natl Acad Sci U S A. 2002;99(5):3129-34. doi:
793 10.1073/pnas.052694299. PubMed PMID: 11854465; PubMed Central PMCID: PMCPMC122484.
794 50. Lo Scrudato M, Blokesch M. The regulatory network of natural competence and transformation
795 of Vibrio cholerae. PLoS Genet. 2012;8(6):e1002778. doi: 10.1371/journal.pgen.1002778. PubMed
796 PMID: 22737089; PubMed Central PMCID: PMCPMC3380833.
797 51. Lo Scrudato M, Blokesch M. A transcriptional regulator linking quorum sensing and chitin
798 induction to render Vibrio cholerae naturally transformable. Nucleic Acids Res. 2013;41(6):3644-58. doi:
799 10.1093/nar/gkt041. PubMed PMID: 23382174; PubMed Central PMCID: PMCPMC3616704.
800 52. Meibom KL, Blokesch M, Dolganov NA, Wu CY, Schoolnik GK. Chitin induces natural competence
801 in Vibrio cholerae. Science. 2005;310(5755):1824-7. doi: 10.1126/science.1120096. PubMed PMID:
802 16357262.
803 53. Dalia AB, Lazinski DW, Camilli A. Identification of a membrane-bound transcriptional regulator
804 that links chitin and natural competence in Vibrio cholerae. MBio. 2014;5(1):e01028-13. Epub
805 2014/01/30. doi: 10.1128/mBio.01028-13. PubMed PMID: 24473132; PubMed Central PMCID:
806 PMCPMC3903286.
807 54. Nero TM, Dalia TN, Wang JC, Kysela DT, Bochman ML, Dalia AB. ComM is a hexameric helicase
808 that promotes branch migration during natural transformation in diverse Gram-negative species. Nucleic

809 Acids Res. 2018;46(12):6099-111. Epub 2018/05/04. doi: 10.1093/nar/gky343. PubMed PMID:
810 29722872; PubMed Central PMCID: PMCPMC6158740.
811 55. Ludtke SJ. Single-Particle Refinement and Variability Analysis in EMAN2.1. Methods Enzymol.
812 2016;579:159-89. Epub 2016/08/31. doi: 10.1016/bs.mie.2016.05.001. PubMed PMID: 27572727;
813 PubMed Central PMCID: PMCPMC5101015.
814 56. Scheres SH. Semi-automated selection of cryo-EM particles in RELION-1.3. J Struct Biol.
815 2015;189(2):114-22. Epub 2014/12/09. doi: 10.1016/j.jsb.2014.11.010. PubMed PMID: 25486611;
816 PubMed Central PMCID: PMCPMC4318617.
817 57. Satyshur KA, Worzalla GA, Meyer LS, Heiniger EK, Aukema KG, Misic AM, et al. Crystal structures
818 of the pilus retraction motor PilT suggest large domain movements and subunit cooperation drive
819 motility. Structure. 2007;15(3):363-76. doi: 10.1016/j.str.2007.01.018. PubMed PMID: 17355871;
820 PubMed Central PMCID: PMCPMC1978094.
821 58. Pettersen EF, Goddard TD, Huang CC, Couch GS, Greenblatt DM, Meng EC, et al. UCSF Chimera--
822 a visualization system for exploratory research and analysis. J Comput Chem. 2004;25(13):1605-12. Epub
823 2004/07/21. doi: 10.1002/jcc.20084. PubMed PMID: 15264254.

824

825

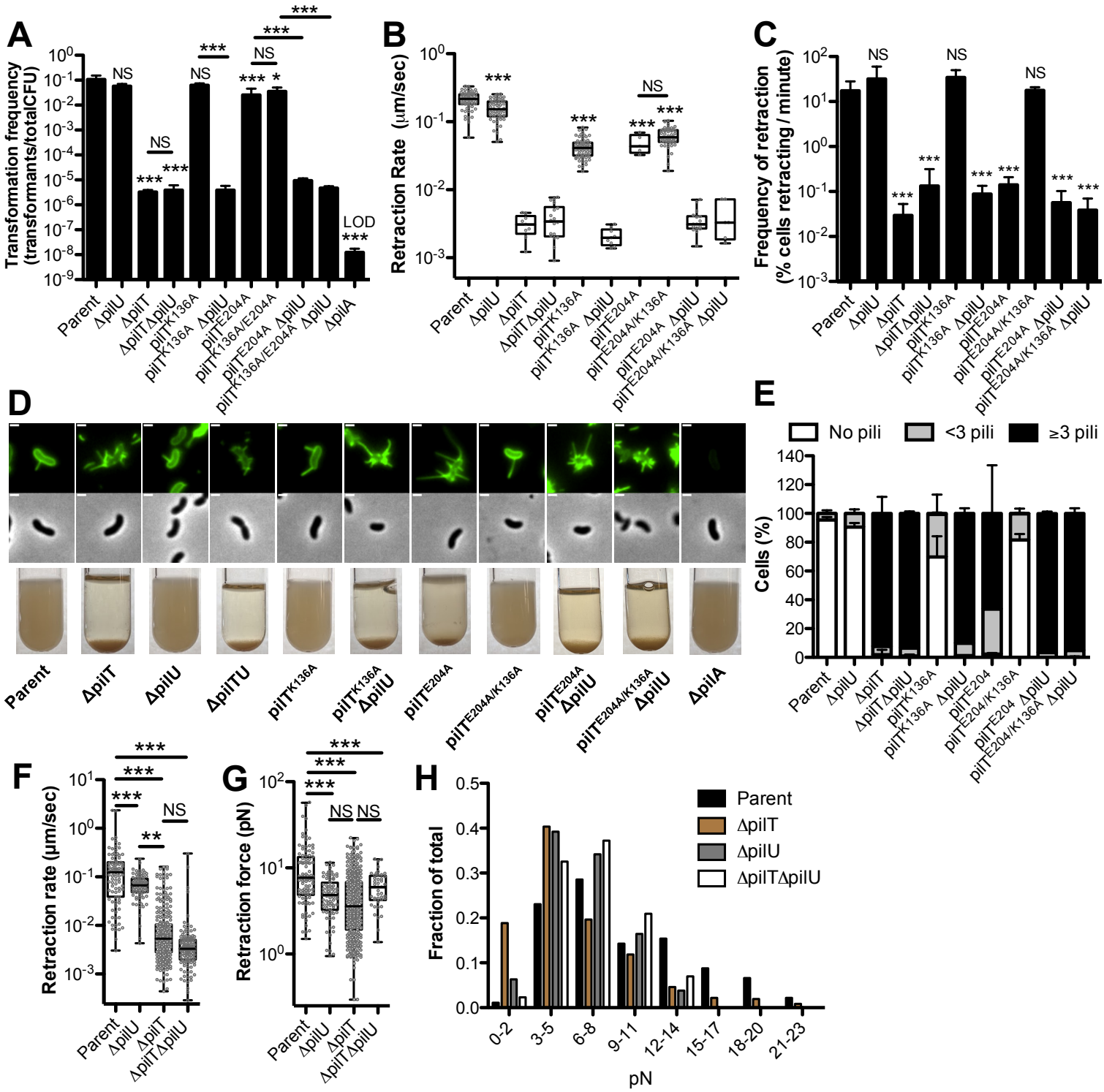

Fig 1. PilU mediates type IVa competence pilus retraction in a PilT-dependent manner in *V. cholerae*. (A) Natural transformation assays of the indicated strains. Reactions were incubated with 500 ng of transforming DNA overnight. Transformation frequency is reported as the fraction of cells that were transformed in each reaction (i.e. the number of transformants / total viable counts). Parent, n = 11, all other strains, n = 4. **(B)** Retraction rates of the indicated strains measured by epifluorescence time-lapse microscopy of AF488-mal labeled cells. Data are from three independent biological replicates; Parent, n = 68. Δ*pilU*, n = 56. Δ*pilT*, n = 9. Δ*pilT*Δ*pilU*, n = 18. *pilT*^{K136A}, n = 66. *pilT*^{K136A}Δ*pilU*, n = 9. *pilT*^{E204A}, n = 5. *pilT*$^{E204A/K136A}$, n = 50. *pilT*^{E204A} Δ*pilU*, n = 17. *pilT*$^{E204A/K136A}$ Δ*pilU*, n = 6. **(C)** Frequency of retraction of the indicated strains measured by counting number of cells that exhibit a retraction event over a given time-lapse. Data are from three independent biological replicates; Parent, n = 1141. Δ*pilU*, n = 824. Δ*pilT*, n = 6681. Δ*pilT*Δ*pilU*, n = 3806. *pilT*^{K136A}, n = 1048. *pilT*^{K136A}Δ*pilU*, n = 997. *pilT*^{E204A}, n = 4311. *pilT*$^{E204A/K136A}$, n = 866. *pilT*^{E204A} Δ*pilU*, n = 7243. *pilT*$^{E204A/K136A}$ Δ*pilU*, n = 6216. **(D)** Representative images of surface piliation (top) and aggregation phenotypes (bottom) for the indicated strains. Scale bar, 1 μm. **(E)** The percentage of cells with 0, <3 or ≥3 surface pili was determined from a static image. Data are from three independent biological replicates; Parent, n = 453. Δ*pilU*, n = 413. Δ*pilT*, n = 381. Δ*pilT*Δ*pilU*, n = 425. *pilT*^{K136A}, n = 417. *pilT*^{K136A} Δ*pilU*, n = 413. *pilT*^{E204A}, n = 579. *pilT*$^{E204A/K136A}$, n = 713. *pilT*^{E204A} Δ*pilU*, n = 806. *pilT*$^{E204A/K136A}$ Δ*pilU*, n = 705. **(F)** Retraction rate (Parent, n = 95. Δ*pilU*, n = 83. Δ*pilT*, n = 324. Δ*pilT* Δ*pilU*, n = 125) and the **(G)** Box plot and **(H)** Histogram of the retraction force (Parent, n = 101. Δ*pilU*, n = 90. Δ*pilT*, n = 372. Δ*pilT* Δ*pilU*, n = 43) was measured via micropillar assays. All bar graphs are shown as the mean ± SD. All Box plots represent the median and the upper and lower quartile, while the whiskers demarcate the range. Asterisk(s) directly above bars denote comparisons to the parent strain. All comparisons were made by one-way ANOVA with Tukey's post test. LOD, limit of detection; NS, not significant; ** = P < 0.01, *** = P < 0.001.

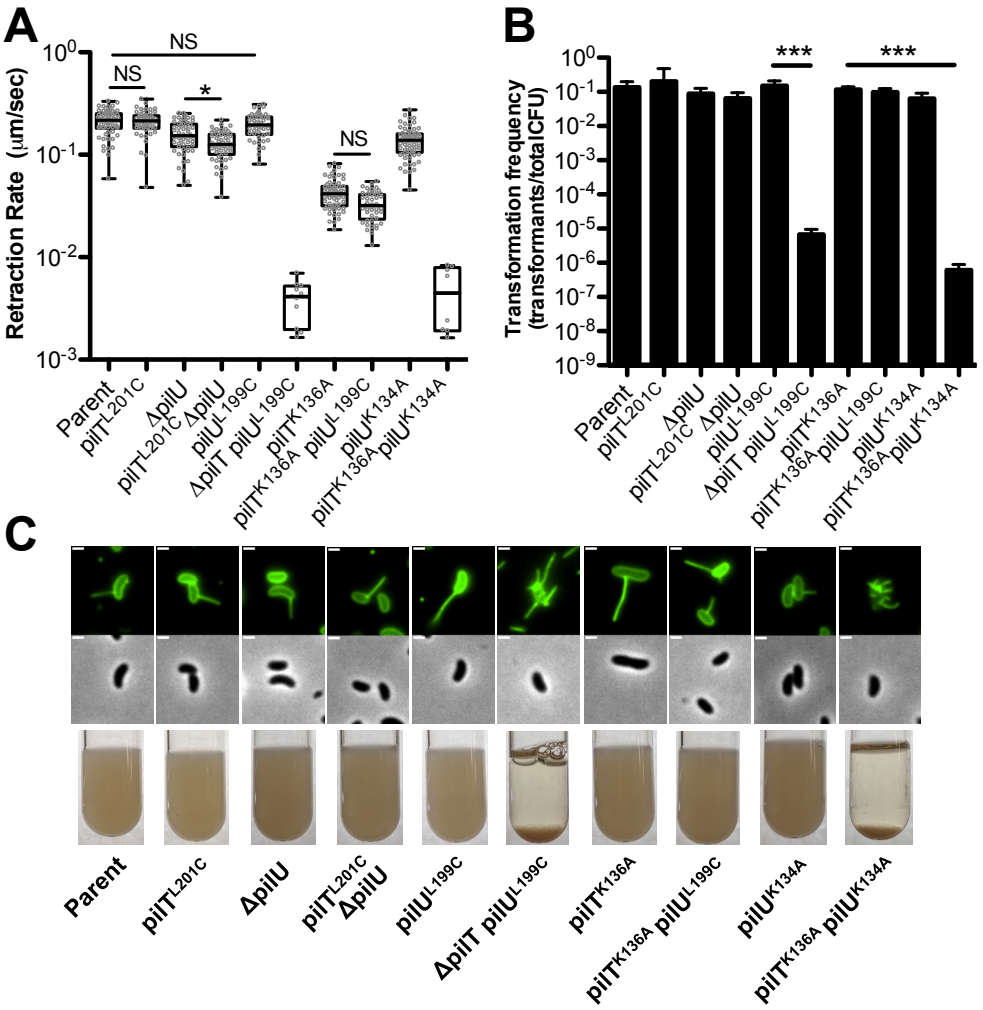

Fig 2. The ATPase activity of PilT and PilU mediate pilus retraction. (A) Retraction rates of the indicated strains measured by epifluorescence time-lapse microscopy of AF488-mal labeled cells. Box plots represent the median and the upper and lower quartile, while the whiskers demarcate the range. Data are from three independent biological replicates; *pilU*^{K134A}, *n* = 70. *pilT*^{K136A} *pilU*^{K134A}, *n* = 8. *pilT*^{K136A} *pilU*^{L199C}, *n* = 46. *pilU*^{L199C}, *n* = 49. *pilT*^{L201C}, *n* = 54. *pilT*^{L201C} Δ*pilU*, *n* = 54. Δ*pilT pilU*^{L199C}, *n* = 11. Data for the retraction rates of the parent, Δ*pilU,* and *pilT*^{K136A} strains are identical to those shown in **Fig 1B** and plotted again here to facilitate comparisons to the mutant strains indicated. **(B)** Natural transformation assays of the indicated strains incubated with 500 ng of transforming DNA overnight. Data are shown as the mean ± SD. Parent, *n* = 6. All other strains, *n* = 4**. (C)** Representative images of surface piliation (top) and aggregation phenotypes (bottom) for the indicated strains. Scale bar, 1 μm. Asterisk(s) directly above bars denote comparisons to the parent strain. All comparisons were made by one-way ANOVA with Tukey's post test. NS, not significant; * = $P < 0.05$, *** = $P < 0.001$.

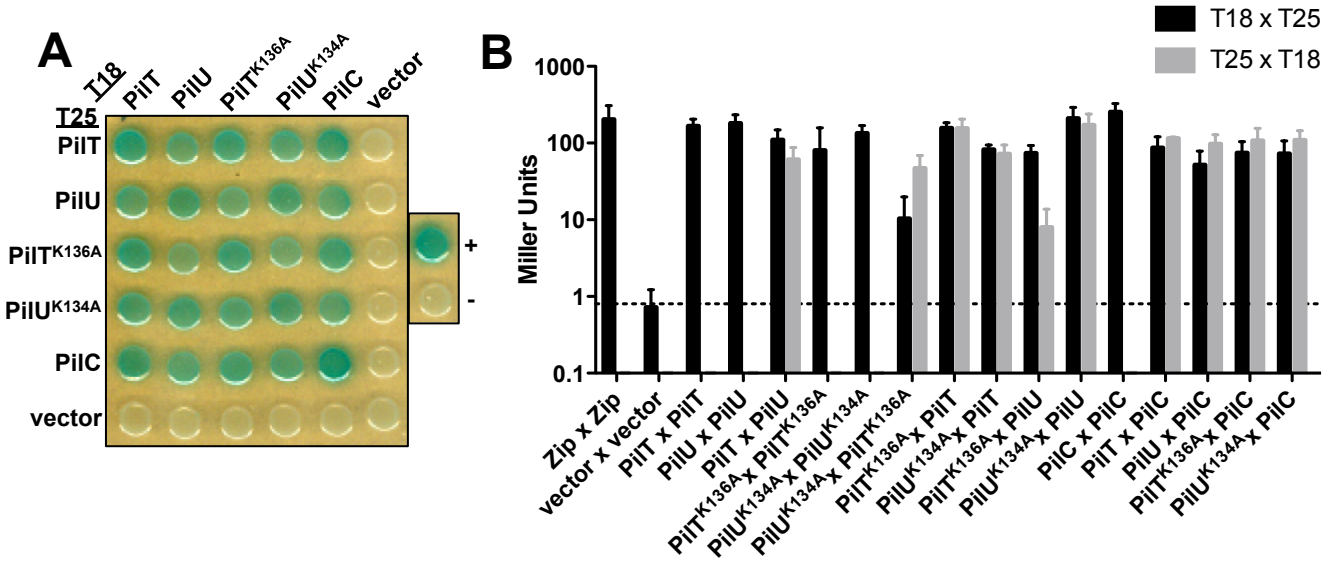

Fig 3. PilT and PilU interact with each other and the pilus platform protein PilC. Bacterial Adenylate Cyclase Two-Hybrid (BACTH) assays were performed to test pair-wise interactions between full length PilT, PilU, PilT^{K136A}, PilU^{K134A}, and PilC that were N-terminally fused to the T18- and T25- fragments of adenylate cyclase. Each construct was also tested for interactions with empty T18 and T25 vectors as a negative control. Leucine zipper fusions to T18 and T25 were used as the positive control (+) and empty T18 and T25 vectors served as an additional negative control (-). **(A)** Representative image of the BACTH assay plated on X-gal-containing media. **(B)** BACTH miller assays of the indicated pairwise interactions. The dotted line represents the β-galactosidase activity of the empty vector negative control. Data are shown as the mean ± SD and are from three independent experiments. Statistical analysis of these data can be found in **S2 Fig**.

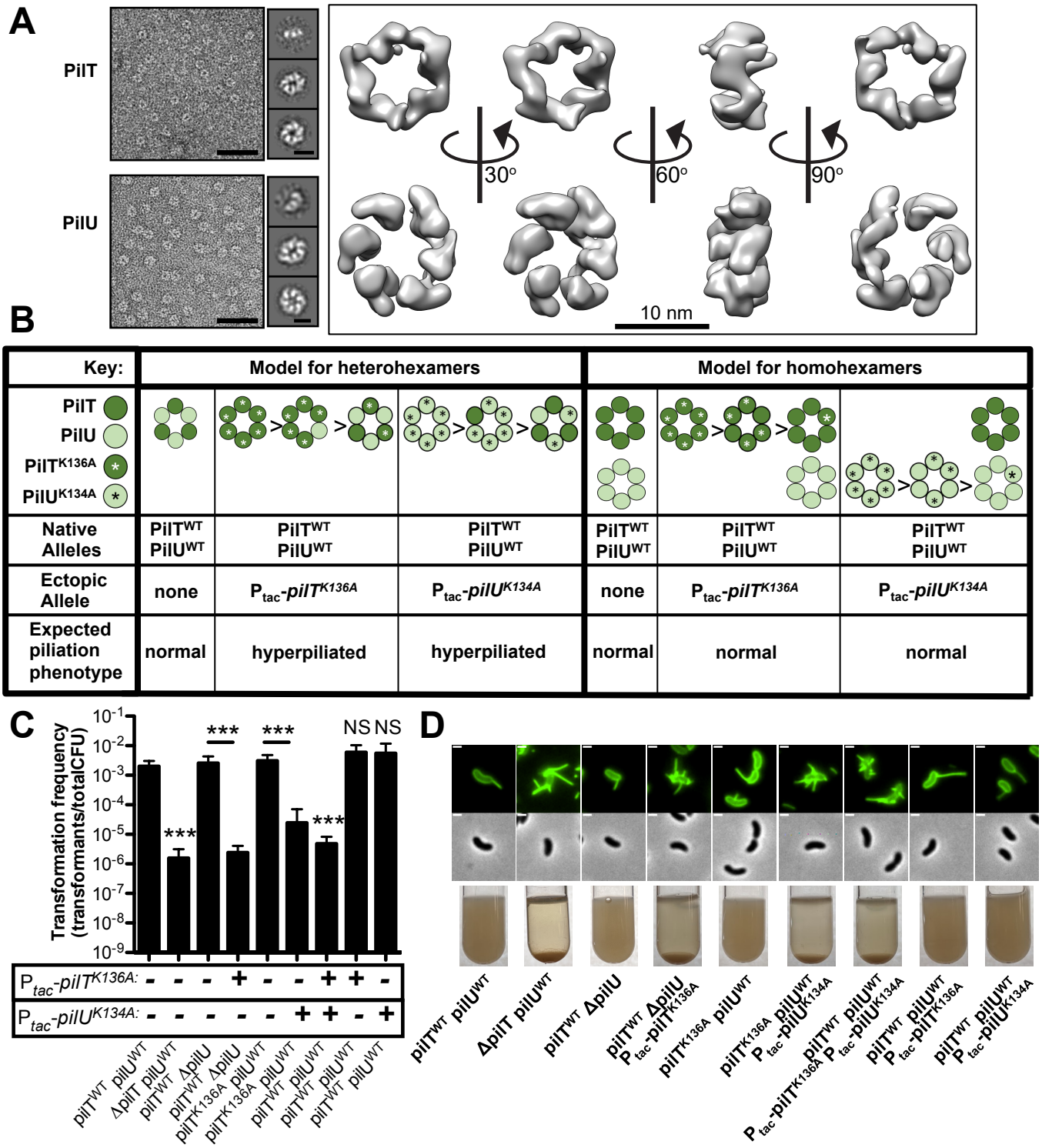

Fig 4. PilT and PilU form independent homomeric complexes *in vitro* and *in vivo* to facilitate pilus retraction. (A) Representative negative stain transmission electron micrographs of purified ^{6X}His-PilT and ^{6X}His-PilU (left; scale bar, 50 nm). 2D class averages revealing hexameric rings (middle; scale bar, 10 nm) and 3D reconstructions (right) of the ring complex. **(B)** Schematic of the experimental approach and expected outcomes for testing whether PilT and PilU form homomeric or heteromeric complexes to facilitate pilus retraction *in vivo*. **(C)** Natural transformation assays of indicated strains incubated with 500 ng of tDNA and after 7 minutes, DNAseI was added to prevent additional DNA uptake. The genotype of native *pilT* and *pilU* alleles are written below each bar graph and the presence or absence of a chromosomally-integrated IPTG-inducible ectopic allele of *pilT*^{K136A} or *pilU*^{K134A} is indicated by a + or -. Strains were grown with 100 μM IPTG if they contained an ectopic expression construct. Data are shown as the mean ± SD and are from four independent biological replicates. **(D)** Representative images of surface piliation (top) and aggregation phenotypes (bottom) for the indicated strains. Scale bar, 1 μm. Asterisk(s) directly above bars denote comparisons to the parent strain. All comparisons were made by one-way ANOVA with Tukey's post test. NS, not significant; *** = $P < 0.001$.

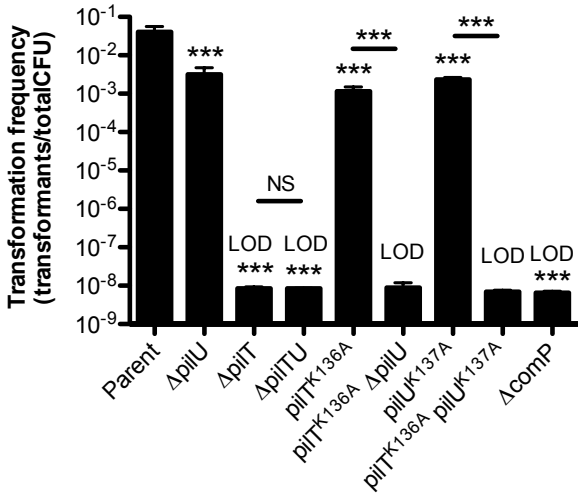

Fig 5. PilU supports pilus retraction in a PilT-dependent manner in *A. baylyi.*
Natural transformation assays of the indicated strains incubated with 500ng of transforming DNA for 5 hours. Data are shown as the mean ± SD. Parent, $n = 5$. Δ*comP*, $n = 6$. All other strains, $n = 4$. Asterisk(s) directly above bars denote comparisons to parent strain. All comparisons were made by one-way ANOVA with Tukey's post test. LOD, limit of detection; NS = not significant; *** = $P < 0.001$.

Supporting Information for

PilT and PilU are homohexameric ATPases that coordinate to retract type IVa pili

Jennifer L. Chlebek[1], Hannah Q. Hughes[1], Aleksandra S. Ratkiewicz[2], Rasman Rayyan[2], Joseph Che-Yen Wang[3], Brittany E. Herrin[1], Triana N. Dalia[1], Nicolas Biais[2], and Ankur B. Dalia[1,*]

[1]Department of Biology, Indiana University, 1001 E. 3rd Street, Bloomington, IN 47405.

[2]Biology Department, CUNY Brooklyn College, 2900 Bedford Avenue, Brooklyn, NY 11210 and Graduate Center of CUNY, 365 5th Avenue, NY 10016.

[3]Electron Microscopy Center, Indiana University, Bloomington, IN 47405.

*Correspondence to: ankdalia@indiana.edu.

This PDF file includes:

S1-S5 Figs
S1-S4 Tables

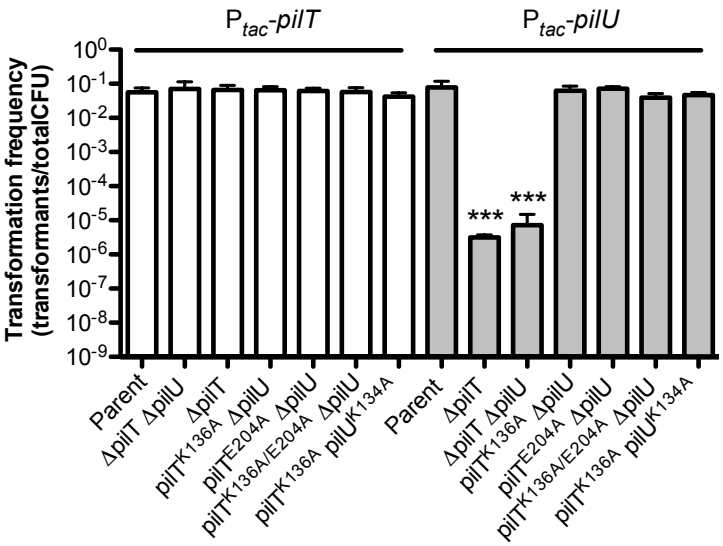

S1 Fig. Complementation analysis of *V. cholerae* mutant strains via ectopic expression of *pilT* or *pilU*. Natural transformation assays of the indicated strains. All strains contain either a chromosomally integrated IPTG-inducible P$_{tac}$-*pilT* (white bars) or P$_{tac}$-*pilU* (gray bars) construct as indicated. Data show that ectopic overexpression of PilT and PilU does not affect the transformation frequency of the parent strain. Ectopic overexpression of PilT rescued the transformation of all strains that showed a substantial reduction in natural transformation in **Fig 1A** and **Fig 2B** (i.e. Δ*pilT*, Δ*pilT* Δ*pilU*, *pilT*^{K136A} Δ*pilU*, *pilT*^{E204A} Δ*pilU*, *pilT*$^{E204A/K136A}$ Δ*pilU*, and *pilT*^{K136A} *pilU*^{K134A}). Ectopic overexpression of PilU rescued all strains except for strains that lacked a copy of *pilT* (i.e. Δ*pilT*, Δ*pilT* Δ*pilU*). All strains were grown with 100 μM IPTG to ectopically induce PilT or PilU. Data are shown as the mean ± SD. Parent, $n = 8$. All other strains, $n = 4$. Asterisk(s) directly above bars denote comparisons to the appropriate parent strain. Comparisons were made by grouping data into the two families indicated by the white and grey bars. A one-way ANOVA was performed for each family with a Dunnet's post to compare each experimental sample to the parent strain. Comparisons were not statistically significantly different unless otherwise noted. *** = $P < 0.001$.

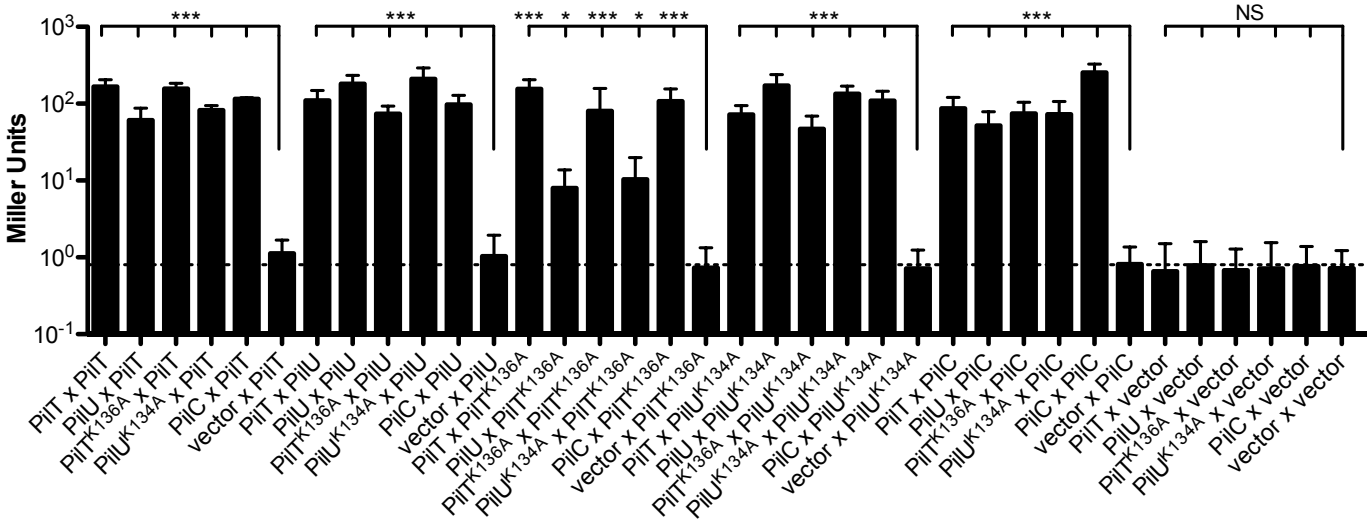

S2 Fig. PilT and PilU interact with each other and the pilus platform protein PilC. BACTH Miller assays showing all data from **Fig 3B** with additional negative controls for every T25- or T18-fusion. Data are shown as the mean ± SD from three independent experiments. The dotted line represents the β-galactosidase activity of the empty vector negative control (T18-empty x T25-empty). Comparisons were made by grouping data into appropriate families indicated by the black lines above the bar graph. A one-way ANOVA was performed on each family with a Dunnet's post test to compare each experimental group to the appropriate negative control (indicated by the longer black line). A single set of asterisks directly above the group line denotes the statistical results for all comparisons in that family unless otherwise noted. NS, not significant; * = $P < 0.05$; *** = $P < 0.001$.

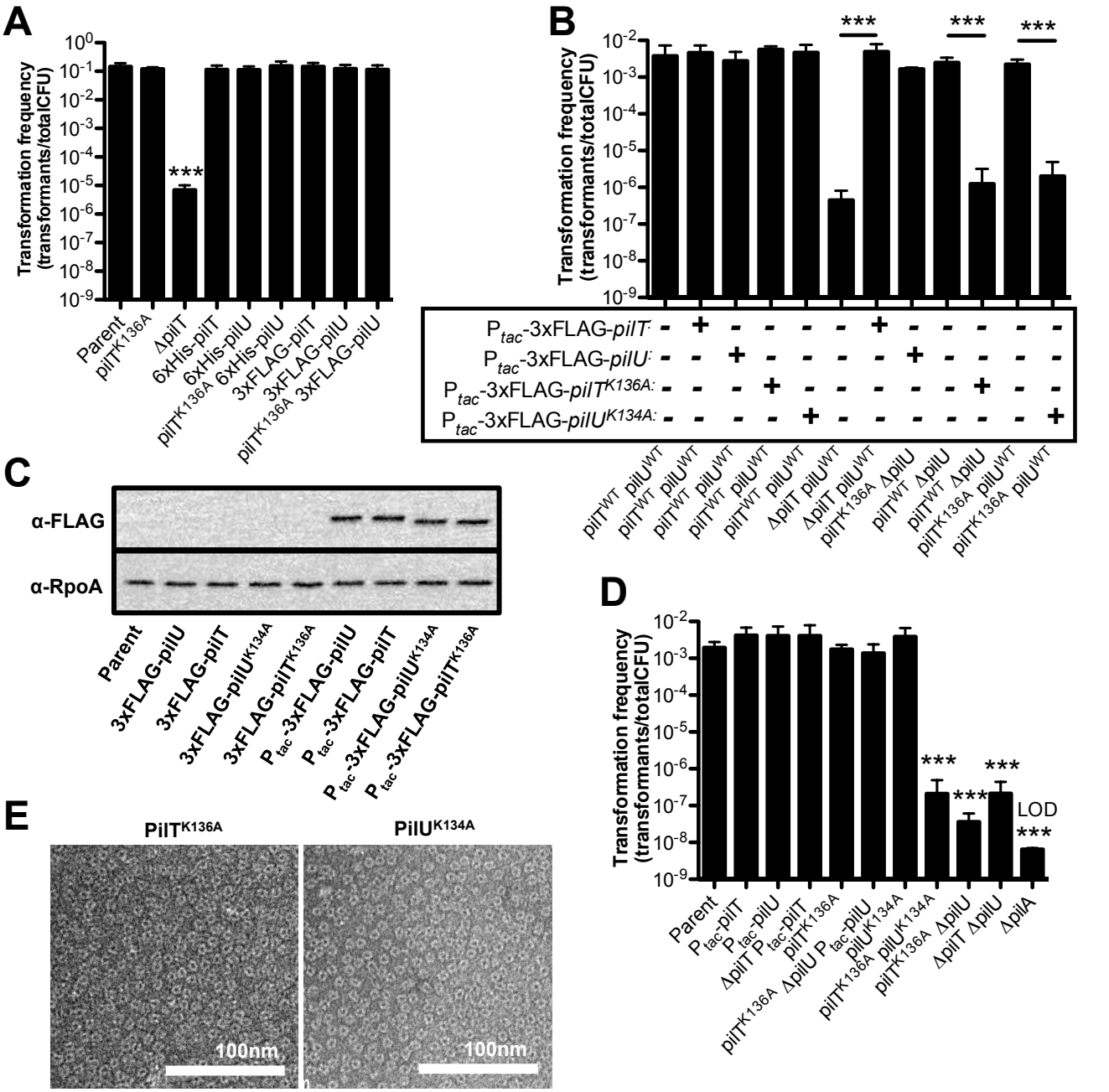

S3 Fig. PilT and PilU form homomeric complexes to facilitate pilus retraction. **(A)** Natural transformation assays showing that 6xHis and 3xFLAG N-terminal fusions to PilT and PilU are functional. The indicated strains were incubated with 500 ng of transforming DNA overnight. Parent, $n = 8$. All others, $n = 4$. **(B)** Natural transformation assays showing that overexpression of 3xFLAG tagged PilT/PilU/PilT^{K136A}/PilU^{K134A} behave the same as non-tagged proteins when ectopically overexpressed in the indicated backgrounds. Strains were incubated with 500 ng of transforming DNA and after 7 minutes, DNAse I was added to prevent additional DNA uptake. Parent, $n = 5$. *pilT^{K136A}*, $n = 5$. All others, $n = 4$. **(C)** Western blot of the indicated strains to detect FLAG tagged-proteins and RpoA as a loading control. Strains containing an IPTG regulated P_{tac} constuct were grown in the presence of 100 μM IPTG. This blot indicates that ectopic induction of 3xFLAG tagged PilT/PilU/PilT^{K136A}/PilU^{K134A} results in robust overexpression of proteins above native levels. Data is representative of three independent experiments. **(D)** Natural transformation assays where the indicated strains were incubated with 500 ng of transforming DNA for 7 minutes prior to the addition of DNAse I to prevent additional DNA uptake. These data indicate that ectopic overexpression of PilT or PilU can rescue strains with a substantial reduction in transformation frequency. All strains with P_{tac} constructs were grown with 100 μM IPTG to overexpress PilT or PilU. All bar graphs are shown as the mean ± SD. Asterisk(s) directly above bars denote comparisons to parent strain. All comparisons were made by one-way ANOVA followed with Tukey's post test. LOD, limit of detection; *** = $P < 0.001$. **(E)** Representative negative stain transmission electron micrographs showing that purified ^{6X}His-PilT^{K136A} and ^{6X}His-PilU^{K134A} form hexamers *in vitro.* Scale bar, 100 nm.

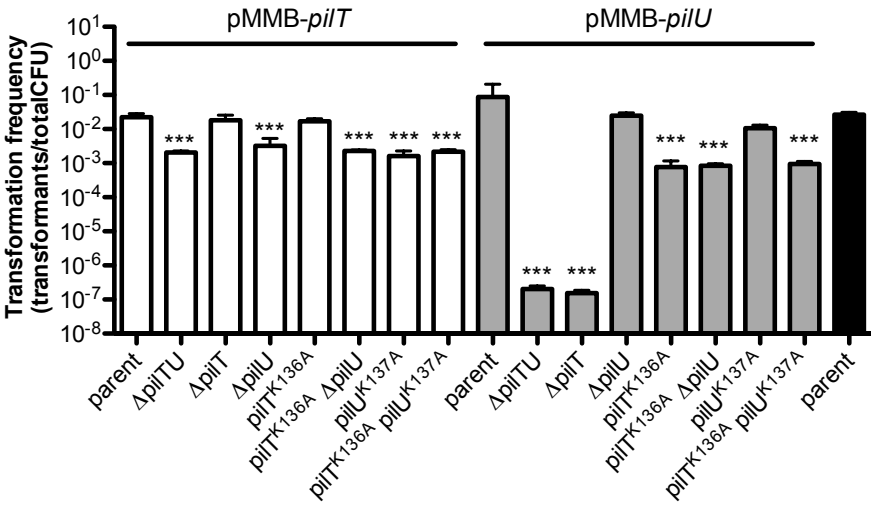

S4 Fig. Complementation analysis of *A. baylyi* mutant strains via ectopic expression of *pilT* or *pilU*. Natural transformation assays of the indicated *A. baylyi* strains. Strains harbored pMMB-*pilT* (white bars), pMMB-*pilU* (gray bars), or no vector (black bar). Data indicate that ectopic overexpression of PilT and PilU do not affect the transformation frequency of the parent strain. Ectopic overexpression of PilT rescued the transformation of all strains that showed a significant reduction in natural transformation in **Fig 5** (i.e. Δ*pilT*, Δ*pilT* Δ*pilU*, *pilT*^{K136A} Δ*pilU*, and *pilT*^{K136A} *pilU*^{K137A}). Ectopic overexpression of PilU rescued all strains except for strains that lacked a copy of pilT (i.e. Δ*pilT* and Δ*pilT* Δ*pilU*). All strains were grown with 100 μM IPTG to induce expression of *pilT* or *pilU*. Data are shown as the mean ± SD and are from three independent experiments. Asterisk(s) directly above bars denote comparisons to the appropriate parent strain. Comparisons were made by grouping data into the two families indicated by the white and grey bars. A one-way ANOVA was performed for each family followed by Dunnet's post test to compare each experimental group to the parent strain. Comparisons were not statistically significantly different from the relevant parent unless otherwise noted. *** = $P < 0.001$.

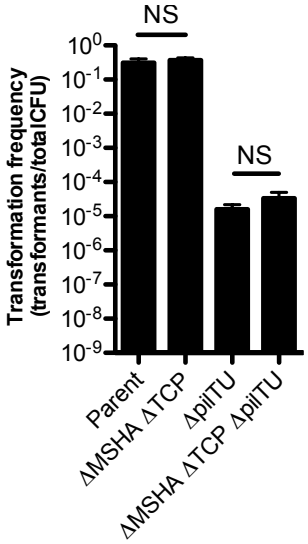

S5 Fig. The components of the *V. cholerae* MSHA or TCP type IV pilus systems do not contribute to PilTU-independent retraction of the competence pilus. Natural transformation assays of the indicated strains. Reactions were incubated with 500 ng of transforming DNA overnight. ΔMSHA and ΔTCP represent deletions of the entire locus for both pilus systems, which includes the extension ATPase associated with each. Data are shown as the mean ± SD and are from four independent biological replicates. All comparisons were made by one-way ANOVA with Tukey's post test. NS, not significant.

S1 Table. Strains used in this study

Strain name in manuscript	Genotype and antibiotic resistances	Figure	Strain #
Parent	E7946 SmR, ΔlacZ::lacIq, P_{tac}-tfoX, ΔluxO::miniFRT, ΔVC1807::ZeoR, pilA S56C	Fig 1, Fig 2	TND0905 (SAD2468)
ΔpilU	E7946 SmR, ΔlacZ::lacIq, P_{tac}-tfoX, ΔluxO::SpecR, ΔVC1807::CmR, pilA S56C, comEA-mCherry, ΔpilU::TmR *	Fig 1, Fig 2	SAD2135
ΔpilT	E7946 SmR, ΔlacZ::lacIq, P_{tac}-tfoX, ΔluxO::miniFRT, ΔVC1807::ZeoR, pilA S56C, ΔpilT::TmR	Fig 1, Supp Fig 3	TND1035 (SAD2469)
ΔpilTU	E7946 SmR, ΔlacZ::lacIq, P_{tac}-tfoX, ΔluxO::miniFRT, ΔVC1807::ZeoR, pilA S56C, ΔpilTU::TmR	Fig 1	JLC227 (SAD2470)
$pilT^{K136A}$	E7946 SmR, ΔlacZ::lacIq, P_{tac}-tfoX, ΔluxO::miniFRT, ΔVC1807::KanR, pilA S56C, $pilT^{K136A}$	Fig 1, Fig 2	TND1077 (SAD2471)
$pilT^{K136A}$ ΔpilU	E7946 SmR, ΔlacZ::lacIq, P_{tac}-tfoX, ΔluxO::miniFRT, ΔVC1807::ZeoR, pilA S56C, $pilT^{K136A}$, ΔpilU::TmR	Fig 1	JLC444 (SAD2472)
$pilT^{E204A}$	E7946 SmR, ΔlacZ::lacIq, P_{tac}-tfoX, ΔluxO::miniFRT, ΔVC1807::CmR, pilA S56C, $pilT^{E204A}$	Fig 1	TND1203 (SAD2473)
$pilT^{E204A/K136A}$	E7946 SmR, ΔlacZ::lacIq, P_{tac}-tfoX, ΔluxO::miniFRT, ΔVC1807::CmR, pilA S56C, $pilT^{E204A/K136A}$	Fig 1	JLC324 (SAD2474)
$pilT^{E204A/K136A}$ ΔpilU	E7946 SmR, ΔlacZ::lacIq, P_{tac}-tfoX, ΔluxO::miniFRT, ΔVC1807::CmR, pilA S56C, $pilT^{E204A/K136A}$, ΔpilU::TmR	Fig 1	JLC530 (SAD2475)
$pilT^{E204A}$ ΔpilU	E7946 SmR, ΔlacZ::lacIq, P_{tac}-tfoX, ΔluxO::miniFRT, ΔVC1807::CmR, pilA S56C, $pilT^{E204A}$, ΔpilU::TmR	Fig 1	JLC531 (SAD2476)
ΔpilA	E7946 SmR, ΔlacZ::lacIq, P_{tac}-tfoX, ΔluxO::SpecR, ΔVC1807::KanR, ΔpilA::miniFRT	Fig 1	TND0855 (SAD2477)
Parent (micropillar assays)	E7946 SmR, ΔlacZ::lacIq, P_{tac}-tfoX, ΔluxO::SpecR, ΔVC1807::CmR, pilA S56C, ΔflaA::CarbR, ΔmshA::miniFRT, Δvps-rbmA::ZeoR, ΔtcpA::KanR	Fig 1	TND0752 (SAD2478)
ΔpilT (micropillar assays)	E7946 SmR, ΔlacZ::lacIq, P_{tac}-tfoX, ΔluxO::SpecR, ΔVC1807::CmR, pilA S56C, ΔflaA::CarbR, ΔmshA::miniFRT, Δvps-rbmA::ZeoR, ΔtcpA::KanR, ΔpilT::TmR	Fig 1	TND0767 (SAD2479)
ΔpilU (micropillar assays)	E7946 SmR, ΔlacZ::lacIq, P_{tac}-tfoX, ΔluxO::SpecR, ΔVC1807::CmR, pilA S56C, ΔflaA::CarbR, ΔmshA::miniFRT, Δvps-rbmA::ZeoR, ΔtcpA::KanR, ΔpilU::TmR	Fig 1	TND1168 (SAD2480)
ΔpilT ΔpilU (micropillar assays)	E7946 SmR, ΔlacZ::lacIq, P_{tac}-tfoX, ΔluxO::SpecR, ΔVC1807::CmR, pilA S56C,	Fig 1	TND1174 (SAD2635)

	ΔflaA::CarbR, ΔmshA::miniFRT, Δvps-rbmA::ZeoR, ΔtcpA::KanR, ΔpilTU::TmR		
P_{tac}-PilT	E7946 SmR, P_{tac}-tfoX, ΔluxO::miniFRT, ΔVC1807::ZeoR, pilA S56C, ΔlacZ::P_{tac}-PilT SpecR	Supp Fig 1	JLC426 (SAD2481)
P_{tac}-PilU	E7946 SmR, P_{tac}-tfoX, ΔluxO::miniFRT, ΔVC1807::ZeoR, pilA S56C, ΔlacZ::P_{tac}-PilU SpecR	Supp Fig 1	JLC427 (SAD2482)
P_{tac}-PilT ΔpilTU	E7946 SmR, P_{tac}-tfoX, ΔluxO::miniFRT, ΔVC1807::ZeoR, pilA S56C, ΔlacZ::P_{tac}-PilT SpecR, ΔpilTU::TmR	Supp Fig 1	JLC420 (SAD2483)
P_{tac}-PilU ΔpilTU	E7946 SmR, P_{tac}-tfoX, ΔluxO::miniFRT, ΔVC1807::ZeoR, pilA S56C, ΔlacZ::P_{tac}-PilU SpecR, ΔpilTU::TmR	Supp Fig 1	JLC421 (SAD2484)
P_{tac}-PilT pilT^{K136A} ΔpilU	E7946 SmR, P_{tac}-tfoX, ΔluxO::miniFRT, ΔVC1807::KanR, pilA S56C, ΔlacZ::P_{tac}-PilT SpecR, pilT ^{K136A}, ΔpilU::TmR	Supp Fig 1	JLC450 (SAD2485)
P_{tac} -PilU pilT^{K136A} ΔpilU	E7946 SmR, P_{tac}-tfoX, ΔluxO::miniFRT, ΔVC1807::KanR, pilA S56C, ΔlacZ::P_{tac}-PilU SpecR, pilT ^{K136A}, ΔpilU::TmR	Supp Fig 1	JLC451 (SAD2486)
P_{tac} -PilT pilT^{K136A} pilU^{K134A}	E7946 SmR, P_{tac}-tfoX, ΔluxO::miniFRT, ΔVC1807::KanR, pilA S56C, ΔlacZ::P_{tac}-PilT SpecR, pilT ^{K136A} pilU ^{K134A}	Supp Fig 1	JLC424 (SAD2487)
P_{tac}-PilU pilT^{K136A} pilU^{K134A}	E7946 SmR, P_{tac}-tfoX, ΔluxO::miniFRT, ΔVC1807::KanR, pilA S56C, ΔlacZ::P_{tac}-PilU SpecR, pilT ^{K136A} pilU ^{K134A}	Supp Fig 1	JLC425 (SAD2488)
P_{tac}-PilT ΔpilTU	E7946 SmR, P_{tac}-tfoX, ΔluxO::miniFRT, ΔVC1807::ZeoR, pilA S56C, ΔlacZ::P_{tac}-PilT SpecR, ΔpilTU::TmR	Supp Fig 1	JLC438 (SAD2489)
P_{tac}-PilU ΔpilTU	E7946 SmR, P_{tac}-tfoX, ΔluxO::miniFRT, ΔVC1807::ZeoR, pilA S56C, ΔlacZ::P_{tac}-PilU SpecR, ΔpilTU::TmR	Supp Fig 1	JLC439 (SAD2490)
P_{tac}-PilT pilT$^{E204A/K136A}$ ΔpilU	E7946 SmR, P_{tac}-tfoX, ΔluxO::miniFRT, ΔVC1807::CmR, pilA S56C, pilT ^{E204A}/^{K136A}, ΔpilU::TmR, ΔlacZ::P_{tac}-PilT SpecR	Supp Fig 1	JLC540 (SAD2491)
P_{tac}-PilU pilT$^{E204A/K136A}$ ΔpilU	E7946 SmR, P_{tac}-tfoX, ΔluxO::miniFRT, ΔVC1807::CmR, pilA S56C, pilT ^{E204A}/^{K136A}, ΔpilU::TmR, ΔlacZ::P_{tac}-PilU SpecR	Supp Fig 1	JLC541 (SAD2492)
P_{tac}-PilT pilT^{E204A} ΔpilU	E7946 SmR, P_{tac}-tfoX, ΔluxO::miniFRT, ΔVC1807::CmR, pilA S56C, pilT ^{E204A}, ΔpilU::TmR, ΔlacZ::P_{tac}-PilT SpecR	Supp Fig 1	JLC542 (SAD2493)
P_{tac}-PilU pilT^{E204A} ΔpilU	E7946 SmR, P_{tac}-tfoX, ΔluxO::miniFRT, ΔVC1807::CmR, pilA S56C, pilT ^{E204A}, ΔpilU::TmR, , ΔlacZ::P_{tac}-PilU SpecR	Supp Fig 1	JLC543 (SAD2494)
PilU^{L199C}	E7946 SmR, ΔlacZ::lacIq, P_{tac}-tfoX, ΔluxO::miniFRT, ΔVC1807::CmR, pilA S56C, pilU ^{L199C}	Fig 2	JLC409 (SAD2495)
ΔpilT PilU^{L199C}	E7946 SmR, ΔlacZ::lacIq, P_{tac}-tfoX, ΔluxO::miniFRT, ΔVC1807::ZeoR, pilA S56C, ΔpilT::TmR, pilU ^{L199C}	Fig 2	JLC411 (SAD2496)

pilT^{K136A} pilU^{L199C}	E7946 SmR, ΔlacZ::lacIq, P_{tac}-tfoX, ΔluxO::miniFRT, ΔVC1807::CmR, pilA S56C, pilU ^{L199C}, pilT ^{K136A}	Fig 2	JLC414 (SAD2497)
pilT^{L201C}	E7946 SmR, ΔlacZ::lacIq, P_{tac}-tfoX, ΔluxO::SpecR, ΔVC1807::CmR, pilA S56C, comEA-mCherry, pilT ^{L201C} *	Fig 2	TND0989 (SAD2498)
pilT^{L201C} ΔpilU	E7946 SmR, ΔlacZ::lacIq, P_{tac}-tfoX, ΔluxO::SpecR, ΔVC1807::CmR, pilA S56C, comEA-mCherry, pilT ^{L201C}, ΔpilU::TmR *	Fig 2	TND1140 (SAD2499)
pilU^{K134A}	E7946 SmR, ΔlacZ::lacIq, P_{tac}-tfoX, ΔluxO::miniFRT, ΔVC1807::KanR, pilA S56C, pilU ^{K134A}	Fig 2	TND1092 (SAD2500)
pilT^{K136A} pilU^{K134A}	E7946 SmR, ΔlacZ::lacIq, P_{tac}-tfoX, ΔluxO::miniFRT, ΔVC1807::KanR, pilA S56C, pilT ^{K136A}, pilU ^{K134A}	Fig 2	TND1094 (SAD2501)
^{6X}His-pilU, pilT^{K136A}	E7946 SmR, ΔlacZ::lacIq, P_{tac}-tfoX, ΔluxO::miniFRT, ΔVC1807::CmR, pilA S56C, ^{6X}His-pilU, pilT ^{K136A}	Supp Fig 3	JLC298 (SAD2502)
^{6X}His-pilT	E7946 SmR, ΔlacZ::lacIq, P_{tac}-tfoX, ΔluxO::miniFRT, ΔVC1807::CmR, pilA S56C, ^{6X}His-pilT	Supp Fig 3	HKQ046 (SAD2503)
^{6X}His-pilU	E7946 SmR, ΔlacZ::lacIq, P_{tac}-tfoX, ΔluxO::miniFRT, ΔVC1807::CmR, pilA S56C, ^{6X}His-pilU	Supp Fig 3	JLC398 (SAD2504)
pilT^{K136A} 3xFLAG-pilU	E7946 SmR, ΔlacZ::lacIq, P_{tac}-tfoX, ΔluxO::miniFRT, ΔVC1807::CmR, pilA S56C, pilT ^{K136A}, 3xFLAG-pilU	Supp Fig 3	JLC396 (SAD2505)
3xFLAG-pilU	E7946 SmR, ΔlacZ::lacIq, P_{tac}-tfoX, ΔluxO::miniFRT, ΔVC1807::CmR, pilA S56C, 3xFLAG-pilU	Supp Fig 3	JLC326 (SAD2506)
3xFLAG-pilU^{K134A}	E7946 SmR, ΔlacZ::lacIq, P_{tac}-tfoX, ΔluxO::miniFRT, ΔVC1807::CmR, pilA S56C, 3xFLAG-pilU^{K134A}	Supp Fig 3	JLC316 (SAD2507)
3xFLAG-pilT	E7946 SmR, ΔlacZ::lacIq, P_{tac}-tfoX, ΔluxO::miniFRT, ΔVC1807::CmR, pilA S56C, 3xFLAG-pilT	Supp Fig 3	JLC310 (SAD2508)
3xFLAG-pilT^{K136A}	E7946 SmR, ΔlacZ::lacIq, P_{tac}-tfoX, ΔluxO::miniFRT, ΔVC1807::CmR, pilA S56C, 3xFLAG-pilT ^{K136A}	Supp Fig 3	JLC349 (SAD2509)
^{6X}His-pilU (purification)	BL21 DE3 pHisTev-6xHis-pilU	Fig 4	HKQ051 (SAD2510)
^{6X}His-pilU^{K134A} (purification)	BL21 DE3 pHisTev-6xHis-pilU ^{K134A}	Supp Fig 3	SAD2316
^{6X}His-pilT (purification)	BL21 DE3 pHisTev-6xHis-pilT	Fig 4	TND1277 (SAD2511)
^{6X}His-pilT^{K136A} (purification)	BL21 DE3 pHisTev-6xHis-pilT ^{K136A}	Supp Fig 3	TND1281 (SAD2512)
PilT x PilT	BTH101 pUT18C-PilT (CarbR), pKT25-PilT (KanR)	Fig 3, Supp Fig 2	JLC465

PilU x PilT	BTH101 pUT18C-PilU (CarbR), pKT25-PilT (KanR)	Fig 3, Supp Fig 2	JLC466
PilT^{K136A} x PilT	BTH101 pUT18C-PilT ^{K136A} (CarbR), pKT25-PilT (KanR)	Fig 3, Supp Fig 2	JLC467
PilU^{K134A} x PilT	BTH101 pUT18C-PilU ^{K134A} (CarbR), pKT25-PilT (KanR)	Fig 3, Supp Fig 2	JLC468
PilC x PilT	BTH101 pUT18C-PilC (CarbR), pKT25-PilT (KanR)	Fig 3, Supp Fig 2	JLC469
vector x PilT	BTH101 pUT18C-vector (CarbR), pKT25-PilT (KanR)	Fig 3, Supp Fig 2	JLC470
PilT x PilU	BTH101 pUT18C-PilT (CarbR), pKT25-PilU (KanR)	Fig 3, Supp Fig 2	JLC471
PilU x PilU	BTH101 pUT18C-PilU (CarbR), pKT25-PilU (KanR)	Fig 3, Supp Fig 2	JLC472
PilT^{K136A} x PilU	BTH101 pUT18C-PilT ^{K136A} (CarbR), pKT25-PilU (KanR)	Fig 3, Supp Fig 2	JLC473
PilU^{K134A} x PilU	BTH101 pUT18C-PilU ^{K134A} (CarbR), pKT25-PilU (KanR)	Fig 3, Supp Fig 2	JLC474
PilC x PilU	BTH101 pUT18C-PilC (CarbR), pKT25-PilU (KanR)	Fig 3, Supp Fig 2	JLC475
vector x PilU	BTH101 pUT18C-vector (CarbR), pKT25-PilU (KanR)	Fig 3, Supp Fig 2	JLC476
PilT x PilT^{K136A}	BTH101 pUT18C-PilT (CarbR), pKT25-PilT ^{K136A} (KanR)	Fig 3, Supp Fig 2	JLC477
PilU x PilT^{K136A}	BTH101 pUT18C-PilU (CarbR), pKT25-PilT ^{K136A} (KanR)	Fig 3, Supp Fig 2	JLC478
PilT^{K136A} x PilT^{K136A}	BTH101 pUT18C-PilT ^{K136A} (CarbR), pKT25-PilT ^{K136A} (KanR)	Fig 3, Supp Fig 2	JLC479
PilU^{K134A} x PilT^{K136A}	BTH101 pUT18C-PilU ^{K134A} (CarbR), pKT25-PilT ^{K136A} (KanR)	Fig 3, Supp Fig 2	JLC480
PilC x PilT^{K136A}	BTH101 pUT18C-PilC (CarbR), pKT25-PilT ^{K136A} (KanR)	Fig 3, Supp Fig 2	JLC481

vector x PilT^{K136A}	BTH101 pUT18C-vector (CarbR), pKT25-PilT ^{K136A} (KanR)	Fig 3, Supp Fig 2	JLC482
PilT x PilU^{K134A}	BTH101 pUT18C-PilT (CarbR), pKT25-PilU ^{K134A} (KanR)	Fig 3, Supp Fig 2	JLC483
PilU x PilU^{K134A}	BTH101 pUT18C-PilU (CarbR), pKT25-PilU ^{K134A} (KanR)	Fig 3, Supp Fig 2	JLC484
PilT^{K136A} x PilU^{K134A}	BTH101 pUT18C-PilT ^{K136A} (CarbR), pKT25-PilU ^{K134A} (KanR)	Fig 3, Supp Fig 2	JLC485
PilU^{K134A} x PilU^{K134A}	BTH101 pUT18C-PilU ^{K134A} (CarbR), pKT25-PilU ^{K134A} (KanR)	Fig 3, Supp Fig 2	JLC486
PilC x PilU^{K134A}	BTH101 pUT18C-PilC (CarbR), pKT25-PilU ^{K134A} (KanR)	Fig 3, Supp Fig 2	JLC487
vector x PilU^{K134A}	BTH101 pUT18C-vector (CarbR), pKT25-PilU ^{K134A} (KanR)	Fig 3, Supp Fig 2	JLC488
PilT x PilC	BTH101 pUT18C-PilT (CarbR), pKT25-PilC (KanR)	Fig 3, Supp Fig 2	JLC489
PilU x PilC	BTH101 pUT18C-PilU (CarbR), pKT25-PilC (KanR)	Fig 3, Supp Fig 2	JLC490
PilT^{K136A} x PilC	BTH101 pUT18C-PilT ^{K136A} (CarbR), pKT25-PilC (KanR)	Fig 3, Supp Fig 2	JLC491
PilU^{K134A} x PilC	BTH101 pUT18C-PilU ^{K134A} (CarbR), pKT25-PilC (KanR)	Fig 3, Supp Fig 2	JLC492
PilC x PilC	BTH101 pUT18C-PilC (CarbR), pKT25-PilC (KanR)	Fig 3, Supp Fig 2	JLC493
vector x PilC	BTH101 pUT18C-vector (CarbR), pKT25-PilC (KanR)	Fig 3, Supp Fig 2	JLC494
PilT x vector	BTH101 pUT18C-PilT (CarbR), pKT25-vector (KanR)	Fig 3, Supp Fig 2	JLC495
PilU x vector	BTH101 pUT18C-PilU (CarbR), pKT25-vector (KanR)	Fig 3, Supp Fig 2	JLC496
PilT^{K136A} x vector	BTH101 pUT18C-PilT ^{K136A} (CarbR), pKT25-vector (KanR)	Fig 3, Supp Fig 2	JLC497

PilU^{K134A} x vector	BTH101 pUT18C-PilU ^{K134A} (CarbR), pKT25-vector (KanR)	Fig 3, Supp Fig 2	JLC498
PilC x vector	BTH101 pUT18C-PilC (CarbR), pKT25-vector (KanR)	Fig 3, Supp Fig 2	JLC499
vector x vector	BTH101 pUT18C-vector (CarbR), pKT25-vector (KanR)	Fig 3, Supp Fig 2	JLC500
Zip x Zip	BTH101 pUT18C-Leucine Zipper (CarbR), pKT25-Leucine Zipper (KanR)	Fig 3, Supp Fig 2	JLC501
Parent (P_{const}-tfoX)	E7946 SmR, ΔlacZ::lacIq, P_{const}-tfoX, ΔluxO::miniFRT, ΔVC1807::KanR, pilA S56C	Fig 4, Supp Fig 3	TND1076 (SAD2513)
ΔpilU	E7946 SmR, ΔlacZ::lacIq, P_{const}-tfoX, ΔluxO::miniFRT, ΔVC1807::KanR, pilA S56C, ΔpilU::TmR	Fig 4, Supp Fig 3	JLC251 (SAD2514)
ΔpilT	E7946 SmR, ΔlacZ::lacIq, P_{const}-tfoX, ΔluxO::miniFRT, ΔVC1807::KanR, pilA S56C, ΔpilT::TmR	Fig 4, Supp Fig 3	JLC250 (SAD2515)
pilT^{K136A}	E7946 SmR, ΔlacZ::lacIq, P_{const}-tfoX, ΔluxO::miniFRT, ΔVC1807::CmR, pilA S56C, pilT ^{K136A}	Fig 4	JLC299 (SAD2516)
P_{tac}-pilT^{K136A}	E7946 SmR, P_{const}-tfoX, ΔluxO::miniFRT, ΔVC1807::KanR, pilA S56C, ΔlacZ::P_{tac} -pilT ^{K136A} SpecR	Fig 4	JLC277 (SAD2517)
ΔpilU P_{tac}-pilT^{K136A}	E7946 SmR, P_{const}-tfoX, ΔluxO::miniFRT, ΔVC1807::KanR, pilA S56C, ΔpilU::TmR, ΔlacZ::Ptac-pilT ^{K136A} SpecR	Fig 4	SAD2243
P_{tac}-pilU^{K134A}	E7946 SmR, P_{const}-tfoX, ΔluxO::miniFRT, ΔVC1807::KanR, pilA S56C, ΔlacZ::P_{tac}-pilU ^{K134A} SpecR	Fig 4	JLC282 (SAD2518)
pilT^{K136A} P_{tac}-pilU^{K134A}	E7946 SmR, P_{const}-tfoX, ΔluxO::miniFRT, ΔVC1807::CmR, pilA S56C, ΔlacZ::P_{tac}-pilU ^{K134A} SpecR, pilT ^{K136A}	Fig 4	JLC300 (SAD2519)
P_{tac}-pilT^{K136A} P_{tac}-pilU^{K134A}	E7946 SmR, P_{const}-tfoX, ΔluxO::miniFRT, pilA S56C, ΔlacZ::P_{tac}-pilU ^{K134A} SpecR, ΔVC1807::Ptac-pilT ^{K136A} CmR	Fig 4	SAD2242
P_{tac}-3xFLAG-PilU	E7946 SmR, P_{const}-tfoX, ΔluxO::miniFRT, ΔVC1807::KanR, pilA S56C, ΔlacZ::P_{tac}-3xFLAG-pilU SpecR	Supp Fig 3	JLC333 (SAD2520)
P_{tac}-3x FLAG-PilU ^{K134A}	E7946 SmR, P_{const}-tfoX, ΔluxO::miniFRT, ΔVC1807::KanR, pilA S56C, ΔlacZ::P_{tac}-3xFLAG-pilU ^{K134A} SpecR	Supp Fig 3	JLC336 (SAD2521)
P_{tac}-3x FLAG-PilT	E7946 SmR, ΔlacZ::lacIq, P_{const}-tfoX, ΔluxO::miniFRT, ΔVC1807::KanR, pilA S56C, ΔlacZ::P_{tac}-3xFLAG-pilT SpecR	Supp Fig 3	JLC337 (SAD2522)

P_{tac}-3x FLAG-PilT^{K136A}	E7946 SmR, P_{const}-tfoX, ΔluxO::miniFRT, ΔVC1807::KanR, pilA S56C, ΔlacZ::P_{tac}-3xFLAG-pilT ^{K136A} SpecR	Supp Fig 3	JLC353 (SAD2523)
ΔpilA	E7946 SmR, ΔlacZ::lacIq, P_{const}-tfoX, ΔluxO::miniFRT, ΔVC1807::TmR, ΔpilA::miniFRT	Supp Fig 3	TND1357 (SAD2524)
ΔpilTU	E7946 SmR, ΔlacZ::lacIq, P_{const}-tfoX, ΔluxO::miniFRT, ΔVC1807::KanR, pilA S56C, ΔpilTU::TmR	Supp Fig 3	JLC252 (SAD2525)
pilU^{K134A}	E7946 SmR, ΔlacZ::lacIq, P_{const}-tfoX, ΔluxO::miniFRT, ΔVC1807::CmR, pilA S56C, pilU ^{K134A}	Supp Fig 3	JLC308 (SAD2526)
pilT^{K136A} ΔpilU	E7946 SmR, ΔlacZ::lacIq, P_{const}-tfoX, ΔluxO::miniFRT, ΔVC1807::KanR, pilA S56C, pilT ^{K136A}, ΔpilU::TmR	Supp Fig 3	JLC447 (SAD2527)
pilT^{K136A} pilU^{K134A}	E7946 SmR, ΔlacZ::lacIq, P_{const}-tfoX, ΔluxO::miniFRT, ΔVC1807::KanR, pilA S56C, pilT ^{K136A}, pilU ^{K134A}	Supp Fig 3	JLC307 (SAD2528)
P_{tac}-pilT	E7946 SmR, P_{const}-tfoX, ΔluxO::miniFRT, ΔVC1807::KanR, pilA S56C, ΔlacZ::P_{tac}-pilT SpecR	Supp Fig 3	JLC279 (SAD2529)
ΔpilT P_{tac}-pilT	E7946 SmR, P_{const}-tfoX, ΔluxO::miniFRT, ΔVC1807::KanR, pilA S56C, ΔlacZ::P_{tac}-pilT SpecR, ΔpilT::TmR	Supp Fig 3	JLC280 (SAD2530)
P_{tac}-pilU	E7946 SmR, P_{const}-tfoX, ΔluxO::miniFRT, ΔVC1807::KanR, pilA S56C, ΔlacZ::P_{tac}-pilU SpecR	Supp Fig 3	JLC283 (SAD2531)
pilT^{K136A} ΔpilU P_{tac}-pilU	E7946 SmR, P_{const}-tfoX, ΔluxO::miniFRT, ΔVC1807::KanR, pilA S56C, ΔlacZ::P_{tac}-pilU SpecR, pilT ^{K136A}, ΔpilU::TmR	Supp Fig 3	JLC449 (SAD2532)
ΔpilT P_{tac}-3xFLAG-pilT	E7946 SmR, P_{const}-tfoX, ΔluxO::miniFRT, ΔVC1807::KanR, pilA S56C, ΔlacZ::P_{tac}-3x-FLAG-pilT SpecR, ΔpilT::TmR	Supp Fig 3	JLC373 (SAD2533)
pilT^{K136A} ΔpilU P_{tac}-3x FLAG-pilU	E7946 SmR, P_{const}-tfoX, ΔluxO::miniFRT, ΔVC1807::KanR, pilA S56C, ΔlacZ::P_{tac}-3x-FLAG-pilU SpecR, pilT ^{K136A}, ΔpilU::TmR	Supp Fig 3	JLC448 (SAD2534)
ΔpilU P_{tac}-3x FLAG-PilT^{K136A}	E7946 SmR, P_{const}-tfoX, ΔluxO::miniFRT, ΔVC1807::KanR, pilA S56C, ΔlacZ::P_{tac}-3xFLAG-pilT ^{K136A} SpecR, ΔpilU::TmR	Supp Fig 3	JLC379 (SAD2535)
pilT^{K136A} P_{tac}-3x FLAG-pilU^{K134A}	E7946 SmR, P_{const}-tfoX, ΔluxO::miniFRT, ΔVC1807::KanR, pilA S56C, ΔlacZ::P_{tac}-3x-FLAG-pilU ^{K134A} SpecR, pilT ^{K136A}	Supp Fig 3	JLC380 (SAD2536)
Parent (*A. baylyi*)	ADP1, comP T129C	Fig 5	TND0428 (SAD2537)
PilT^{K136A} ΔpilU	ADP1, comP T129C, PilT ^{K136A} ΔpilU::ZeoR	Fig 5	TND1135 (SAD2538)
PilT^{K136A} PilU^{K137A}	ADP1, , comP T129C, PilT ^{K136A} PilU ^{K137A}	Fig 5	TND1142 (SAD2539)
PilT^{K136A}	ADP1, comP T129C, PilT ^{K136A}	Fig 5	TND1122 (SAD2540)

PilU^{K137A}	ADP1, comP T129C, PilU ^{K137A}	Fig 5	TND1111 (SAD2541)
ΔpilT	ADP1, comP T129C, ΔpilT::SpecR	Fig 5	TND0779 (SAD2542)
ΔpilU	ADP1, comP T129C, ΔpilU::ZeoR	Fig 5	TND0798 (SAD2543)
ΔpilTU	ADP1, comP T129C, ΔpilTU::ZeoR	Fig 5	TND0799 (SAD2544)
ΔcomP	ADP1, ΔcomP::SpecR	Fig 5	TND0115 (SAD2545)
P_{tac}-pilT	ADP1, comP T129C, pMMB67EH- P_{tac}-pilT	Supp Fig 4	TND1703 (SAD2546)
P_{tac}-pilT ΔpilTU	ADP1, comP T129C, pMMB67EH- P_{tac}-pilT, ΔpilTU::ZeoR	Supp Fig 4	TND1704 (SAD2547)
P_{tac}-pilT ΔpilT	ADP1, comP T129C, pMMB67EH- P_{tac}-pilT, ΔpilT::SpecR	Supp Fig 4	TND1705 (SAD2548)
P_{tac}-pilT ΔpilU	ADP1, comP T129C, pMMB67EH- P_{tac}-pilT, ΔpilU::ZeoR	Supp Fig 4	TND1706 (SAD2549)
P_{tac}-pilT pilT^{K136A}	ADP1, comP T129C, pMMB67EH- P_{tac}-pilT, pilT ^{K136A}	Supp Fig 4	TND1707 (SAD2550)
P_{tac}-pilT pilT^{K136A} ΔpilU	ADP1, comP T129C, pMMB67EH- P_{tac}-pilT, pilT ^{K136A}, ΔpilU::ZeoR	Supp Fig 4	TND1708 (SAD2551)
P_{tac}-pilT pilU^{K137A}	ADP1, comP T129C, pMMB67EH- P_{tac}-pilT, pilU ^{K137A}	Supp Fig 4	TND1709 (SAD2552)
P_{tac}-pilT pilT^{K136A} pilU^{K137A}	ADP1, comP T129C, pMMB67EH- P_{tac}-pilT, pilT ^{K136A}, pilU ^{K137A}	Supp Fig 4	TND1710 (SAD2553)
P_{tac}-pilU	ADP1, comP T129C, pMMB67EH- P_{tac}-pilU	Supp Fig 4	TND1711 (SAD2554)
P_{tac}-pilU ΔpilTU	ADP1, comP T129C, pMMB67EH- P_{tac}-pilU, ΔpilTU::ZeoR	Supp Fig 4	TND1712 (SAD2555)
P_{tac}-pilU ΔpilT	ADP1, comP T129C, pMMB67EH- P_{tac}-pilU, ΔpilT::SpecR	Supp Fig 4	TND1713 (SAD2556)
P_{tac}-pilU ΔpilU	ADP1, comP T129C, pMMB67EH- P_{tac}-pilU, ΔpilU::ZeoR	Supp Fig 4	TND1714 (SAD2557)
P_{tac}-pilU pilT^{K136A}	ADP1, comP T129C, pMMB67EH- P_{tac}-pilU, pilT ^{K136A}	Supp Fig 4	TND1715 (SAD2558)
P_{tac}-pilU pilT^{K136A} ΔpilU	ADP1, comP T129C, pMMB67EH- P_{tac}-pilU, pilT ^{K136A}, ΔpilU::ZeoR	Supp Fig 4	TND1716 (SAD2559)
P_{tac}-pilU pilU^{K137A}	ADP1, comP T129C, pMMB67EH- P_{tac}-pilU, pilU ^{K137A}	Supp Fig 4	TND1717 (SAD2560)
P_{tac}-pilU pilT^{K136A} pilU^{K137A}	ADP1, comP T129C, pMMB67EH- P_{tac}-pilU, pilT ^{K136A}, pilU ^{K137A}	Supp Fig 4	TND1718 (SAD2561)
Parent	E7946 SmR, ΔlacZ::lacIq, P_{tac}-tfoX, ΔluxO::miniFRT, ΔVC1807::CmR, pilA S56C, comEA-mCherry	Supp Fig 5	TND0904 (SAD2636)
ΔMSHA ΔTCP	E7946 SmR, ΔlacZ::lacIq, P_{tac}-tfoX, ΔluxO::miniFRT, ΔVC1807::CmR, pilA S56C, comEA-mCherry, ΔMSHA::CarbR, ΔTCP::ZeoR	Supp Fig 5	SAD2087 (SAD2637)

ΔpilTU	E7946 SmR, ΔlacZ::lacIq, P_{tac}-tfoX, ΔluxO::miniFRT, ΔVC1807::CmR, pilA S56C, comEA-mCherry, ΔpilTU::TmR	Supp Fig 5	JLC765 (SAD2638)
ΔpilTU ΔMSHA ΔTCP	E7946 SmR, ΔlacZ::lacIq, P_{tac}-tfoX, ΔluxO::miniFRT, ΔVC1807::CmR, pilA S56C, comEA-mCherry, ΔpilTU::TmR, ΔMSHA::CarbR, ΔTCP::ZeoR	Supp Fig 5	JLC832 (SAD2639)

* comEA-mCherry does not affect natural transformation or retraction rates [17].

S2 Table. Primers used in this study

Primer name	Sequence (5' –> 3')	Description
BBC374	TGGCAAAAAGCGAGAGAAGAAG	ΔluxO F1
BBC375	gtcgacggatccccggaatCATGAGGACATATTTTGTTTTCTGC	ΔluxO R1
BBC376	gaagcagctccagcctacaTAAGCGATGAGAGAATGGATCAAC	ΔluxO F2
BBC377	TCACACCCGAATTTCCATCATGC	ΔluxO R2
ABD344	GATTAGCAACGATTCTAGCGCAGGAG	ΔVC1807 F1
ABD340	gtcgacggatccccggaatACGTTTCATTAGTCACCTCTATTGT TAACTTGTTC	ΔVC1807 R1
ABD341	gaagcagctccagcctacaTAGTCGAAAATAAAAAAAAGAGG CTCGCCTC	ΔVC1807 F2
ABD345	CTTGCTAACCGTTGGTGTTACCAGC	ΔVC1807 R2
pilA S81C F	AAAACTAATATTGAAGATTATATTGCGACAGAAGGC TgTTTTCCTGCAACAACTGCAGG	pilA S56C F
pilA R2	CATTAATCGCGGTTTCAAAGTGCA	pilA S56C R2
DOG0400	ACTTCTGGCTGAAGGTCAATTTTC	ΔpilT/U F1
DOG0401	gtcgacggatccccggaatCATTTAAATTCCTTAATAAAGTCTG GC	ΔpilT R1
DOG0402	gaagcagctccagcctacaTAGGTAGGTAAAGACAGATGGAG	ΔpilT F2
DOG0403	TCACGTGTTCGGCCAAAATC	ΔpilT/U R2
HQP0001	GGGCTCGGGTgctTCGACGACCTTGGCG	PilT ^{K136A} R1
HQP0002	CGCCAAGGTCGTCGAagcACCCGAGCCC	PilT ^{K136A} F2
BBC2508	GTTTCTTGGTCACGCAGagCACCGACGAGGATCAC	PilT ^{E204A} R1
BBC2509	GTGATCCTCGTCGGTGctCTGCGTGACCAAGAAAC	PilT ^{E204A} F2
BBC401	ACCAGCAAAGCTAATAAAATCGAG	ΔpilA F1
BBC402	gtcgacggatccccggaatGAGCATATGCCTTGCTACACAAG	ΔpilA R1
BBC403	gaagcagctccagcctacaACTGCAGGTGCAACAATTAACTAA	ΔpilA F2
BBC404	CGCCATACTAACCCAATACACTC	ΔpilA R2
BBC1752	CTGAATGATTTCCATGAGACG	ΔflaA F1
BBC1753	gtcgacggatccccggaatCATAGTTTGCTCTCCTATCGAG	ΔflaA R1
BBC1754	gaagcagctccagcctacaTTGCAGTAGTTCACGGTACCTTC	ΔflaA F2
BBC1755	TTATACGCTCTTTTGCGTGATGG	ΔflaA R2
BBC1450	CACTCAACGAGCTCAATACG	ΔmshA F1
ABD653	gtcgacggatccccggaatCATCTCTCTTTCATGTGAATACGCA GC	ΔmshA R1
ABD654	gaagcagctccagcctacaGCGCAATAATTTAAATATGGCTCG TGC	ΔmshA F2

BBC1453	ATAGCCTTGCTGTTCATTTTGG	ΔmshA R2
BBC2022	TGCCGATCTCGTTTATGGACG	Δvps-rbmA locus F1
BBC2023	gtcgacggatccccggaatTGCCATTTTGATTGCCTCTGG	Δvps-rbmA locus R1
BBC2024	gaagcagctccagcctacaCAAAGAGAGCCTTATTAGGCTCTC	Δvps-rbmA locus F2
BBC2025	TGAAAGAGGTTGCTCTAGAACTCG	Δvps-rbmA locus R2
BBC1457	TTTCAAGACTTTGGGCAATAG	ΔtcpA F1
BBC1968	gtcgacggatccccggaatCTGTTTTAATAATTGCATATTTATA TAACTCCACC	ΔtcpA R1
BBC1969	gaagcagctccagcctacaTTTGGTAACAGTTAATCTACACCAT TATCTTG	ΔtcpA F2
BBC1463	TTGAATTCGTCCATCATCTAAG	ΔtcpA R2
BBC1833	GATATCCATGTCCATGTCCCAG	comEA-mCherry F1
BBC1834	cttgctcactccaccacttccacctgcTAACAAGATCCTTGCGGCATTG	comEA-mCherry R1
BBC1837	acgagctgtacaagtaaGCTGCAATCATGTGTCTCG	comEA-mCherry F2
BBC1838	GTCTTTCTATCAGTTCGGACTTAGTC	comEA-mCherry R2
BBC1835	gcaggtggaagtggtggaGTGAGCAAGGGCGAGGAGG	mCherry (for comEAmCherry) F
BBC1836	gattgcagcTTACTTGTACAGCTCGTCC	mCherry (for comEAmCherry) R
DOG0405	gtcgacggatccccggaatCATCTGTCTTTACCTACCTAAAATGC	ΔpilU R1
DOG0406	gaagcagctccagcctacaTAGCGATGGTTACTTTGTGCG	ΔpilU F2
JCP048	CAAGCCCCCGATATGATTTgcATTGGTGAAATCCGCAGC	PilU ^{L199C} F
JCP049	GCTGCGGATTTCACCAATgcAAATCATATCGGGGGCTTG	PilU ^{L199C} R
BBC2287	CATTGCGCTCGGCATTGCGTGAAGACCCAGATGTGATCtgtGTCGGTGAGCTGCGTGAC	PilT ^{L201C} F2
BBC2288	CGCAATGCCGAGCGCAATG	PilT ^{L201C} R1
BBC2369	GGCTGCCATAGTGGTCGAggcACCCGAACCGGTTGCGC	PilU ^{K134A} R1
BBC2347	GCGCAACCGGTTCGGGTgccTCGACCACTATGGCAGCC	PilU ^{K134A} F2
BBC2313	gcaggtggaagtggtggaCATCATCATCATCATCACgcaggtggagcaggtgga	6xHis (for 6xHis-PilU/T) F
BBC2314	tccacctgctccacctgcGTGATGATGATGATGATGtccaccacttccacctgc	6xHis (for 6xHis-PilU/T) R
BBC2272	gcaggtggaagtggtggagattataaagaccatgatggtgactacaaggatcacgacattgattataaggatgacgatgacaaagcaggtggagcaggtgga	3xFLAG (for 3xFLAG-PilU/T) F
BBC2273	tccacctgctccacctgctttgtcatcgtcatccttataatcaatgtcgtgatccttgtagtcaccatcatggtctttataatctccaccacttccacctgc	3xFLAG (for 3xFLAG-PilU/T) R
JCP028	tccaccacttccacctgcCATCTGTCTTTACCTACCTAAAATGC	X-PilU (N-term tags) R1

JCP029	gcaggtggagcaggtggaGAGTTGAATCAATATCTGGATGGC	X-PilU (N-term tags OR BACTH TXX-pilU) F2
JCP026	tccaccacttccacctgcCATTTAAATTCCTTAATAAAGTCTGGCTATG	X-PilT (N-term tags) R1
JCP027	gcaggtggagcaggtggaGATATCGCTGAGTTACTGGAATTTAG	X-PilT (N-term tags or BACTH TXX-pilT) F2
ABD332	GGCTGAACGTGGTTGTCGAAAATGAC	P_{tac}-PilT/U @lacZ F1
BBC244	CCCGGGATCCTGTGTGAAATTGTTATCCGC	P_{tac}-PilT/U @lacZ or @VC1807 R1
ABD255	TTAAGCTACTAAAGCGTAGTTTTCG	P_{tac}-PilT/U @lacZ F2
ABD256	CAATTTCACACAGGATCCCGGGAGGAGGTAACGTAATGGTGAGCAAAGGCGAAG	P_{tac}-PilT/U @lacZ R2
BBC1723	caatttcacacaggatcccgggAGGAGGTATTTAAATGGATATCGCTGAGTTAC	Amplify pilT (for P_{tac}-pilT) F
BBC1724	tgtaggctggagctgcttcCTAAAATGCTTTTAAATCCAACTCG	Amplify pilT (for P_{tac}-pilT OR BACTH TXX-pilT) R
BBC1725	caatttcacacaggatcccgggAGGAGGTAGACAGATGGAGTTGAATCAATATC	Amplify pilU (for P_{tac}-pilU) F
BBC1726	tgtaggctggagctgcttcCTACTCCATATCAATCTTCACATTC	Amplify pilU (for P_{tac}-pilU OR BACTH TXX-pilU) R
ABD342	ATTTTTCAGTTGGCCTACAATGCTTTCC	P_{tac}-PilT/U @VC1807 F1
BBC719	CACCATACCCACGCCGAAACAAGGATTTTGAATTAAACGTTTCATTAGTC	P_{tac}-PilT/U @VC1807 R1
BBC243	TTGTTTCGGCGTGGGTATGGTG	P_{tac}-PilT/U @VC1807 F2
BBC2667	tccaccacttccacctgcCATTACGTTACCTCCTCCCG	P_{tac}-X-PilT/U (X is 3xFLAG or 6xHis) R
BBC2513	gaagcagctccagcctacaGATCCCCGGGTACCTAAGTAAC	BACTH pKT25-X F
BBC2512	tccacctgctccacctgcCTCTAGAGTCGACCCTGCAG	BACTH pKT25-X R
BBC2515	gaagcagctccagcctacaCCGAGCTCGAATTCATCGATATAAC	BACTH pUT18C-X F
BBC2514	tccacctgctccacctgcCTCTAGAGTCGACCTGCAG	BACTH pUT18C-X R
BBC2518	gcaggtggagcaggtggaAAAGCGACCCAAACCTTACC	BACTH TXX-PilC F
BBC2524	tgtaggctggagctgcttcTTAACCCAATACACTCATTAAGTTAAAG	BACTH TXX-PilC R
BBC2358	GGTATATCTCCTTCTTAAAGTTAAACAAAATTATTTCTAGAGGGGAATTGTTATCC	pHisTev-X F
BBC2360	cggatccGGCTGCTAACAAAGCCCGAAAGGAAGCTGAGTTGGCTGCTGC	pHisTev-X R
BBC2478	TTTTGTTTAACTTTAAGAAGGAGATATACCATGgcaggtggaagtggtgga	Amplify 6xHis-pilT or 6xHis-PilU to clone into pHistev F
BBC2479	CCTTTCGGGCTTTGTTAGCAGCCggatccgCTAAAATGCTTTTAAATCCAACTCG	Amplify 6xHis-pilT to clone into pHistev R
BBC2480	CCTTTCGGGCTTTGTTAGCAGCCggatccgCTACTCCATATCAATCTTCACATTCTG	Amplify 6xHis-pilU to clone into pHistev R
BBC706	CCACACATTATACGAGCCGATG	P_{const}-tfoX R1
BBC2226	catcggctcgtataatgtgtggaGGGGAACGTGATTAAAGGA	P_{const}-tfoX F2

ABD332	GGCTGAACGTGGTTGTCGAAAATGAC	ΔlacZ::lacIq F1
ABD331	GAACATGGGGTGTACGGCAGTGCtATTTAACGATGTGCGGGTTTTGCCAATCTTG	ΔlacZ::lacIq R1
ABD255	gaagcagctccagcctacaCCACAATAAGCCAGAGAGCCTTAAG	ΔlacZ::lacIq F2
ABD256	CCCAAATACGGCAACTTGGCG	ΔlacZ::lacIq R2
ABD841	GGCACTGCCGTACACCCCATGTTCCGGTACCCGACACCATCGAATG	Amplify lacIq F
ABD842	GGCTCTCTGGCTTATTGTGGGGGGAAACCTGTCGTGCCAGCTGC	Amplify lacIq R
DOG0175	AAACTATCCAGATAAGGGAAAGC	comP (*A. baylyi*) F1
CE87	GAAGTTGTCGTACATTTCCAacaTACAGCGCCACTAGCATATG	comP T129C (*A. baylyi*) R1
CE88	CATATGCTAGTGGCGCTGTATGTTGGAAATGTACGACAACTTC	comP T129C (*A. baylyi*) F2
DOG0178	AGGATCTGTAATGACGGGTTGAG	comP (*A. baylyi*) R2
DOG0176	gtcgacggatccccggaatCATAAAATTTCTCCACCAATGTTG	ΔcomP (*A. baylyi*) R1
DOG0177	gaagcagctccagcctacaTGATAGTAGTACTATATGGCTTTAAAAG	ΔcomP (*A. baylyi*) F2
BBC1934	GTTACAAAGTCAGGGACGTAAAG	pilT or pilU (*A. baylyi*) F1
BBC1935	gtcgacggatccccggaatATCCATATTTTCCCCGAAGATCG	ΔpilT (*A. baylyi*) R1
BBC1936	gaagcagctccagcctacaTAAGAATAACGCTACTCGATCTG	ΔpilT (*A. baylyi*) F2
BBC1939	GGTATTCAGATTGATCGTCAGTTAG	pilT or pilU (*A. baylyi*) R2
BBC1937	gtcgacggatccccggaatCATCGTATTGTTTTCCTCTCAGATC	ΔpilU (*A. baylyi*) R1
BBC1938	gaagcagctccagcctacaCGCCGTAATCTCAAATAAAAGAG	ΔpilU (*A. baylyi*) F2
BBC2403	GCTGCAAGGGTGGTTGAagcACCGGAACCAGTGG	pilT^{K136A} (*A. baylyi*) R1
BBC2404	CCACTGGTTCCGGTgctTCAACCACCCTTGCAGC	pilT^{K136A} (*A. baylyi*) F2
BBC2408	GGATGCCAAAGACGTGGAagcTCCTGTACCAGTTGC	pilU^{K137A} (*A. baylyi*) R1
BBC2409	GCAACTGGTACAGGAgctTCCACGTCTTTGGCATCC	pilU^{K137A} (*A. baylyi*) F2
BBC2807	caatttcacacaggatcccgggAGGAGGTGAAAATATGGATATAACAGAATTACTCG	pilT amplify for insertion into P_{tac} construct (*A. baylyi*) F
BBC2808	tgtaggctggagctgcttcTTAGAACGACTCTGGAGATTTTG	pilT amplify for insertion into P_{tac} construct or pMMB67EH (*A. baylyi*) R
BBC2809	caatttcacacaggatcccgggAGGAGGTAATACGATGGACTTTAATGATTTACTC	pilU amplify for insertion into P_{tac} construct (*A. baylyi*) F
BBC2810	tgtaggctggagctgcttcTTATTTGAGATTACGGCGTTGAC	pilU amplify for insertion into P_{tac} construct or pMMB67EH (*A. baylyi*) R

BBC2822	aatttcacacaggaaacagaattcgagctcTTGTTTCGGCGTGGGTATGGTG	Clone P_{tac}-pilT or P_{tac}-PilU into pMMB67EH (*A. baylyi*) F
BBC2824	gagctcgaattctgtttcctgtgtgaaattTTTGCCAGAACCGTTATGATGTC	Amplify pMMB67EH to clone P_{tac}-pilT or P_{tac}-pilU (*A. baylyi*) F
BBC2357	GGTACCCGGGGATCCTCTAGAGTCGACCTGCAGGCATGCAAGCTTGGC	Amplify pMMB67EH to clone P_{tac}-pilT or P_{tac}-pilU (*A. baylyi*) R
DOG0436	AAGCGTTCTGGTTCAATCACC	ΔMSHA locus (VC0399-VC0414) F1
DOG0434	gtcgacggatccccggaatCATTCTCTACCACTGCTATTTGGTTC	ΔMSHA locus (VC0399-VC0414) R1
BBC2129	gaagcagctccagcctacaTAATGATTAAGCACTCAATGGATCCAG	ΔMSHA locus (VC0399-VC0414) F2
BBC2130	TTTTGCATCAGCAAAATCACGC	ΔMSHA locus (VC0399-VC0414) R2
BBC2123	TGATGGTAACTACTATAGGGTCG	ΔTCP locus (VC0825-VC0838) F1
BBC2124	gtcgacggatccccggaatTAAATTAGGCTAGTGCCAGTCAG	ΔTCP locus (VC0825-VC0838) R1
BBC2125	gaagcagctccagcctacaACAGGAGTTGCAGAAAAATAATGG	ΔTCP locus (VC0825-VC0838) F2
BBC2126	ACTAAGATAATTGCTTCACGCATG	ΔTCP locus (VC0825-VC0838) R2

S3 Table. Mean values for each data set

Figure	Strain Name	Mean		Figure	Strain Name	Mean
Fig 1A	Parent	1.08E-01		S2 Fig	PilT x PilT	1.67E+02
Fig 1A	ΔpilA	1.22E-08		S2 Fig	PilU x PilT	6.10E+01
Fig 1A	ΔpilU	5.78E-02		S2 Fig	$PilT^{K136A}$ x PilT	1.57E+02
Fig 1A	ΔpilT	3.29E-06		S2 Fig	$PilU^{K134A}$ x PilT	8.23E+01
Fig 1A	ΔpilTΔpilU	3.91E-06		S2 Fig	PilC x PilT	1.15E+02
Fig 1A	$pilT^{K136A}$	6.22E-02		S2 Fig	vector x PilT	1.13E+00
Fig 1A	$pilT^{K136A}$ ΔpilU	3.89E-06		S2 Fig	PilT x PilU	1.10E+02
Fig 1A	$pilT^{E204A}$	2.55E-02		S2 Fig	PilU x PilU	1.81E+02
Fig 1A	$pilT^{K136A/E204A}$	3.53E-02		S2 Fig	$PilT^{K136A}$ x PilU	7.37E+01
Fig 1A	$pilT^{E204A}$ ΔpilU	9.36E-06		S2 Fig	$PilU^{K134A}$ x PilU	2.11E+02
Fig 1A	$pilT^{K136A/E204A}$ ΔpilU	4.66E-06		S2 Fig	PilC x PilU	9.71E+01
Fig 1B	Parent	2.12E-01		S2 Fig	vector x PilU	1.04E+00
Fig 1B	ΔpilU	1.57E-01		S2 Fig	PilT x $PilT^{K136A}$	1.56E+02
Fig 1B	ΔpilT	3.07E-03		S2 Fig	PilU x $PilT^{K136A}$	7.99E+00
Fig 1B	ΔpilTΔpilU	3.85E-03		S2 Fig	$PilT^{K136A}$ x $PilT^{K136A}$	8.06E+01
Fig 1B	$pilT^{K136A}$	4.26E-02		S2 Fig	$PilU^{K134A}$ x $PilT^{K136A}$	1.04E+01
Fig 1B	$pilT^{K136A}$ ΔpilU	2.06E-03		S2 Fig	PilC x $PilT^{K136A}$	1.08E+02
Fig 1B	$pilT^{E204A}$	4.82E-02		S2 Fig	vector x $PilT^{K136A}$	7.32E-01
Fig 1B	$pilT^{E204A/K136A}$	6.12E-02		S2 Fig	PilT x $PilU^{K134A}$	7.20E+01
Fig 1B	$pilT^{E204A}$ ΔpilU	3.58E-03		S2 Fig	PilU x $PilU^{K134A}$	1.72E+02
Fig 1B	$pilT^{E204A/K136A}$ ΔpilU	4.09E-03		S2 Fig	$PilT^{K136A}$ x $PilU^{K134A}$	4.69E+01
Fig 1C	Parent	1.73E+01		S2 Fig	$PilU^{K134A}$ x $PilU^{K134A}$	1.34E+02
Fig 1C	ΔpilU	3.16E+01		S2 Fig	PilC x $PilU^{K134A}$	1.10E+02
Fig 1C	ΔpilT	2.93E-02		S2 Fig	vector x $PilU^{K134A}$	7.14E-01
Fig 1C	ΔpilTΔpilU	1.33E-01		S2 Fig	PilT x PilC	8.69E+01
Fig 1C	$pilT^{K136A}$	3.43E+01		S2 Fig	PilU x PilC	5.20E+01
Fig 1C	$pilT^{K136A}$ ΔpilU	8.75E-02		S2 Fig	$PilT^{K136A}$ x PilC	7.43E+01
Fig 1C	$pilT^{E204A}$	1.41E-01		S2 Fig	$PilU^{K134A}$ x PilC	7.25E+01
Fig 1C	$pilT^{E204A/K136A}$	1.77E+01		S2 Fig	PilC x PilC	2.55E+02
Fig 1C	$pilT^{E204A}$ΔpilU	5.65E-02		S2 Fig	vector x PilC	8.15E-01
Fig 1C	$pilT^{E204A/K136A}$ΔpilU	3.86E-02		S2 Fig	PilT x vector	6.59E-01
Fig 1F	Parent	1.05E+01		S2 Fig	PilU x vector	7.85E-01
Fig 1F	ΔpilT	4.93E+00		S2 Fig	$PilT^{K136A}$ x vector	6.81E-01
Fig 1F	ΔpilU	5.08E+00		S2 Fig	$PilU^{K134A}$ x vector	7.14E-01
Fig 1F	ΔpilTΔpilU	6.08E+00		S2 Fig	PilC x vector	7.68E-01
Fig 1H	Parent	1.93E-01		S2 Fig	vector x vector	7.22E-01
Fig 1H	ΔpilT	1.37E-02		S3-A Fig	Parent	1.46E-01

Fig 1H	ΔpilU	7.23E-02
Fig 1H	ΔpilTΔpilU	8.19E-03
Fig 2A	Parent	1.37E-01
Fig 2A	pilU^{L199C}	1.51E-01
Fig 2A	pilT^{K136A}pilU^{L199C}	9.81E-02
Fig 2A	ΔpilT pilU^{L199C}	6.79E-06
Fig 2A	pilT^{L201C}	2.04E-01
Fig 2A	pilT^{L201C} ΔpilU	6.47E-02
Fig 2A	pilT^{K136A}	1.17E-01
Fig 2A	pilU^{K134A}	6.33E-02
Fig 2A	pilT^{K136A}pilU^{K134A}	6.07E-07
Fig 2A	ΔpilU	8.80E-02
Fig 2B	Parent	2.12E-01
Fig 2B	ΔpilU	1.57E-01
Fig 2B	pilT^{K136A}	4.26E-02
Fig 2B	pilU^{K134A}	1.37E-01
Fig 2B	pilT^{K136A}pilU^{K134A}	4.77E-03
Fig 2B	pilT^{K136A} pilU^{L199C}	3.26E-02
Fig 2B	pilU^{L199C}	1.96E-01
Fig 2B	pilT^{L201C}	2.11E-01
Fig 2B	pilT^{L201C}ΔpilU	1.28E-01
Fig 2B	ΔpilT pilU^{L199C}	3.91E-03
Fig 4C	Parent	2.02E-03
Fig 4C	ΔpilU	2.57E-03
Fig 4C	ΔpilT	1.57E-06
Fig 4C	pilT^{K136A}	3.08E-03
Fig 4C	Ptac-pilT^{K136A}	5.94E-03

S3-A Fig	ΔpilT	6.94E-06
S3-A Fig	pilT^{K136A}, 6xHis-pilU	1.53E-01
S3-A Fig	6xHis-pilT	1.14E-01
S3-A Fig	6xHis-pilU	1.11E-01
S3-A Fig	pilT^{K136A}, 3xFLAG-pilU	1.14E-01
S3-A Fig	3xFLAG-pilT	1.45E-01
S3-A Fig	3xFLAG-pilU	1.23E-01
S3-A Fig	pilT^{K136A}	1.20E-01
S3-B Fig	Parent	3.75E-03
S3-B Fig	ΔpilT	4.46E-07
S3-B Fig	Ptac-3xFLAG-pilT	4.60E-03
S3-B Fig	Ptac-3xFLAG-pilT ΔpilT	4.94E-03
S3-B Fig	Ptac-3xFLAG-pilU	2.78E-03
S3-B Fig	Ptac-3xFLAG-pilU, pilT^{K136A} ΔpilU	1.66E-03
S3-B Fig	Ptac-3xFLAG-pilT^{K136A}	5.66E-03
S3-B Fig	Ptac-3xFLAG-pilU^{K134A}	4.71E-03
S3-B Fig	Ptac-3xFLAG-pilT^{K136A}, ΔpilU	1.25E-06
S3-B Fig	P_{tac}-3xFLAG-pilU^{K134A}, pilT^{K136A}	2.00E-06
S3-B Fig	ΔpilU	2.48E-03
S3-B Fig	pilT^{K136A}	2.24E-03
S3-D Fig	Parent	1.97E-03
S3-D Fig	ΔpilT ΔpilU	2.15E-07
S3-D Fig	pilU^{K134A}	3.90E-03
S3-D Fig	pilT^{K136A} ΔpilU	3.62E-08
S3-D Fig	pilT^{K136A} pilU^{K134A}	2.12E-07
S3-D Fig	P_{tac}-pilT	4.18E-03
S3-D Fig	ΔpilT Ptac-pilT	4.08E-03

Fig 4C	Ptac-pilT^{K136A} ΔpilU	2.41E-06		S3-D Fig	P_{tac}-pilU	4.07E-03
Fig 4C	Ptac-pilU^{K134A}	5.55E-03		S3-D Fig	pilT^{K136A} ΔpilU Ptac-pilU	1.39E-03
Fig 4C	Ptac-pilU^{K134A} pilT^{K136A}	2.46E-05		S3-D Fig	ΔpilA	6.49E-09
Fig 4C	Ptac-pilT^{K136A} Ptac-pilU^{K134A}	4.82E-06		S3-D Fig	pilT^{K136A}	1.75E-03
Fig 5	pilT^{K136A} ΔpilU	8.95E-09		S4 Fig	Parent pmmB-pilT	2.23E-02
Fig 5	pilT^{K136A} pilU^{K137A}	7.00E-09		S4 Fig	ΔpilTU pmmB-pilT	2.05E-03
Fig 5	pilT^{K136A}	1.17E-03		S4 Fig	ΔpilT pmmB-pilT	1.80E-02
Fig 5	pilU^{K137A}	2.34E-03		S4 Fig	ΔpilU pmmB-pilT	3.24E-03
Fig 5	Parent	4.10E-02		S4 Fig	pilT^{K136A} pmmB-pilT	1.68E-02
Fig 5	ΔpilT	8.52E-09		S4 Fig	pilT^{K136A} ΔpilU pmmB-pilT	2.30E-03
Fig 5	ΔpilU	3.17E-03		S4 Fig	pilU^{K137A} pmmB-pilT	1.63E-03
Fig 5	ΔpilTU	8.48E-09		S4 Fig	pilT^{K136A} pilU^{K137A} pmmB-pilT	2.19E-03
Fig 5	ΔcomP	6.53E-09		S4 Fig	Parent pmmB-pilU	8.67E-02
S1 Fig	ΔpilT ΔpilU Ptac-PilT	7.05E-02		S4 Fig	ΔpilTU pmmB-pilU	2.04E-07
S1 Fig	ΔpilT ΔpilU Ptac-PilU	7.26E-06		S4 Fig	ΔpilT pmmB-pilU	1.55E-07
S1 Fig	pilT^{K136A} ΔpilU Ptac-PilT	6.53E-02		S4 Fig	ΔpilU pmmB-pilU	2.48E-02
S1 Fig	pilT^{K136A} ΔpilU Ptac-PilU	6.27E-02		S4 Fig	pilT^{K136A} pmmB-pilU	7.66E-04
S1 Fig	pilT^{K136A} pilU^{K134A} Ptac-PilT	4.21E-02		S4 Fig	pilT^{K136A} ΔpilU pmmB-pilU	8.35E-04
S1 Fig	pilT^{K136A} pilU^{K134A} Ptac-PilU	4.65E-02		S4 Fig	pilU^{K137A} pmmB-pilU	1.07E-02
S1 Fig	Parent Ptac-PilT	6.74E-02		S4 Fig	pilT^{K136A} pilU^{K137A} pmmB-pilU	9.52E-04
S1 Fig	Parent Ptac-PilU	8.85E-02		S4 Fig	Parent pmmB-pilU	2.66E-02
S1 Fig	ΔpilT Ptac-PilT	6.55E-02		S5 Fig	Parent	3.12E-01
S1 Fig	ΔpilT Ptac-PilU	3.13E-06		S5 Fig	ΔMSHA ΔTCP	3.73E-01
S1 Fig	pilT$^{K136A/E204A}$ ΔpilU Ptac-PilT	6.32E-02		S5 Fig	ΔpilTU	1.59E-05
S1 Fig	pilT$^{K136A/E204A}$ ΔpilU Ptac-PilU	4.05E-02		S5 Fig	ΔpilTU ΔMSHA ΔTCP	3.34E-05
S1 Fig	pilT^{E204A} ΔpilU Ptac-PilT	6.02E-02				
S1 Fig	pilT^{E204A} ΔpilU Ptac-PilU	7.81E-02				

S4 Table. Statistical Comparisons.

Comparison	P value[#]		Information
Figure 1A - Tukey's multiple comparison test			
Parent vs. ΔpilA	****	<0.0001	# of families = 1
Parent vs. ΔpilU	ns	0.6432	# of comparisons per family = 55
Parent vs. ΔpilT	****	<0.0001	Alpha = 0.05
Parent vs. ΔpilTΔpilU	****	<0.0001	
Parent vs. pilT^{K136A}	ns	0.804	
Parent vs. pilT^{K136A} ΔpilU	****	<0.0001	
Parent vs. pilT^{E204A}	****	<0.0001	
Parent vs. pilT$^{K136A/E204A}$	*	0.0135	
Parent vs. pilT^{E204A} ΔpilU	****	<0.0001	
Parent vs. pilT$^{K136A/E204A}$ ΔpilU	****	<0.0001	
ΔpilA vs. ΔpilU	****	<0.0001	
ΔpilA vs. ΔpilT	****	<0.0001	
ΔpilA vs. ΔpilTΔpilU	****	<0.0001	
ΔpilA vs. pilT^{K136A}	****	<0.0001	
ΔpilA vs. pilT^{K136A} ΔpilU	****	<0.0001	
ΔpilA vs. pilT^{E204A}	****	<0.0001	
ΔpilA vs. pilT$^{K136A/E204A}$	****	<0.0001	
ΔpilA vs. pilT^{E204A} ΔpilU	****	<0.0001	
ΔpilA vs. pilT$^{K136A/E204A}$ ΔpilU	****	<0.0001	
ΔpilU vs. ΔpilT	****	<0.0001	
ΔpilU vs. ΔpilTΔpilU	****	<0.0001	
ΔpilU vs. pilT^{K136A}	ns	>0.9999	
ΔpilU vs. pilT^{K136A} ΔpilU	****	<0.0001	
ΔpilU vs. pilT^{E204A}	ns	0.0523	
ΔpilU vs. pilT$^{K136A/E204A}$	ns	0.8854	
ΔpilU vs. pilT^{E204A} ΔpilU	****	<0.0001	
ΔpilU vs. pilT$^{K136A/E204A}$ ΔpilU	****	<0.0001	
ΔpilT vs. ΔpilTΔpilU	ns	>0.9999	
ΔpilT vs. pilT^{K136A}	****	<0.0001	
ΔpilT vs. pilT^{K136A} ΔpilU	ns	>0.9999	
ΔpilT vs. pilT^{E204A}	****	<0.0001	
ΔpilT vs. pilT$^{K136A/E204A}$	****	<0.0001	
ΔpilT vs. pilT^{E204A} ΔpilU	ns	0.1222	
ΔpilT vs. pilT$^{K136A/E204A}$ ΔpilU	ns	0.994	
ΔpilTΔpilU vs. pilT^{K136A}	****	<0.0001	
ΔpilTΔpilU vs. pilT^{K136A} ΔpilU	ns	>0.9999	
ΔpilTΔpilU vs. pilT^{E204A}	****	<0.0001	
ΔpilTΔpilU vs. pilT$^{K136A/E204A}$	****	<0.0001	

ΔpilTΔpilU vs. pilT^{E204A} ΔpilU	ns	0.1655	
ΔpilTΔpilU vs. pilT$^{K136A/E204A}$ ΔpilU	ns	0.9983	
pilT^{K136A} vs. pilT^{K136A} ΔpilU	****	<0.0001	
pilT^{K136A} vs. pilT^{E204A}	*	0.03	
pilT^{K136A} vs. pilT$^{K136A/E204A}$	ns	0.7787	
pilT^{K136A} vs. pilT^{E204A} ΔpilU	****	<0.0001	
pilT^{K136A} vs. pilT$^{K136A/E204A}$ ΔpilU	****	<0.0001	
pilT^{K136A} ΔpilU vs. pilT^{E204A}	****	<0.0001	
pilT^{K136A} ΔpilU vs. pilT$^{K136A/E204A}$	****	<0.0001	
pilT^{K136A} ΔpilU vs. pilT^{E204A} ΔpilU	ns	0.1909	
pilT^{K136A} ΔpilU vs. pilT$^{K136A/E204A}$ ΔpilU	ns	0.9992	
pilT^{E204A} vs. pilT$^{K136A/E204A}$	ns	0.7599	
pilT^{E204A} vs. pilT^{E204A} ΔpilU	****	<0.0001	
pilT^{E204A} vs. pilT$^{K136A/E204A}$ ΔpilU	****	<0.0001	
pilT$^{K136A/E204A}$ vs. pilT^{E204A} ΔpilU	****	<0.0001	
pilT$^{K136A/E204A}$ vs. pilT$^{K136A/E204A}$ ΔpilU	****	<0.0001	
pilT^{E204A} ΔpilU vs. pilT$^{K136A/E204A}$ ΔpilU	ns	0.6405	
Figure 1B - Tukey's multiple comparison test			
Parent vs. ΔpilU	****	<0.0001	# of families = 1
Parent vs. ΔpilT	****	<0.0001	# of comparisons per family = 45
Parent vs. ΔpilTΔpilU	****	<0.0001	Alpha = 0.05
Parent vs. pilT^{K136A}	****	<0.0001	
Parent vs. pilT^{K136A} ΔpilU	****	<0.0001	
Parent vs. pilT^{E204A}	****	<0.0001	
Parent vs. pilT$^{E204A/K136A}$	****	<0.0001	
Parent vs. pilT^{E204A} ΔpilU	****	<0.0001	
Parent vs. pilT^{E204A}/^{K136A} ΔpilU	****	<0.0001	
ΔpilU vs. ΔpilT	****	<0.0001	
ΔpilU vs. ΔpilTΔpilU	****	<0.0001	
ΔpilU vs. pilT^{K136A}	****	<0.0001	
ΔpilU vs. pilT^{K136A} ΔpilU	****	<0.0001	
ΔpilU vs. pilT^{E204A}	****	<0.0001	
ΔpilU vs. pilT^{E204A}/^{K136A}	****	<0.0001	
ΔpilU vs. pilT^{E204A} ΔpilU	****	<0.0001	
ΔpilU vs. pilT^{E204A}/^{K136A} ΔpilU	****	<0.0001	
ΔpilT vs. ΔpilTΔpilU	ns	>0.9999	
ΔpilT vs. pilT^{K136A}	ns	0.0674	
ΔpilT vs. pilT^{K136A} ΔpilU	ns	>0.9999	
ΔpilT vs. pilT^{E204A}	ns	0.4312	
ΔpilT vs. pilT^{E204A}/^{K136A}	***	0.0005	
ΔpilT vs. pilT^{E204A} ΔpilU	ns	>0.9999	
ΔpilT vs. pilT^{E204A}/^{K136A} ΔpilU	ns	>0.9999	

ΔpilTΔpilU vs. pilT^{K136A}	**	0.0027	
ΔpilTΔpilU vs. pilT^{K136A} ΔpilU	ns	>0.9999	
ΔpilTΔpilU vs. pilT^{E204A}	ns	0.3118	
ΔpilTΔpilU vs. pilT$^{E204A/K136A}$	****	<0.0001	
ΔpilTΔpilU vs. pilT^{E204A} ΔpilU	ns	>0.9999	
ΔpilTΔpilU vs. pilT$^{E204A/K136A}$ ΔpilU	ns	>0.9999	
pilT^{K136A} vs. pilT^{K136A} ΔpilU	ns	0.0538	
pilT^{K136A} vs. pilT^{E204A}	ns	>0.9999	
pilT^{K136A} vs. pilT$^{E204A/K136A}$	ns	0.1608	
pilT^{K136A} vs. pilT^{E204A} ΔpilU	**	0.0034	
pilT^{K136A} vs. pilT$^{E204A/K136A}$ ΔpilU	ns	0.2706	
pilT^{K136A} ΔpilU vs. pilT^{E204A}	ns	0.3977	
pilT^{K136A} ΔpilU vs. pilT$^{E204A/K136A}$	***	0.0004	
pilT^{K136A} ΔpilU vs. pilT^{E204A} ΔpilU	ns	>0.9999	
pilT^{K136A} ΔpilU vs. pilT$^{E204A/K136A}$ ΔpilU	ns	>0.9999	
pilT^{E204A} vs. pilT$^{E204A/K136A}$	ns	0.9989	
pilT^{E204A} vs. pilT^{E204A} ΔpilU	ns	0.3122	
pilT^{E204A} vs. pilT$^{E204A/K136A}$ ΔpilU	ns	0.5871	
pilT$^{E204A/K136A}$ vs. pilT^{E204A} ΔpilU	****	<0.0001	
pilT$^{E204A/K136A}$ vs. pilT$^{E204A/K136A}$ ΔpilU	*	0.0109	
pilT^{E204A} ΔpilU vs. pilT$^{E204A/K136A}$ ΔpilU	ns	>0.9999	
Figure 1C - Tukey's multiple comparison test			
Parent vs. ΔpilU	ns	>0.9999	# of families = 1
Parent vs. ΔpilT	****	<0.0001	# of comparisons per family = 45
Parent vs. ΔpilTΔpilU	****	<0.0001	Alpha = 0.05
Parent vs. pilT^{K136A}	ns	0.9963	
Parent vs. pilT^{K136A} ΔpilU	***	0.0002	
Parent vs. pilT^{E204A}	***	0.0006	
Parent vs. pilT$^{E204A/K136A}$	ns	>0.9999	
Parent vs. pilT^{E204A} ΔpilU	****	<0.0001	
Parent vs. pilT$^{E204A/K136A}$ ΔpilU	****	<0.0001	
ΔpilU vs. ΔpilT	****	<0.0001	
ΔpilU vs. ΔpilTΔpilU	****	<0.0001	
ΔpilU vs. pilT^{K136A}	ns	>0.9999	
ΔpilU vs. pilT^{K136A} ΔpilU	****	<0.0001	
ΔpilU vs. pilT^{E204A}	***	0.0002	
ΔpilU vs. pilT$^{E204A/K136A}$	ns	>0.9999	
ΔpilU vs. pilT^{E204A} ΔpilU	****	<0.0001	
ΔpilU vs. pilT$^{E204A/K136A}$ ΔpilU	****	<0.0001	
ΔpilT vs. ΔpilTΔpilU	ns	0.9878	
ΔpilT vs. pilT^{K136A}	****	<0.0001	
ΔpilT vs. pilT^{K136A} ΔpilU	ns	0.9085	

ΔpilT vs. pilT^{E204A}	ns	0.6143	
ΔpilT vs. pilT$^{E204A/K136A}$	****	<0.0001	
ΔpilT vs. pilT^{E204A} ΔpilU	ns	>0.9999	
ΔpilT vs. pilT$^{E204A/K136A}$ ΔpilU	ns	>0.9999	
ΔpilTΔpilU vs. pilT^{K136A}	****	<0.0001	
ΔpilTΔpilU vs. pilT^{K136A} ΔpilU	ns	>0.9999	
ΔpilTΔpilU vs. pilT^{E204A}	ns	0.9904	
ΔpilTΔpilU vs. pilT$^{E204A/K136A}$	****	<0.0001	
ΔpilTΔpilU vs. pilT^{E204A} ΔpilU	ns	>0.9999	
ΔpilTΔpilU vs. pilT$^{E204A/K136A}$ ΔpilU	ns	0.9718	
pilT^{K136A} vs. pilT^{K136A} ΔpilU	****	<0.0001	
pilT^{K136A} vs. pilT^{E204A}	****	<0.0001	
pilT^{K136A} vs. pilT$^{E204A/K136A}$	ns	0.9992	
pilT^{K136A} vs. pilT^{E204A} ΔpilU	****	<0.0001	
pilT^{K136A} vs. pilT$^{E204A/K136A}$ ΔpilU	****	<0.0001	
pilT^{K136A} ΔpilU vs. pilT^{E204A}	ns	0.9998	
pilT^{K136A} ΔpilU vs. pilT$^{E204A/K136A}$	***	0.0001	
pilT^{K136A} ΔpilU vs. pilT^{E204A} ΔpilU	ns	0.9936	
pilT^{K136A} ΔpilU vs. pilT$^{E204A/K136A}$ ΔpilU	ns	0.8538	
pilT^{E204A} vs. pilT$^{E204A/K136A}$	***	0.0004	
pilT^{E204A} vs. pilT^{E204A} ΔpilU	ns	0.8779	
pilT^{E204A} vs. pilT$^{E204A/K136A}$ ΔpilU	ns	0.5286	
pilT$^{E204A/K136A}$ vs. pilT^{E204A} ΔpilU	****	<0.0001	
pilT$^{E204A/K136A}$ vs. pilT$^{E204A/K136A}$ ΔpilU	****	<0.0001	
pilT^{E204A} ΔpilU vs. pilT$^{E204A/K136A}$ ΔpilU	ns	0.9996	
Figure 1F - Tukey's multiple comparison test			
Parent vs. ΔpilT	****	<0.0001	# of families = 1
Parent vs. ΔpilU	****	<0.0001	# of comparisons per family = 6
Parent vs. ΔpilTΔpilU	****	<0.0001	Alpha = 0.05
ΔpilT vs. ΔpilU	ns	0.9956	
ΔpilT vs. ΔpilTΔpilU	ns	0.5137	
ΔpilU vs. ΔpilTΔpilU	ns	0.738	
Figure 1H - Tukey's multiple comparison test			
Parent vs. ΔpilT	****	<0.0001	# of families = 1
Parent vs. ΔpilU	****	<0.0001	# of comparisons per family = 6
Parent vs. ΔpilTΔpilU	****	<0.0001	Alpha = 0.05
ΔpilT vs. ΔpilU	**	0.0028	
ΔpilT vs. ΔpilTΔpilU	ns	0.9806	
ΔpilU vs. ΔpilTΔpilU	**	0.0051	
Figure 2A - Tukey's multiple comparison test			
Parent vs. pilU^{L199C}	ns	>0.9999	# of families = 1
Parent vs. pilT^{K136A} pilU^{L199C}	ns	0.9978	# of comparisons per family = 45
Parent vs. ΔpilT pilU^{L199C}	****	<0.0001	Alpha = 0.05

Parent vs. pilT^{L201C}	ns	>0.9999	
Parent vs. pilT^{L201C} ΔpilU	ns	0.4971	
Parent vs. pilT^{K136A}	ns	>0.9999	
Parent vs. pilU^{K134A}	ns	0.4696	
Parent vs. pilT^{K136A} pilU^{K134A}	****	<0.0001	
Parent vs. ΔpilU	ns	0.9608	
pilU^{L199C} vs. pilT^{K136A} pilU^{L199C}	ns	0.9864	
pilU^{L199C} vs. ΔpilT pilU^{L199C}	****	<0.0001	
pilU^{L199C} vs. pilT^{L201C}	ns	0.9999	
pilU^{L199C} vs. pilT^{L201C} ΔpilU	ns	0.4266	
pilU^{L199C} vs. pilT^{K136A}	ns	>0.9999	
pilU^{L199C} vs. pilU^{K134A}	ns	0.403	
pilU^{L199C} vs. pilT^{K136A} pilU^{K134A}	****	<0.0001	
pilU^{L199C} vs. ΔpilU	ns	0.9085	
pilT^{K136A} pilU^{L199C} vs. ΔpilT pilU^{L199C}	****	<0.0001	
pilT^{K136A} pilU^{L199C} vs. pilT^{L201C}	ns	>0.9999	
pilT^{K136A} pilU^{L199C} vs. pilT^{L201C} ΔpilU	ns	0.9608	
pilT^{K136A} pilU^{L199C} vs. pilT^{K136A}	ns	>0.9999	
pilT^{K136A} pilU^{L199C} vs. pilU^{K134A}	ns	0.9525	
pilT^{K136A} pilU^{L199C} vs. pilT^{K136A} pilU^{K134A}	****	<0.0001	
pilT^{K136A} pilU^{L199C} vs. ΔpilU	ns	>0.9999	
ΔpilT pilU^{L199C} vs. pilT^{L201C}	****	<0.0001	
ΔpilT pilU^{L199C} vs. pilT^{L201C} ΔpilU	****	<0.0001	
ΔpilT pilU^{L199C} vs. pilT^{K136A}	****	<0.0001	
ΔpilT pilU^{L199C} vs. pilU^{K134A}	****	<0.0001	
ΔpilT pilU^{L199C} vs. pilT^{K136A} pilU^{K134A}	****	<0.0001	
ΔpilT pilU^{L199C} vs. ΔpilU	****	<0.0001	
pilT^{L201C} vs. pilT^{L201C} ΔpilU	ns	0.7827	
pilT^{L201C} vs. pilT^{K136A}	ns	>0.9999	
pilT^{L201C} vs. pilU^{K134A}	ns	0.7604	
pilT^{L201C} vs. pilT^{K136A} pilU^{K134A}	****	<0.0001	
pilT^{L201C} vs. ΔpilU	ns	0.9968	
pilT^{L201C} ΔpilU vs. pilT^{K136A}	ns	0.7609	
pilT^{L201C} ΔpilU vs. pilU^{K134A}	ns	>0.9999	
pilT^{L201C} ΔpilU vs. pilT^{K136A} pilU^{K134A}	****	<0.0001	
pilT^{L201C} ΔpilU vs. ΔpilU	ns	0.9969	
pilT^{K136A} vs. pilU^{K134A}	ns	0.7378	
pilT^{K136A} vs. pilT^{K136A} pilU^{K134A}	****	<0.0001	
pilT^{K136A} vs. ΔpilU	ns	0.9956	
pilU^{K134A} vs. pilT^{K136A} pilU^{K134A}	****	<0.0001	
pilU^{K134A} vs. ΔpilU	ns	0.9957	
pilT^{K136A} pilU^{K134A} vs. ΔpilU	****	<0.0001	

Figure 2B - Tukey's multiple comparison test			
Parent vs. ΔpilU	****	<0.0001	# of families = 1
Parent vs. pilT^{K136A}	****	<0.0001	# of comparisons per family = 45
Parent vs. pilU^{K134A}	****	<0.0001	Alpha = 0.05
Parent vs. pilT^{K136A} pilU^{K134A}	****	<0.0001	
Parent vs. pilT^{K136A} pilU^{L199C}	****	<0.0001	
Parent vs. pilU^{L199C}	ns	0.6117	
Parent vs. pilT^{L201C}	ns	>0.9999	
Parent vs. pilT^{L201C} ΔpilU	****	<0.0001	
Parent vs. ΔpilT pilU^{L199C}	****	<0.0001	
ΔpilU vs. pilT^{K136A}	****	<0.0001	
ΔpilU vs. pilU^{K134A}	ns	0.1821	
ΔpilU vs. pilT^{K136A} pilU^{K134A}	****	<0.0001	
ΔpilU vs. pilT^{K136A} pilU^{L199C}	****	<0.0001	
ΔpilU vs. pilU^{L199C}	***	0.0003	
ΔpilU vs. pilT^{L201C}	****	<0.0001	
ΔpilU vs. pilT^{L201C} ΔpilU	*	0.014	
ΔpilU vs. ΔpilT pilU^{L199C}	****	<0.0001	
pilT^{K136A} vs. pilU^{K134A}	****	<0.0001	
pilT^{K136A} vs. pilT^{K136A} pilU^{K134A}	ns	0.3556	
pilT^{K136A} vs. pilT^{K136A} pilU^{L199C}	ns	0.9694	
pilT^{K136A} vs. pilU^{L199C}	****	<0.0001	
pilT^{K136A} vs. pilT^{L201C}	****	<0.0001	
pilT^{K136A} vs. pilT^{L201C} ΔpilU	****	<0.0001	
pilT^{K136A} vs. ΔpilT pilU^{L199C}	ns	0.1504	
pilU^{K134A} vs. pilT^{K136A} pilU^{K134A}	****	<0.0001	
pilU^{K134A} vs. pilT^{K136A} pilU^{L199C}	****	<0.0001	
pilU^{K134A} vs. pilU^{L199C}	****	<0.0001	
pilU^{K134A} vs. pilT^{L201C}	****	<0.0001	
pilU^{K134A} vs. pilT^{L201C} ΔpilU	ns	0.9841	
pilU^{K134A} vs. ΔpilT pilU^{L199C}	****	<0.0001	
pilT^{K136A} pilU^{K134A} vs. pilT^{K136A} pilU^{L199C}	ns	0.8001	
pilT^{K136A} pilU^{K134A} vs. pilU^{L199C}	****	<0.0001	
pilT^{K136A} pilU^{K134A} vs. pilT^{L201C}	****	<0.0001	
pilT^{K136A} pilU^{K134A} vs. pilT^{L201C} ΔpilU	****	<0.0001	
pilT^{K136A} pilU^{K134A} vs. ΔpilT pilU^{L199C}	ns	>0.9999	
pilT^{K136A} pilU^{L199C} vs. pilU^{L199C}	****	<0.0001	
pilT^{K136A} pilU^{L199C} vs. pilT^{L201C}	****	<0.0001	
pilT^{K136A} pilU^{L199C} vs. pilT^{L201C} ΔpilU	****	<0.0001	
pilT^{K136A} pilU^{L199C} vs. ΔpilT pilU^{L199C}	ns	0.6067	
pilU^{L199C} vs. pilT^{L201C}	ns	0.7303	

pilU^{L199C} vs. pilT^{L201C} ΔpilU	****	<0.0001	
pilU^{L199C} vs. ΔpilT pilU^{L199C}	****	<0.0001	
pilT^{L201C} vs. pilT^{L201C} ΔpilU	****	<0.0001	
pilT^{L201C} vs. ΔpilT pilU^{L199C}	****	<0.0001	
pilT^{L201C} ΔpilU vs. ΔpilT pilU^{L199C}	****	<0.0001	
Figure 4C - Tukey's multiple comparison test			
Parent vs. ΔpilU	ns	>0.9999	# of families = 1
Parent vs. ΔpilT	****	<0.0001	# of comparisons per family = 36
Parent vs. pilT^{K136A}	ns	0.9998	Alpha = 0.05
Parent vs. Ptac-pilT^{K136A}	ns	0.9537	
Parent vs. Ptac-pilT^{K136A} ΔpilU	****	<0.0001	
Parent vs. Ptac-pilU^{K134A}	ns	0.9996	
Parent vs. Ptac-pilU^{K134A} pilT^{K136A}	****	<0.0001	
Parent vs. Ptac-pilT^{K136A} Ptac-pilU^{K134A}	****	<0.0001	
ΔpilU vs. ΔpilT	****	<0.0001	
ΔpilU vs. pilT^{K136A}	ns	>0.9999	
ΔpilU vs. Ptac-pilT^{K136A}	ns	0.9844	
ΔpilU vs. Ptac-pilT^{K136A} ΔpilU	****	<0.0001	
ΔpilU vs. Ptac-pilU^{K134A}	ns	>0.9999	
ΔpilU vs. Ptac-pilU^{K134A} pilT^{K136A}	****	<0.0001	
ΔpilU vs. Ptac-pilT^{K136A} Ptac-pilU^{K134A}	****	<0.0001	
ΔpilT vs. pilT^{K136A}	****	<0.0001	
ΔpilT vs. Ptac-pilT^{K136A}	****	<0.0001	
ΔpilT vs. Ptac-pilT^{K136A} ΔpilU	ns	0.9408	
ΔpilT vs. Ptac-pilU^{K134A}	****	<0.0001	
ΔpilT vs. Ptac-pilU^{K134A} pilT^{K136A}	ns	0.3939	
ΔpilT vs. Ptac-pilT^{K136A} Ptac-pilU^{K134A}	ns	0.542	
pilT^{K136A} vs. Ptac-pilT^{K136A}	ns	0.9988	
pilT^{K136A} vs. Ptac-pilT^{K136A} ΔpilU	****	<0.0001	
pilT^{K136A} vs. Ptac-pilU^{K134A}	ns	>0.9999	
pilT^{K136A} vs. Ptac-pilU^{K134A} pilT^{K136A}	****	<0.0001	
pilT^{K136A} vs. Ptac-pilT^{K136A} Ptac-pilU^{K134A}	****	<0.0001	
Ptac-pilT^{K136A} vs. Ptac-pilT^{K136A} ΔpilU	****	<0.0001	
Ptac-pilT^{K136A} vs. Ptac-pilU^{K134A}	ns	0.9994	
Ptac-pilT^{K136A} vs. Ptac-pilU^{K134A} pilT^{K136A}	****	<0.0001	
Ptac-pilT^{K136A} vs. Ptac-pilT^{K136A} Ptac-pilU^{K134A}	****	<0.0001	
Ptac-pilT^{K136A} ΔpilU vs. Ptac-pilU^{K134A}	****	<0.0001	
Ptac-pilT^{K136A} ΔpilU vs. Ptac-pilU^{K134A} pilT^{K136A}	ns	0.9789	
Ptac-pilT^{K136A} ΔpilU vs. Ptac-pilT^{K136A} Ptac-pilU^{K134A}	ns	0.9964	
Ptac-pilU^{K134A} vs. Ptac-pilU^{K134A} pilT^{K136A}	****	<0.0001	
Ptac-pilU^{K134A} vs. Ptac-pilT^{K136A} Ptac-pilU^{K134A}	****	<0.0001	

Ptac-pilU^{K134A} pilT^{K136A} vs. Ptac-pilT^{K136A} Ptac-pilU^{K134A}	ns	>0.9999	
Figure 5 - Tukey's multiple comparison test			
pilT^{K136A} ΔpilU vs. pilT^{K136A} pilU^{K137A}	ns	0.9546	# of families = 1
pilT^{K136A} ΔpilU vs. pilT^{K136A}	****	<0.0001	# of comparisons per family = 36
pilT^{K136A} ΔpilU vs. pilU^{K137A}	****	<0.0001	Alpha = 0.05
pilT^{K136A} ΔpilU vs. Parent	****	<0.0001	
pilT^{K136A} ΔpilU vs. ΔpilT	ns	>0.9999	
pilT^{K136A} ΔpilU vs. ΔpilU	****	<0.0001	
pilT^{K136A} ΔpilU vs. ΔpilTU	ns	>0.9999	
pilT^{K136A} ΔpilU vs. ΔcomP	ns	0.7185	
pilT^{K136A} pilU^{K137A} vs. pilT^{K136A}	****	<0.0001	
pilT^{K136A} pilU^{K137A} vs. pilU^{K137A}	****	<0.0001	
pilT^{K136A} pilU^{K137A} vs. Parent	****	<0.0001	
pilT^{K136A} pilU^{K137A} vs. ΔpilT	ns	0.9681	
pilT^{K136A} pilU^{K137A} vs. ΔpilU	****	<0.0001	
pilT^{K136A} pilU^{K137A} vs. ΔpilTU	ns	0.9694	
pilT^{K136A} pilU^{K137A} vs. ΔcomP	ns	>0.9999	
pilT^{K136A} vs. pilU^{K137A}	**	0.0082	
pilT^{K136A} vs. Parent	****	<0.0001	
pilT^{K136A} vs. ΔpilT	****	<0.0001	
pilT^{K136A} vs. ΔpilU	***	0.0003	
pilT^{K136A} vs. ΔpilTU	****	<0.0001	
pilT^{K136A} vs. ΔcomP	****	<0.0001	
pilU^{K137A} vs. Parent	****	<0.0001	
pilU^{K137A} vs. ΔpilT	****	<0.0001	
pilU^{K137A} vs. ΔpilU	ns	0.9315	
pilU^{K137A} vs. ΔpilTU	****	<0.0001	
pilU^{K137A} vs. ΔcomP	****	<0.0001	
Parent vs. ΔpilT	****	<0.0001	
Parent vs. ΔpilU	****	<0.0001	
Parent vs. ΔpilTU	****	<0.0001	
Parent vs. ΔcomP	****	<0.0001	
ΔpilT vs. ΔpilU	****	<0.0001	
ΔpilT vs. ΔpilTU	ns	>0.9999	
ΔpilT vs. ΔcomP	ns	0.7633	
ΔpilU vs. ΔpilTU	****	<0.0001	
ΔpilU vs. ΔcomP	****	<0.0001	
ΔpilTU vs. ΔcomP	ns	0.7681	
Supplemental Figure 1 - Dunnett's multiple comparison test			
Parent Ptac-PilT vs. ΔpilT ΔpilU Ptac-PilT	ns	0.9999	# of families = 2
Parent Ptac-PilT vs. pilT^{K136A} ΔpilU Ptac-PilT	ns	0.9999	# of comparisons per family = 6

Parent Ptac-PilT vs. pilT^{K136A} pilU^{K134A} Ptac-PilT	ns	0.37	Alpha = 0.05
Parent Ptac-PilT vs. ΔpilT Ptac-PilT	ns	0.9999	
Parent Ptac-PilT vs. pilT$^{K136A/E204A}$ ΔpilU Ptac-PilT	ns	0.9996	
Parent Ptac-PilT vs. pilT^{E204A} ΔpilU Ptac-PilT	ns	0.9779	
Parent Ptac-PilU vs. ΔpilT ΔpilU Ptac-PilU	****	0.0001	
Parent Ptac-PilU vs. pilT^{K136A} ΔpilU Ptac-PilU	ns	0.8282	
Parent Ptac-PilU vs. pilT^{K136A} pilU^{K134A} Ptac-PilU	ns	0.3199	
Parent Ptac-PilU vs. ΔpilT Ptac-PilU	****	0.0001	
Parent Ptac-PilU vs. pilT$^{K136A/E204A}$ ΔpilU Ptac-PilU	ns	0.0732	
Parent Ptac-PilU vs. pilT^{E204A} ΔpilU Ptac-PilU	ns	0.9999	
Supplemental Figure 2 (T18 x T25) - Dunnett's multiple comparison test			
vector x PilT vs. PilT x PilT	****	<0.0001	# of families = 6
vector x PilT vs. PilU x PilT	*	0.0343	# of comparisons per family = 6
vector x PilT vs. PilT^{K136A} x PilT	****	<0.0001	Alpha = 0.05
vector x PilT vs. PilU^{K134A} x PilT	**	0.0043	
vector x PilT vs. PilC x PilT	***	0.0002	
vector x PilU vs. PilT x PilU	*	0.0464	
vector x PilU vs. PilU x PilU	**	0.0016	
vector x PilU vs. PilT^{K136A} x PilU	ns	0.2389	
vector x PilU vs. PilU^{K134A} x PilU	***	0.0005	
vector x PilU vs. PilC x PilU	ns	0.0849	
vector x PilT^{K136A} vs. PilT x PilT^{K136A}	**	0.0031	
vector x PilT^{K136A} vs. PilU x PilT^{K136A}	ns	0.9997	
vector x PilT^{K136A} vs. PilT^{K136A} x PilT^{K136A}	ns	0.1368	
vector x PilT^{K136A} vs. PilU^{K134A} x PilT^{K136A}	ns	0.9984	
vector x PilT^{K136A} vs. PilC x PilT^{K136A}	*	0.0349	
vector x PilU^{K134A} vs. PilT x PilU^{K134A}	ns	0.1185	
vector x PilU^{K134A} vs. PilU x PilU^{K134A}	***	0.0004	
vector x PilU^{K134A} vs. PilT^{K136A} x PilU^{K134A}	ns	0.4273	
vector x PilU^{K134A} vs. PilU^{K134A} x PilU^{K134A}	**	0.003	
vector x PilU^{K134A} vs. PilC x PilU^{K134A}	*	0.013	
vector x PilC vs. PilT x PilC	ns	0.0724	
vector x PilC vs. PilU x PilC	ns	0.4038	
vector x PilC vs. PilT^{K136A} x PilC	ns	0.1408	
vector x PilC vs. PilU^{K134A} x PilC	ns	0.1544	
vector x PilC vs. PilC x PilC	****	0.0001	
vector x vector vs. PilT x vector	ns	0.9999	
vector x vector vs. PilU x vector	ns	0.9999	
vector x vector vs. PilT^{K136A} x vector	ns	0.9999	
vector x vector vs. PilU^{K134A} x vector	ns	0.9999	
vector x vector vs. PilC x vector	ns	0.9999	

Supplemental Figure 3A - Tukey's multiple comparison test			
Parent vs. ΔpilT	***	0.0002	# of families = 1
Parent vs. pilT^{K136A}, 6xHis-pilU	ns	>0.9999	# of comparisons per family = 36
Parent vs. 6xHis-pilT	ns	0.9508	Alpha = 0.05
Parent vs. 6xHis-pilU	ns	0.9235	
Parent vs. pilT^{K136A}, 3xFLAG-pilU	ns	0.9553	
Parent vs. 3xFLAG-pilT	ns	>0.9999	
Parent vs. 3xFLAG-pilU	ns	0.9949	
Parent vs. pilT^{K136A}	ns	0.9865	
ΔpilT vs. pilT^{K136A}, 6xHis-pilU	***	0.0007	
ΔpilT vs. 6xHis-pilT	*	0.0209	
ΔpilT vs. 6xHis-pilU	*	0.0261	
ΔpilT vs. pilT^{K136A}, 3xFLAG-pilU	*	0.0201	
ΔpilT vs. 3xFLAG-pilT	**	0.0014	
ΔpilT vs. 3xFLAG-pilU	**	0.0093	
ΔpilT vs. pilT^{K136A}	*	0.0126	
pilT^{K136A}, 6xHis-pilU vs. 6xHis-pilT	ns	0.9279	
pilT^{K136A}, 6xHis-pilU vs. 6xHis-pilU	ns	0.8986	
pilT^{K136A}, 6xHis-pilU vs. pilT^{K136A}, 3xFLAG-pilU	ns	0.9329	
pilT^{K136A}, 6xHis-pilU vs. 3xFLAG-pilT	ns	>0.9999	
pilT^{K136A}, 6xHis-pilU vs. 3xFLAG-pilU	ns	0.9862	
pilT^{K136A}, 6xHis-pilU vs. pilT^{K136A}	ns	0.9724	
6xHis-pilT vs. 6xHis-pilU	ns	>0.9999	
6xHis-pilT vs. pilT^{K136A}, 3xFLAG-pilU	ns	>0.9999	
6xHis-pilT vs. 3xFLAG-pilT	ns	0.98	
6xHis-pilT vs. 3xFLAG-pilU	ns	>0.9999	
6xHis-pilT vs. pilT^{K136A}	ns	>0.9999	
6xHis-pilU vs. pilT^{K136A}, 3xFLAG-pilU	ns	>0.9999	
6xHis-pilU vs. 3xFLAG-pilT	ns	0.9671	
6xHis-pilU vs. 3xFLAG-pilU	ns	>0.9999	
6xHis-pilU vs. pilT^{K136A}	ns	>0.9999	
pilT^{K136A}, 3xFLAG-pilU vs. 3xFLAG-pilT	ns	0.982	
pilT^{K136A}, 3xFLAG-pilU vs. 3xFLAG-pilU	ns	>0.9999	
pilT^{K136A}, 3xFLAG-pilU vs. pilT^{K136A}	ns	>0.9999	
3xFLAG-pilT vs. 3xFLAG-pilU	ns	0.9983	
3xFLAG-pilT vs. pilT^{K136A}	ns	0.9951	
3xFLAG-pilU vs. pilT^{K136A}	ns	>0.9999	
Supplemental Figure 3B - Tukey's multiple comparison test			
Parent vs. ΔpilT	ns	0.2194	# of families = 1
Parent vs. Ptac-3xFLAG-pilT	ns	>0.9999	# of comparisons per family = 66
Parent vs. Ptac-3xFLAG-pilT ΔpilT	ns	0.9989	Alpha = 0.05
Parent vs. Ptac-3xFLAG-pilU	ns	0.9995	
Parent vs. Ptac-3xFLAG-pilU, pilT^{K136A} ΔpilU	ns	0.9127	

Parent vs. Ptac-3xFLAG-pilT^{K136A}	ns	0.9505	
Parent vs. Ptac-3xFLAG-pilU^{K134A}	ns	0.9999	
Parent vs. Ptac-3xFLAG-pilT^{K136A}, ΔpilU	ns	0.2197	
Parent vs. Ptac-3xFLAG-pilU^{K134A}, pilT^{K136A}	ns	0.2199	
Parent vs. ΔpilU	ns	0.998	
Parent vs. pilT^{K136A}	ns	0.9912	
ΔpilT vs. Ptac-3xFLAG-pilT	ns	0.0832	
ΔpilT vs. Ptac-3xFLAG-pilT ΔpilT	*	0.0472	
ΔpilT vs. Ptac-3xFLAG-pilU	ns	0.5898	
ΔpilT vs. Ptac-3xFLAG-pilU, pilT^{K136A} ΔpilU	ns	0.9879	
ΔpilT vs. Ptac-3xFLAG-pilT^{K136A}	*	0.0123	
ΔpilT vs. Ptac-3xFLAG-pilU^{K134A}	ns	0.0697	
ΔpilT vs. Ptac-3xFLAG-pilT^{K136A}, ΔpilU	ns	>0.9999	
ΔpilT vs. Ptac-3xFLAG-pilU^{K134A}, pilT^{K136A}	ns	>0.9999	
ΔpilT vs. ΔpilU	ns	0.8312	
ΔpilT vs. pilT^{K136A}	ns	0.9042	
Ptac-3xFLAG-pilT vs. Ptac-3xFLAG-pilT ΔpilT	ns	>0.9999	
Ptac-3xFLAG-pilT vs. Ptac-3xFLAG-pilU	ns	0.9531	
Ptac-3xFLAG-pilT vs. Ptac-3xFLAG-pilU, pilT^{K136A} ΔpilU	ns	0.6364	
Ptac-3xFLAG-pilT vs. Ptac-3xFLAG-pilT^{K136A}	ns	0.9998	
Ptac-3xFLAG-pilT vs. Ptac-3xFLAG-pilU^{K134A}	ns	>0.9999	
Ptac-3xFLAG-pilT vs. Ptac-3xFLAG-pilT^{K136A}, ΔpilU	ns	0.0833	
Ptac-3xFLAG-pilT vs. Ptac-3xFLAG-pilU^{K134A}, pilT^{K136A}	ns	0.0834	
Ptac-3xFLAG-pilT vs. ΔpilU	ns	0.9305	
Ptac-3xFLAG-pilT vs. pilT^{K136A}	ns	0.8688	
Ptac-3xFLAG-pilT ΔpilT vs. Ptac-3xFLAG-pilU	ns	0.8682	
Ptac-3xFLAG-pilT ΔpilT vs. Ptac-3xFLAG-pilU, pilT^{K136A} ΔpilU	ns	0.4801	
Ptac-3xFLAG-pilT ΔpilT vs. Ptac-3xFLAG-pilT^{K136A}	ns	>0.9999	
Ptac-3xFLAG-pilT ΔpilT vs. Ptac-3xFLAG-pilU^{K134A}	ns	>0.9999	
Ptac-3xFLAG-pilT ΔpilT vs. Ptac-3xFLAG-pilT^{K136A}, ΔpilU	*	0.0473	
Ptac-3xFLAG-pilT ΔpilT vs. Ptac-3xFLAG-pilU^{K134A}, pilT^{K136A}	*	0.0473	
Ptac-3xFLAG-pilT ΔpilT vs. ΔpilU	ns	0.8381	
Ptac-3xFLAG-pilT ΔpilT vs. pilT^{K136A}	ns	0.7454	
Ptac-3xFLAG-pilU vs. Ptac-3xFLAG-pilU, pilT^{K136A} ΔpilU	ns	0.9991	
Ptac-3xFLAG-pilU vs. Ptac-3xFLAG-pilT^{K136A}	ns	0.5332	
Ptac-3xFLAG-pilU vs. Ptac-3xFLAG-pilU^{K134A}	ns	0.9319	
Ptac-3xFLAG-pilU vs. Ptac-3xFLAG-pilT^{K136A}, ΔpilU	ns	0.5902	

Ptac-3xFLAG-pilU vs. Ptac-3xFLAG-pilU^{K134A}, pilT^{K136A}	ns	0.5906	
Ptac-3xFLAG-pilU vs. ΔpilU	ns	>0.9999	
Ptac-3xFLAG-pilU vs. pilT^{K136A}	ns	>0.9999	
Ptac-3xFLAG-pilU, pilT^{K136A} ΔpilU vs. Ptac-3xFLAG-pilT^{K136A}	ns	0.2052	
Ptac-3xFLAG-pilU, pilT^{K136A} ΔpilU vs. Ptac-3xFLAG-pilU^{K134A}	ns	0.5864	
Ptac-3xFLAG-pilU, pilT^{K136A} ΔpilU vs. Ptac-3xFLAG-pilT^{K136A}, ΔpilU	ns	0.988	
Ptac-3xFLAG-pilU, pilT^{K136A} ΔpilU vs. Ptac-3xFLAG-pilU^{K134A}, pilT^{K136A}	ns	0.988	
Ptac-3xFLAG-pilU, pilT^{K136A} ΔpilU vs. ΔpilU	ns	>0.9999	
Ptac-3xFLAG-pilU, pilT^{K136A} ΔpilU vs. pilT^{K136A}	ns	>0.9999	
Ptac-3xFLAG-pilT^{K136A} vs. Ptac-3xFLAG-pilU^{K134A}	ns	>0.9999	
Ptac-3xFLAG-pilT^{K136A} vs. Ptac-3xFLAG-pilT^{K136A}, ΔpilU	*	0.0123	
Ptac-3xFLAG-pilT^{K136A} vs. Ptac-3xFLAG-pilU^{K134A}, pilT^{K136A}	*	0.0123	
Ptac-3xFLAG-pilT^{K136A} vs. ΔpilU	ns	0.5225	
Ptac-3xFLAG-pilT^{K136A} vs. pilT^{K136A}	ns	0.4139	
Ptac-3xFLAG-pilU^{K134A} vs. Ptac-3xFLAG-pilT^{K136A}, ΔpilU	ns	0.0698	
Ptac-3xFLAG-pilU^{K134A} vs. Ptac-3xFLAG-pilU^{K134A}, pilT^{K136A}	ns	0.0699	
Ptac-3xFLAG-pilU^{K134A} vs. ΔpilU	ns	0.906	
Ptac-3xFLAG-pilU^{K134A} vs. pilT^{K136A}	ns	0.8338	
Ptac-3xFLAG-pilT^{K136A}, ΔpilU vs. Ptac-3xFLAG-pilU^{K134A}, pilT^{K136A}	ns	>0.9999	
Ptac-3xFLAG-pilT^{K136A}, ΔpilU vs. ΔpilU	ns	0.8315	
Ptac-3xFLAG-pilT^{K136A}, ΔpilU vs. pilT^{K136A}	ns	0.9044	
Ptac-3xFLAG-pilU^{K134A}, pilT^{K136A} vs. ΔpilU	ns	0.8318	
Ptac-3xFLAG-pilU^{K134A}, pilT^{K136A} vs. pilT^{K136A}	ns	0.9046	
ΔpilU vs. pilT^{K136A}	ns	>0.9999	
Supplemental Figure 3D - Tukey's multiple comparison test			
Parent vs. ΔpilT ΔpilU	****	<0.0001	# of families = 1
Parent vs. pilU^{K134A}	ns	0.9994	# of comparisons per family = 55
Parent vs. pilT^{K136A} ΔpilU	****	<0.0001	Alpha = 0.05
Parent vs. pilT^{K136A} pilU^{K134A}	****	<0.0001	
Parent vs. P_{tac}-pilT	ns	0.999	
Parent vs. ΔpilT Ptac-pilT	ns	>0.9999	
Parent vs. P_{tac}-pilU	ns	0.999	
Parent vs. pilT^{K136A} ΔpilU Ptac-pilU	ns	0.9481	
Parent vs. ΔpilA	****	<0.0001	

Parent vs. pilT^{K136A}	ns	>0.9999	
ΔpilT ΔpilU vs. pilU^{K134A}	****	<0.0001	
ΔpilT ΔpilU vs. pilT^{K136A} ΔpilU	ns	0.4878	
ΔpilT ΔpilU vs. pilT^{K136A} pilU^{K134A}	ns	>0.9999	
ΔpilT ΔpilU vs. Ptac-pilT	****	<0.0001	
ΔpilT ΔpilU vs. ΔpilT Ptac-pilT	****	<0.0001	
ΔpilT ΔpilU vs. Ptac-pilU	****	<0.0001	
ΔpilT ΔpilU vs. pilT^{K136A} ΔpilU Ptac-pilU	****	<0.0001	
ΔpilT ΔpilU vs. ΔpilA	**	0.0028	
ΔpilT ΔpilU vs. pilT^{K136A}	****	<0.0001	
pilU^{K134A} vs. pilT^{K136A} ΔpilU	****	<0.0001	
pilU^{K134A} vs. pilT^{K136A} pilU^{K134A}	****	<0.0001	
pilU^{K134A} vs. P_{tac}-pilT	ns	>0.9999	
pilU^{K134A} vs. ΔpilT Ptac-pilT	ns	>0.9999	
pilU^{K134A} vs. P_{tac}-pilU	ns	>0.9999	
pilU^{K134A} vs. pilT^{K136A} ΔpilU Ptac-pilU	ns	0.6391	
pilU^{K134A} vs. ΔpilA	****	<0.0001	
pilU^{K134A} vs. pilT^{K136A}	ns	0.9972	
pilT^{K136A} ΔpilU vs. pilT^{K136A} pilU^{K134A}	ns	0.6518	
pilT^{K136A} ΔpilU vs. Ptac-pilT	****	<0.0001	
pilT^{K136A} ΔpilU vs. ΔpilT Ptac-pilT	****	<0.0001	
pilT^{K136A} ΔpilU vs. Ptac-pilU	****	<0.0001	
pilT^{K136A} ΔpilU vs. pilT^{K136A} ΔpilU Ptac-pilU	****	<0.0001	
pilT^{K136A} ΔpilU vs. ΔpilA	ns	0.4692	
pilT^{K136A} ΔpilU vs. pilT^{K136A}	****	<0.0001	
pilT^{K136A} pilU^{K134A} vs. P_{tac}-pilT	****	<0.0001	
pilT^{K136A} pilU^{K134A} vs. ΔpilT Ptac-pilT	****	<0.0001	
pilT^{K136A} pilU^{K134A} vs. P_{tac}-pilU	****	<0.0001	
pilT^{K136A} pilU^{K134A} vs. pilT^{K136A} ΔpilU Ptac-pilU	****	<0.0001	
pilT^{K136A} pilU^{K134A} vs. ΔpilA	**	0.0057	
pilT^{K136A} pilU^{K134A} vs. pilT^{K136A}	****	<0.0001	
Ptac-pilT vs. ΔpilT Ptac-pilT	ns	>0.9999	
P_{tac}-pilT vs. P_{tac}-pilU	ns	>0.9999	
Ptac-pilT vs. pilT^{K136A} ΔpilU Ptac-pilU	ns	0.6089	
Ptac-pilT vs. ΔpilA	****	<0.0001	
P_{tac}-pilT vs. pilT^{K136A}	ns	0.9957	
ΔpilT Ptac-pilT vs. Ptac-pilU	ns	>0.9999	
ΔpilT Ptac-pilT vs. pilT^{K136A} ΔpilU Ptac-pilU	ns	0.7364	
ΔpilT Ptac-pilT vs. ΔpilA	****	<0.0001	
ΔpilT Ptac-pilT vs. pilT^{K136A}	ns	0.9995	
Ptac-pilU vs. pilT^{K136A} ΔpilU Ptac-pilU	ns	0.6068	
Ptac-pilU vs. ΔpilA	****	<0.0001	

P_{tac}-pilU vs. pilT^{K136A}	ns	0.9956	
pilT^{K136A} ΔpilU Ptac-pilU vs. ΔpilA	****	<0.0001	
pilT^{K136A} ΔpilU Ptac-pilU vs. pilT^{K136A}	ns	0.9772	
ΔpilA vs. pilT^{K136A}	****	<0.0001	
Supplemental Figure 4 - Dunnett's multiple comparison test			
Parent pmmB-pilT vs. ΔpilTU pmmB-pilT	****	0.0001	# of families = 2
Parent pmmB-pilT vs. ΔpilT pmmB-pilT	ns	0.8827	# of comparisons per family = 8
Parent pmmB-pilT vs. ΔpilU pmmB-pilT	****	0.0001	Alpha = 0.05
Parent pmmB-pilT vs. pilT^{K136A} pmmB-pilT	ns	0.8666	
Parent pmmB-pilT vs. pilT^{K136A} ΔpilU pmmB-pilT	****	0.0001	
Parent pmmB-pilT vs. pilU^{K137A} pmmB-pilT	****	0.0001	
Parent pmmB-pilT vs. pilT^{K136A} pilU^{K137A} pmmB-pilT	****	0.0001	
Parent pmmB-pilU vs. ΔpilTU pmmB-pilU	Yes	****	
Parent pmmB-pilU vs. ΔpilT pmmB-pilU	Yes	****	
Parent pmmB-pilU vs. ΔpilU pmmB-pilU	No	ns	
Parent pmmB-pilU vs. pilT^{K136A} pmmB-pilU	Yes	****	
Parent pmmB-pilU vs. pilT^{K136A} ΔpilU pmmB-pilU	Yes	****	
Parent pmmB-pilU vs. pilU^{K137A} pmmB-pilU	Yes	*	
Parent pmmB-pilU vs. pilT^{K136A} pilU^{K137A} pmmB-pilU	Yes	****	
Parent pmmB-pilU vs. Parent pmmB-pilU	No	ns	
Supplemental Figure 5 - Tukey's multiple comparison test			
Parent vs. ΔMSHA ΔTCP	ns	0.8726	# of families = 1
Parent vs. ΔpilTU	****	<0.0001	# of comparisons per family = 6
Parent vs. ΔpilTU ΔMSHA ΔTCP	****	<0.0001	Alpha = 0.05
ΔMSHA ΔTCP vs. ΔpilTU	****	<0.0001	
ΔMSHA ΔTCP vs. ΔpilTU ΔMSHA ΔTCP	****	<0.0001	
ΔpilTU vs. ΔpilTU ΔMSHA ΔTCP	ns	0.0927	

[#]Statistical differences were assessed by one-way ANOVA tests followed by a multiple comparisons post test (either Tukey's or Dunnett's) using GraphPad Prism software. For all transformation frequency experiments and frequency of pilus retraction experiments, statistical analyses were performed on the log transformed data (i.e. **Figs 1A, 1C, 2B, 4C** and **S1, S3A, S3B, S3D, S4, S5 Figs**).